國 立 交 通 大 學

光電工程研究所

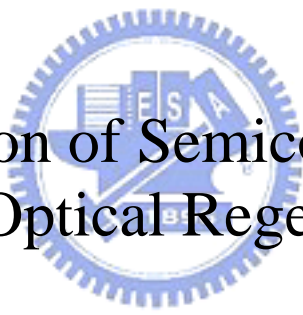## 博士論文

半導體雷射於全光再生之應用

The Application of Semiconductor Laser
on All-Optical Regeneration

研 究 生：錢鴻章

指導教授：祁　甡 教授

李健仲 博士

中華民國 九十五 年 七 月

半導體雷射於全光再生之應用

The Applications of Semiconductor Laser on All-Optical Regeneration

研 究 生：錢鴻章　　　　　　　Student : Hung-Chang Chien

指導教授：祁　甡　　　　　　　Advisors : Sien Chi
　　　　　李健仲　　　　　　　　　　　　Chien-Chung Lee

國立交通大學 電機學院
光電工程研究所
博士論文

A Dissertation
Submitted in Partial Fulfillment of the Requirements
for the Degree of Doctor of Philosophy in
The Institute of Electro-Optical Engineering
College of Electrical and Computer Engineering
National Chiao Tung University
Hsin-Chu, Taiwan, R.O.C.

中華民國 九十五 年 七 月

半導體雷射於全光再生之應用

研究生：錢鴻章　　　　　　　　　　　指導教授：祁　甡
　　　　　　　　　　　　　　　　　　　　　　　李健仲

國立交通大學 電機學院

光電工程研究所

摘要

在本篇論文中我們探討了全光再生技術。而半導體雷射這種常見的經濟型光源，最近被發現其在被失真訊號注入鎖定之下能夠成為一個理想的光決策元件進而提供全光振幅及波形再生功能。本論文探討了其理論分析以及實驗論證。以傳統雙模注入鎖定技術為基礎，我們提出了兩種基於半導體雷射之振幅及波形全光再生方法。第一種方式是一種簡化的架構，係使用高集成之自我注入鎖定 Fabry-Pérot 雷射二極體來達成全光振幅及波形再生而不需要傳統架構所需的外部連續光源。此外，我們也提出了一個將自我注入鎖定 Fabry-Pérot 雷射二極體併入雙向光放大器的整合性模組。另一種方式為第一種方式的免放大器模式。藉由技巧性的使用與第一種方式的不同操作狀態，甚至可以不需要外部放大器即可達到 1.3/1.5 μm 全光振幅及波形再生。實驗結果證明了這兩種提出的方法皆為針對系統缺陷之經濟且有效率的解決方案，並對於未來光網路的發展有著廣闊的前景。

The Application of Semiconductor Laser on All-Optical Regeneration

Student: Hung-Chang Chien

Advisor: Sien Chi

Chien-Chung Lee

Institute of Electro-Optical Engineering
College of Electrical and Computer Engineering
National Chiao Tung University

ABSTRACT

In this dissertation, we investigate the all-optical regeneration techniques. A semiconductor laser, a commonly available low-cost light source, is recently found to be an ideal optical decision element, which can provide all-optical 2R regenerating function when injection-locked by a degraded signal. Both theoretical analysis and experimental demonstration are studied. Based on the traditional two-mode injection locking (TMIL) technique, two types of semiconductor-laser-based 2R schemes are presented. The first scheme has a simplified structure which employs a compact self-seed Fabry-Pérot laser diode (SSFP-LD) to execute all-optical 2R regeneration without the help from the traditionally required external probe lasers. Additionally, an integrated module using this SSFP-LD incorporated in a bidirectional optical amplifier is also proposed. Another scheme is an amplifier-free edition of the first one. By skillfully using different operation conditions from those of the first scheme, even the outside amplifiers are not required for 1.3/1.5 μm all-optical 2R regeneration. The proposed schemes are proved to be cost-effective solutions for the system impairments, and are promising for future deployment of optical networks.

誌　謝

(Acknowledgements)

Contents

Chapter 1. Introduction

Chapter 2. Overview of All-Optical Regeneration

Chapter 3. Semiconductor-Laser-based All-Optical 2R Regeneration Using Injection Locking Technique

Chapter 4. All-Optical 2R Regeneration Using Simplified TMIL Scheme

Chapter 5. Amplifier-Free All-Optical 2R Regeneration

Chapter 6. Conclusions and Future Work

List of Figures

List of Tables

List of Acronyms

Acronyms	Descriptions
1R	Reamplification
2R	Reamplification and Reshaping
3R	Reamplification, Reshaping and Retiming
WDM	Wavelength Division Multiplexing
TDM	Time Division Multiplexing
ECC	Error Correcting Code
SOA	Semiconductor Optical Amplifier
EAM	Electro-Absorber Modulator
MMIL	Main-Mode Injection Locking
SMIL	Side-Mode Injection Locking
TMIL	Two-Mode Injection Locking
EDFA	Erbium-Doped Fiber Amplifier
SSFP-LD	Self-Seeded Fabry-Pérot Laser Diode
DFB-LD	Distributed Feedback Laser Diode
ER	Extinction Ratio
SOA-MZI	SOA-based Mach–Zehnder Interferometer
CW	Continuous Wave
XPM	Cross Phase Modulation
SPM	Self-Phase Modulation
NOLM	Nonlinear Optical Loop Mirror
ML	Master Laser
SL	Salve Laser
TL	Tunable Laser

ODE	Ordinary Differential Equation
BER	Bit Error Rate
EOM	Electro-Optic Modulator
OC	Optical Circulator
PC	Polarization Controller
SMSR	Side Mode Suppression Ratio
BPF	Bandpass Filter
CDR	Clock and Data Receiver
VOA	Variable Optical Attenuator
BERT	Bit-Error-Ratio Tester
FWM	Four Wave Mixing
SLM	Single Longitudinal Mode
OSNR	Optical Signal to Noise Ratio
FBG	Fiber Bragg Grating
PDFA	Praseodymium Doped-Fiber Amplifier
RA	Raman Amplifier
LAN	Local Area Network
MAN	Metropolitan Area Network
ROF	Relaxation Oscillation Frequency

List of Symbols

Symbols	Descriptions
ω_0	Free-running oscillation frequency
I_0	Free-running oscillation intensity
E_i	Injected optical field
E_c	Optical field in laser cavity
$\widetilde{G}_{rt}(\omega)$	Net complex round-trip field gain
$G_{rt}(\omega)$	Net round-trip magnitude
α_m	Laser Gain
a	Insertion loss
$\phi(\omega)$	Round-trip phase shift
$\widetilde{g}_{reg}(\omega)$	Overall regenerative field gain
t	Transmission coefficient of the input mirror
T	Transmittance
t_{rt}	Transit time for one round trip inside the cavity
r_e	External decay rate
$\beta(t)$	Normalized electric field of the slave laser
$\beta_I(t)$	Electric field coupled into the SL cavity
G	Material gain
G_N	Derivatives of G with respect to N
G_I	Derivatives of G with respect to I
$N(t)$	Carrier density
N_0	Threshold carrier density
ϕ	Phase difference between SL and ML
τ_s	Spontaneous lifetime of minority carriers

τ_i	Group round-trip time of SL
$\Delta\omega$	Frequency detuning
ρ	Normalized optical injection level
f_r	Relaxation oscillation frequency
τ_p	Average photon life time in the laser cavity
υ	Group velocity of light
S_0	Photon density in steady state
P_{peak}	Field intensities of the peak (main) mode
P_{side}	Field intensities of the side (target) mode
P_{in}	Field intensities of the input signal
ϕ_{side}	Phase difference between the side mode and the input signal
δn	Deviations of the carrier numbers around the threshold values
p	Ratio of the effective mode index to the effective group index
v	Angular frequencies of the input signal
ω_{th}	Angular frequencies of the side mode
α	Linewidth broadening factor
C	Carrier injection rate
$C_{sp\text{-}peak}$	Spontaneous emission rates of the peak mode
$C_{sp\text{-}side}$	Spontaneous emission rates of the side mode
β_k	Slowly varying field envelope of the locked mode
β_k^{in}	Injected field

Chapter 1

Introduction

1.1 WDM/TDM Network Impairments

The advent of optical amplification and WDM/TDM technologies make a high-capacity fiber-optic communication system realized [1-10]. A given capacity can be implemented through a large number of WDM channels, a reduced number of high-speed TDM channels, or the hybrid of them. It is well known that the trend for future WDM/TDM transmission system is to pursue a higher channel rate. However, such high-speed system may exhibit sensitive to several impairments like amplifier noise accumulation [11], fiber dispersion [12-14], fiber nonlinearity [15, 16], and inter/intrachannel interactions [17], which may result in three main types of signal degradation: intensity noise, timing jitter, and pulse-envelope distortion [18].

To overcome the above limitations and improve the performance of lightwave transmission performance, error correcting codes (ECC) at transmitter and receiver are usually applied to provide extra information for identifying and correcting the bit errors caused by transmission channel [21]. However, such coding criterion shows limited improvement and can not be viewed as actual signal regeneration. Therefore, a fundamental development of practical inline optical signal processing is required [18, 22, 23]. In this way, signal can directly be recovered in optical domain.

1.2 Motivation

In a high data rate system, there exists a challenge for the development of broadband high-speed electronics. Thus, signal regeneration in all-optical domain becomes a promising inline signal processing technique. It performs the same signal-restoring functions as the conventional electronic approach, but with far reduced complexity and enhanced capabilities. As a result, the motivation of this dissertation lies in the investigation of a reliable and economic solution for all-optical regeneration in WDM/TDM network. It is also proved that a semiconductor laser diode [20], which is commonly available as a low-cost lighting source, has a good change to provide all-optical regenerating functions when injection-locked by an external degraded optical signal.

1.3 Organization of the Dissertation

In Chapter 1, the system impairments in WDM/TDM network and the motivation to overcome such limitation using cost-effective and elegant approaches are introduced. In Chapter 2, an overview of all-optical regeneration is studied. Four different types of all-optical 2R regeneration methods by using the SOA-based, fiber-based, EAM-based, and semiconductor-laser-based techniques are presented, respectively. In Chapter 3, we briefly introduce the theory of laser injection locking, and review three types of conventional semiconductor-laser-based all-optical 2R regeneration schemes: main-mode (MM), side-mode (SM), and two-mode (TM) injection locking. In addition, the pros and cons of these 2R techniques are also discussed. Based on the traditional TMIL method, we propose two types of new TMIL schemes. The first type has a simplified structure without the help from external probe lasers and another one is an amplifier-free method in which the outside EDFAs are not required.

In chapter 4, two simplified TMIL schemes for all-optical 2R regeneration are presented.

In section 4.2, a cost-effective method, based on the injection locking technique of a compact self-seeded Fabry-Pérot laser diode (SSFP-LD) with a 10mm-long embedded fiber Bragg grating cavity, is proposed, in which the external probe lasers are not required. Additionally, in section 4.3, an all-optical 2R regenerator, based on a compact self-seeded Fabry-Pérot laser diode (SSFP-LD) with a 10mm-long embedded fiber Bragg grating cavity, and a bidirectional EDFA, is presented to execute all-optical 2R regeneration at 10 Gb/s with 6.4-dB power-penalty improvement and reduced number of EDFAs.

Chapter 5 presents an EDFA-free all-optical 2R regeneration scheme. The proposed 2R regenerator achieves a straight line transmission at 10 Gb/s over 76 km without either the EDFA or the external probe laser, both of which are traditionally required. On the other hand, a novel and cost-effective 1.3 μm all-optical 2R regenerator based on a two-mode injection-locked distributed feedback laser diode (TMIL DFB-LD) is also proposed to provide adequate all-optical reamplification and reshaping in the second window. Finally, concluding remarks and suggestions for future works are given in Chapter 6.
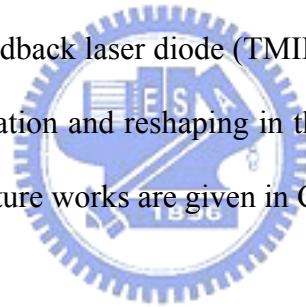
References for Chapter 1:

[1] Y. Sun, G. Luo, J. L. Zyskind, A. A. M. Saleh, A. K. Srivastava, and J. W. Sulhoff, "Model for gain dynamics in erbium-doped fiber amplifiers," *Electron. Lett.*, vol. 32, no. 16, pp. 1490-1491, Aug. 1996.

[2] Y. Sun, A. K. Srivastava, J. L. Zyskind, J. W. Sulhoff, C. Wolf, and R. W. Tkach, "Fast power transients in WDM optical networks with cascaded EDFA's," *Electron. Lett.*, vol. 33, no. 4, pp. 313-314, Feb. 1997.

[3] Y. Sun, A. A. M. Saleh, J. L. Zyskind, D. L. Wilson, A. K. Srivastava, and J. W. Sulhoff, "Time dependent perturbation theory and tones in cascaded Erbium-doped fiber amplifier systems," *J. Lightwave Technol.*, vol. 15, pp. 1083-1087, July 1997.

[4] A. Bononi and L. A. Rusch, "Doped-fiber amplifier dynamics: A system perspective," *J. Lightwave Technol.*, vol. 16, pp. 945-956, May 1998.

[5] C. Qiao, "Optical buffer switching—A novel paradigm for gigabit WDM optical networks," *Proc. Gigabit Networking Symp.* San Francisco, CA, Mar. 1998.

[6] E. Desurvire, Erbium-Doped Fiber Amplifiers, New York: Wiley, 1994.

[7] T. Georges and E. Delevaque, "Analytic modeling of high-gain Erbium-doped fiber amplifiers," *Opt. Lett.*, vol. 17, no. 16, pp. 1113-1115, Aug. 1992.

[8] W. Zeiler, F. Di Pasquale, P. Bayvel, and J. E. Midwinter, "Modeling of four-wave mixing and gain peaking in amplified WDM optical communication systems and networks," *J. Lightwave Technol.*, vol. 14, pp. 1933-1942, Sept. 1996.

[9] A. E. Willner and S. Hwang, "Transmission of many WDM channels through a cascade of EDFA's in long-distance links and ring networks," *J. Lightwave Technol.*, vol. 13, pp. 802-816, May 1995.

[10] M. A. Ali, A. F. Elrefaie, R. E. Wagner, and S. A. Ahmed, "A detailed comparison of the

overall performance of 980 and 1480 nm pumped EDFA cascades in WDM multiple-access lightwave networks," *J. Lightwave Technol.*, vol. 14, pp. 1436-1448, June 1996.

[11] C. Lorattanasane, K. Kikuchi, "Parametric instability of optical amplifier noise in long-distance optical transmission systems," *IEEE J. Sel. Topics Quantum. Electron.*, vol. 33, pp. 1068-1074, July 1997.

[12] M. Suzuki, I. Morita, N. Edagawa, S. Yamamoto, and S. Akiba, "20Gbit/s-based soliton WDM transmission over transoceanic distances using periodic compensation of dispersion and its slope," *Electron. Lett.*, vol. 23, pp. 691-692, 1997.

[13] M. Stern, J. P. Heritage, R. N. Thurston, and S. Tu, "Self-phase modulation and dispersion in high data rate fiber-optic transmission systems," *J. Lightwave Technol.*, vol. 8, pp. 1009-1016, 1990.

[14] M. Suzuki, N. Edagawa, "Dispersion-managed high-capacity ultra-long-haul transmission," *J. Lightwave Technol.*, vol. 21, pp. 916-929, 2003.

[15] F. Forghieri, "Granularity in WDM networks: the role of fiber nonlinearities," *IEEE Photon. Technol. Lett.*, vol. 8, pp. 1400-1402, 1996.

[16] M. Wu, W. I. Way, "Fiber nonlinearity limitations in ultra-dense WDM systems," *J. Lightwave Technol.*, vol. 22, pp. 1483-1498, 2004.

[17] T. Hirooka, M. J. Ablowitz, "Suppression of intrachannel dispersion-managed pulse interactions by distributed amplification," *IEEE Photon. Technol. Lett.*, vol. 14, pp. 316-318, 2002.

[18] S. Waiyapot, S.K. Turitsyn, V.K. Mezentsev, "Optical regeneration at 40 Gb/s and beyond," *J. Lightwave Technol.*, vol. 21, pp. 2779-2790, 2003.

[19] M.Tomizawa, Y. Yamabayshi, K. Murata, T. Ono, Y. Kobayashi, K. Hagimoto, "Forward error correcting codes in synchronous fiber optic transmission systems," *J. Lightwave*

Technol., vol. 15, pp. 43-52, 1997.

[20] A. Poustie, "Semiconductor devices for all-optical signal processing," in *Proc. Eur. Conf. Optical Communication (ECOC 2005)*, vol. 3, pp. 475-478, 2005.

[21] K. Uchiyama, T. Morioka, "All-optical signal processing for 160 Gbit/s/channel OTDM/WDM systems," in *Proc. Optical Fiber Communication Conf. (OFC) 2001*, pp. ThH2-1 - ThH2-3.

Chapter 2

Overview of All-Optical Regeneration

2.1 Introduction

Recently, the advent of the optical amplification and wavelength division multiplexed (WDM) technologies have realized ultrahigh transmission bandwidth up to several THz. Current optical communication networks have the trends toward greater capacities and higher spectral efficiencies. However, the rapid growth of channel bit rate would result in the increase of some propagation impairments owing to noise accumulation, fiber dispersion, fiber nonlinearities, and inter-channel interactions. Therefore, in-line optical signal regeneration is a promising alternative for overcome system limitations. There are two kinds of optical signal regeneration. The first one is called optoelectronic regeneration. As its name imply, a degraded optical signal will be converted to the electrical domain for signal restoration, and then be converted back to the optical domain with regenerated waveform and clock. However, the power consumption at each routing node from optical-to-electrical-to-optical (OEO) conversion and the existence of electrical bottleneck at high bit rate will limit the development of optoelectronic regeneration. Therefore, another solution called all-optical regeneration is attracting much interest. Such signal regeneration in all-optical domain features enhanced capacities and far reduced complexity, and are ready to be implemented in a commercial communication system in the near future.

There are three basic functions of all-optical regeneration: reamplication, reshaping, and retiming. Therefore, by definition, "1R" regeneration means only optical amplification. When reshaping capability is added, we call it "2R" regeneration. In addition, when the retiming is further included, all-optical "3R" regeneration is obtained [1-5]. Throughout this thesis, we focus on the study of all-optical 2R regeneration schemes.

2.2 Classification of All-Optical 2R Regeneration

The device or module for all-optical 2R regeneration usually contains nonlinear elements, that is, a step-like transfer function is provided for the incoming signal. As shown is Fig. 2.1, a distorted signal, with noise accumulation over its mark and space, is fed into the 2R regenerating system. After nonlinear transferring, the degraded signal is amplified, and the output signal exhibits a noise-suppressed and reshaped waveform with improved extinction ratio (ER). Generally speaking, nonlinear optical decision element with ideal step-like transfer function is unavailable. So far, all-optical 2R regeneration can be achieved by four types of medias: SOA-based, Fiber-based, EAM-based, and semiconductor-laser-based.

2.2.1 SOA-Based

The first type of device to consider is all-optical 2R regeneration based on semiconductor optical amplifier (SOA) [6, 7]. The modulation of carrier density in the active region of SOA is used to achieve a nonlinear intensity transfer function. Figure 2.2 shows the most common structure: SOA-based Mach–Zehnder interferometer (SOA-MZI). An input signal at wavelength λ_1 acting as a control signal and a continuous-wave (CW) signal at wavelength λ_2 acting as a probe. The output power is given by

$$P_{out}(\lambda_2) \propto P_{cw}(\lambda_2)[1 + \cos(\Delta\Phi(P_{in,\lambda_1}))] \tag{2.1}$$

where $\Delta\Phi(P_{in,\lambda_1}) = \Phi_2(P_{in,\lambda_1}) - \Phi_1$. The injection signal at λ_1 will induce a phase shift through cross phase modulation (XPM), and the amount of which depends upon its power level P_{in,λ_1}. As a result, phase modulation is attempted to change the amplitude on the signal at λ_2, and 2R regeneration can be achieved.

8

2.2.2　Fiber-Based

In the case of fiber-based devices such as the nonlinear optical loop mirror (NOLM) illustrated in Fig. 2.3, the phase shift is induced through Kerr effect in an optical fiber [8]. Such cross-phase modulation (XPM) induced optical phase change will determinate whether the input signal is transmitted or reflected. The fiber-based devices have fast response of the Kerr nonlinearity, which is suitable for ultrahigh bit-rate operation. However, major limitations lay in environmental instability, strong polarization dependence, and difficult integration, resulting from the requirement of kilometer-scale fiber lengths.

2.2.3　EAM-Based

Another choice is using an electro-absorber modulator (EAM) as a saturable absorber to achieve ER improvement and reduce noise variation [9]. Such device absorbs low intensity noise, for example amplified spontaneous emission (ASE), while high intensity pulses are transmitted with low loss. The optical nonlinearities induced in an EAM is based on real process of carrier generation by absorption of injected optical pulse, and the absorption recovery time is faster than gain recovery time of an SOA.

2.2.4　Semiconductor-Laser-Based

In addition to semiconductor optical amplifier, semiconductor laser have also been applied as all-optical 2R regenerator [10]. Such 2R regeneration features an injection locking phenomenon which can only be observed within an oscillator above certain threshold condition. Laser injection locking exhibits an on-off threshold for the incoming signal. Therefore, a step-like nonlinear intensity transfer function can be provided. Besides, compared with SOA, the semiconductor diode laser has far reduced cost and compatible regeneration efficiency, and thus become the main subject of our study.

Reference for Chapter 2

[1] B. Sartorius, M. Möhrle, S. Reichenbacher, H. Preir, H. J. Wünsche, and U. Bandelow, "Dispersive self-Q-switching in self-pulsating DFB lasers," *IEEE J. Quantum Electron.*, vol. 33, pp. 211-218, Feb. 1997.

[2] C. Bornholdt, B. Sartorius, and M. Möhrle, "All-optical clock recovery at 40 Gbit/s," *Proc. Eur. Conf. Optical Communications (ECOC'99)*, Nice, France, 1999, postdeadline paper PD 3-5, p. 54.

[3] D. Chiaroni, B. Lavigne, A. Dupas, P. Guerber,A. Jourdan, F. Devaux, C. Bornholdt, S. Bauer, B. Sartorius, and M. Möhrle, *Proc. Eur. Conf. Optical Communications (ECOC'2000)*, vol. 4, Munich, Germany, 2000, paper 10.4.5, p. 69.

[4] B. Sartorius, C. Bornholdt, S. Bauer, M. Möhrle, P. Brindel, and O. Leclerc, "System application of 40 GHz all-optical clock in a 40 Gbit/soptical 3R regenerator," *Proc. Conf. Optical Communications (OFC'2000)*, Washington, DC, 2000, postdeadline paper PD11.

[5] B. Lavigne, P. Guerber, C. Janz, A. Jourdan, and M. Renaud, "Full validation of an optical 3R regenerator at 20 Gbit/s," *Proc. Conf. Optical Communications (OFC'2000)*, vol. 4, Washington, DC, paper ThF7, p. 93.

[6] T. Durhuus, B. Mikkelsen, C. Joergensen, S. L. Danielsen, and K. E. Stubkjaer, "All-optical wavelength conversion by semiconductor optical amplifiers," *J. Lightwave Technol.*, vol. 14, no. 6, 1996.

[7] S. Fischer, M. Dülk, E. Gamper, W. Vogt, E. Gini, H. Melchior, WHunziker, D. Nesset, and A. D. Ellis, "Optical 3R regenerator for 40 Gbit/s networks," *Electron. Lett.*, vol. 35, no. 23, 1999.

[8] S. Bigo, O. Leclerc, and E. Desurvire, "All-optical fiber signal processing and regeneration for soliton communications," *IEEE J. Select. Topics Quantum Electron.*, vol.

3, pp. 1208–1223, Sept./Oct. 1997.

[9] K. Nishimura, R. Inohara, M. Usami, and S. Akiba, "All-Optical Regeneration by Electro-Absorption Modulator", *IEICE Trans. Electron.*, vol. E88-C, no. 3, pp. 319–326, 2006.

[10] S. Yamashita and J. Suzuki, "All-optical 2R regeneration using a two-mode injection-locked Fabry-Pérot laser diode," *IEEE Photon. Technol. Lett.*, vol. 16, no. 4, pp. 1176-1178, Apr. 2004.
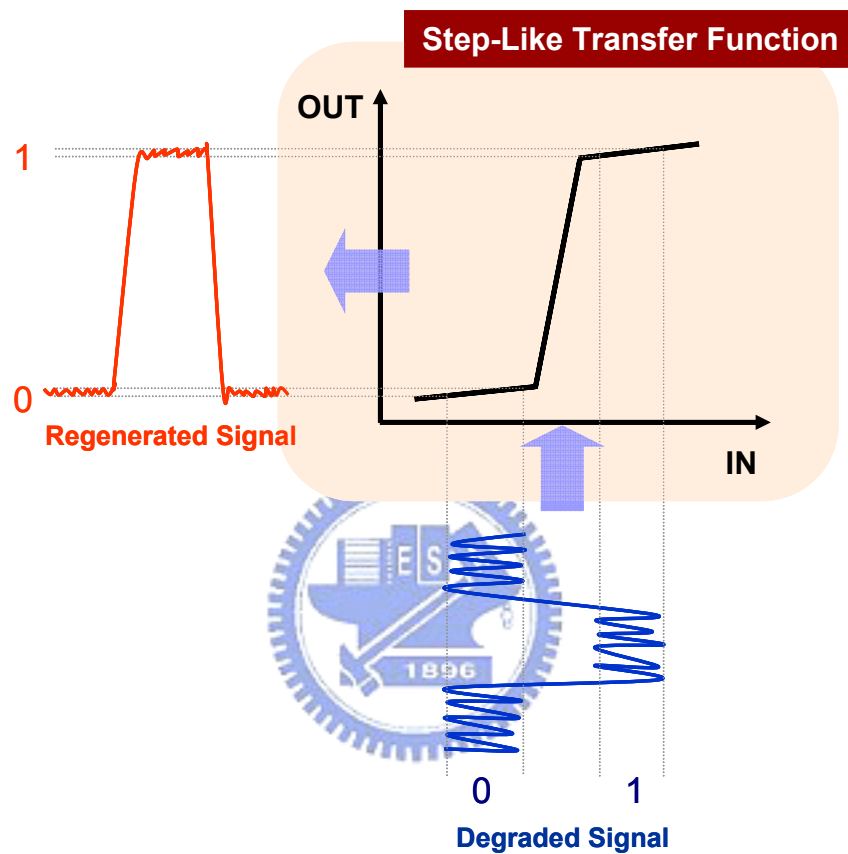
Fig. 2.1 Principle of all-optical 2R regeneration with step-like intensity transfer function.
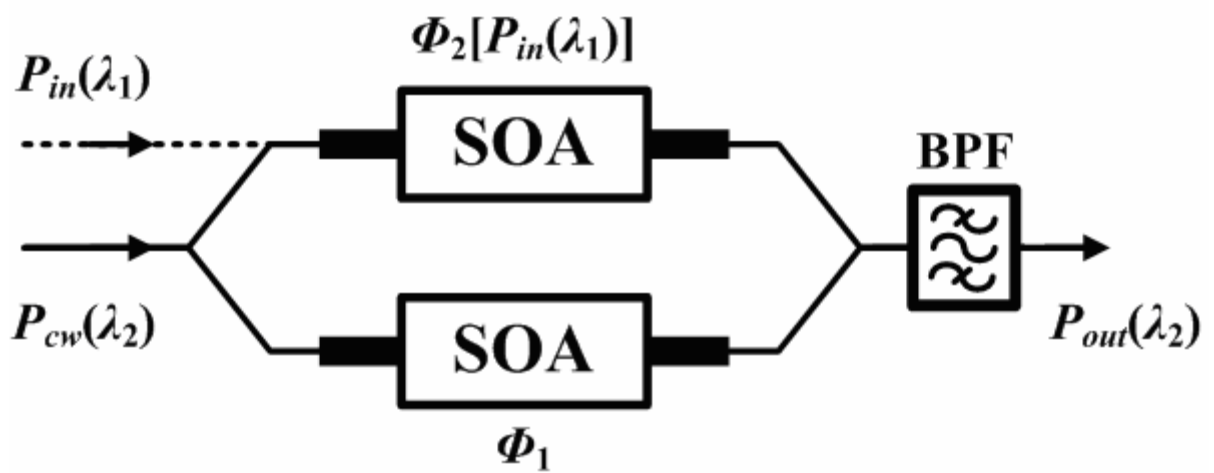
Fig. 2.2 Schematic diagram of SOA-based Mach-Zehnder

interferometer (SOA-MZI).
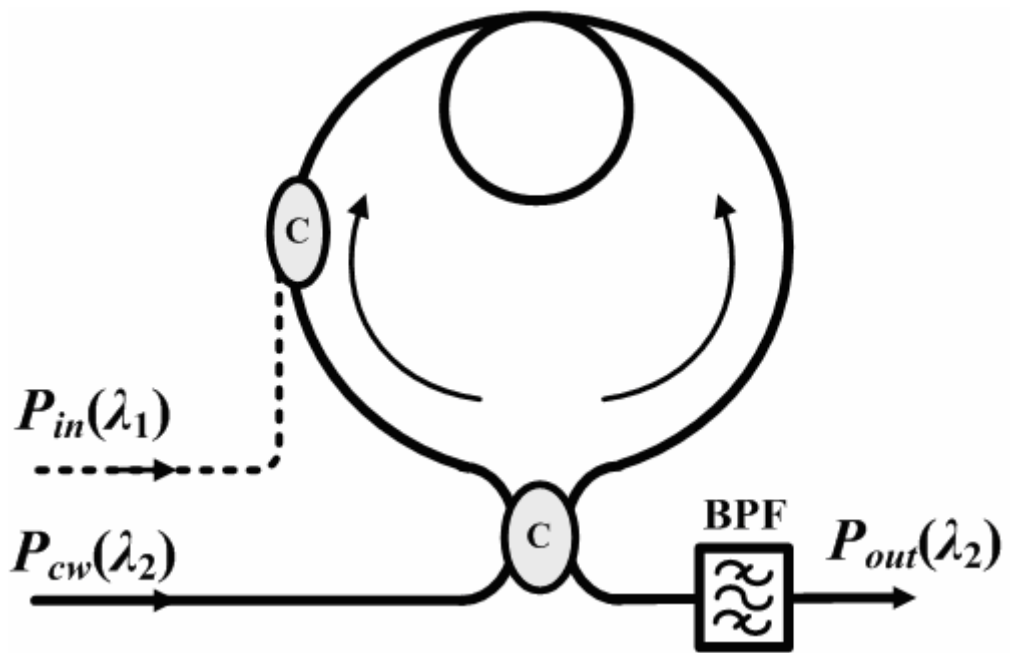
Fig. 2.3 Schematic diagram of nonlinear loop mirror (NOLM).

Chapter 3

Semiconductor-Laser-Based All-Optical 2R Regeneration Using Injection Locking Technique

3.1 Introduction

In this chapter, we briefly introduce the theory of laser injection locking, and review three types of conventional semiconductor-laser-based all-optical 2R regeneration schemes: main-mode (MM), side-mode (SM), and two-mode (TM) injection locking. In addition, the pro and con of these 2R techniques are also discussed. Based on the traditional TMIL method, we propose two types of new TMIL schemes. The first type has a simplified structure without the help from external probe lasers and another one is an amplify-free method in which the outside EDFAs are not required.

3.2 Laser Injection Locking Technique

Semiconductor lasers have several intrinsic imperfections like partition noise, mode instability, and broad linewidth, which are disadvantageous in a coherent optical communication system. Recently, the injection-locking technique has been widely used to improve the static and dynamic performance of different kinds of oscillators, and its application on semiconductor lasers have also aroused great interest. Injection locking of a semiconductor laser can improve the coherence properties of the emitted signal, suppress the mode hopping effect, eliminate the partition the noise [1, 2], reduce the relaxation oscillations under direct modulation [3-6], achieve high-speed single-mode operation, narrow the laser linewidth [7-10], reduce the frequency chirping [11].

In addition to the above-mentioned improvements of laser properties, such injection locking technique also offers several optical signal processing functions in coherent telecommunications such as wavelength conversion [12], signal regeneration [13-16], data-format conversion [17], fast optical switching [18], and optical buffering [19].

3.2.1 Regenerative Amplification

Injection locking, as its name imply, is to inject a weak signal into a more powerful free-running oscillator that can produce an interesting and useful effects. The injected signal can then capture or lock the subsequent oscillator behavior, so that the oscillator is more or less completely controlled by the injected signal. To qualitatively describe this phenomenon in a simple fashion, a simple model of laser as a regeneratively amplifying interferometer cavity is employed. Figure 3.1 shows the conceptual model of ring laser oscillator with simultaneous injected and free-running signals [20]. A laser oscillator is initially oscillating at a free-running oscillation frequency ω_0 and producing coherent output intensity I_0 at that frequency. Suppose now that a weak external signal is injected into this laser oscillator via some suitable coupling method, at a frequency ω_1 which is close to but not exactly coincident with the free-running oscillation frequency ω_0 of the laser. As shown in Fig. 3.1, an optical field E_i is injected into the laser cavity with optical field E_c through an input mirror, and has the following self-consistent relationship [20]:

$$E_c = E_c\widetilde{G}_{rt}(\omega) + tE_i \qquad (3.1)$$

where the total E_c is sum of the amplified E_c plus a effectively injected field E_i. $\widetilde{G}_{rt}(\omega)$ is the net complex round-trip field gain inside the laser cavity:

$$\widetilde{G}_{rt}(\omega) \equiv G_{rt}(\omega)e^{[-i\phi(\omega)]} \qquad (3.2)$$

where $G_{rt}(\omega)$ is the gain magnitude including laser gain α_m, internal loss a, and $\phi(\omega)$ is the

round-trip phase shift. Therefore, the overall regenerative field gain from input to output, which is defined by the ratio of the transmitted field over the injected one, can be written in the form:

$$\widetilde{g}_{reg}(\omega) \equiv \frac{E_t}{E_i} = \frac{tE_c}{E_i} = \frac{t^2}{1 - \widetilde{G}_{rt}(\omega)} = \frac{T}{1 - G_{rt}(\omega)\cos\phi(\omega) + iG_{rt}(\omega)\sin\phi(\omega)} \quad (3.3)$$

where t is the transmission coefficient of the input mirror, and $T = t^2$ is the transmittance. There exists a highly regenerative limit when $G_{rt}(\omega)$ approaches 1 and the overall regenerative gain near any axial-mode frequency ω_0 would simplify to the form

$$\widetilde{g}_{reg}(\omega) \approx \frac{T}{1 - G_{rt} + iG_{rt}t_{rt}(\omega - \omega_0)} \quad (3.4)$$

where t_{rt} is the transit time for one round trip inside the cavity. That is, if the net round-trip magnitude $G_{rt}(\omega)$ inside the laser cavity rises to be exactly unity at free-running oscillation frequency, an oscillation threshold would occur. Such oscillation threshold would thus correspond to the point where the overall regenerative gain goes to infinity for an externally injected signal tuned exactly to the oscillation frequency of the laser. Therefore, a laser injection locking is achieved.

Actually, the $G_{rt}(\omega)$ would be clamped at the value of unity, which means that the overall regenerative gain for an externally applied signal at any other frequency away from the resonance frequency is still finite and limited as illustrated in Fig. 3.2. The regenerative power gain has the form

$$\left|\widetilde{g}_{reg}(\omega)\right|^2 \approx \left|\frac{T}{iG_{rt}t_{rt}(\omega - \omega_0)}\right|^2 = \frac{r_e^2}{(\omega - \omega_0)^2} \quad (3.5)$$

where r_e is the external decay rate defined by T/t_{rt}. Therefore, more or less exactly a this point, on either side of the free-running frequency ω_0, the amplified signal begin to steal enough gain from the laser medium, or begin to saturate the laser gain down, that the free-running

laser oscillation at ω_0 will be turned off or goes out, leaving only the injected signal at ω_1. However, the amplified output power at the injected frequency ω_1 will no longer continue to rise as ω_1 is tuned further inside this range, since the amplifying medium α_m inside the oscillator just can not supply enough power. Instead, the amplified output at ω_1 will be limited to the free-running oscillation intensity I_0, or slightly above this to account for the additional signal power that is being injected. For an injected signal tuned outside this locking point, therefore, the laser output consists of the strong free-running oscillation with intensity I_0, plus the weaker amplified intensity at the injected signal frequency ω_1. Inside the locking range, however, the output of the oscillator will consist entirely of the regeneratively amplified but amplitude-limited signal at ω_1.

3.2.2 Injection Locking Bandwidth

In 1991, the static and dynamic injection locking ranges of a distributed feedback (DFB) semiconductor laser was first investigated by R. Hui [21]. The reason why a DFB laser was employed is because the common Fabry-Perot laser has mode hopping effect among different longitudinal modes, and injection locking phenomenon in some phase conditions are difficult to observe.

A theoretical model, which consisted of a well-known single mode Van der Pol equation and a carrier density rate equation, was presented including a nonlinear gain saturation term to stabilize the injection locking [21]:

$$\frac{d\beta(t)}{dt} = \left[-i\omega + \frac{1-i\alpha}{2} G_N (N - N_0) + \frac{1}{2} G_I |\beta(t)|^2 \right] \cdot \beta(t) + \frac{1}{\tau_i} \beta_1(t) \tag{3.6}$$

$$\frac{dN(t)}{dt} = C(t) - \frac{N(t)}{\tau_s} - G|\beta(t)|^2 \tag{3.7}$$

where $\beta(t) = I^{1/2} exp[-i(\omega_1 t - \phi)]$ is the normalized electric field of the slave laser (SL) inside the

laser cavity, and $\beta_1(t) = I_1^{1/2} exp[-i\omega_1 t]$ is that coupled into the SL cavity from master laser

(ML); I and I_1 are the field intensity of SL, and that coupled from ML; G is the material gain;

G_N and G_I are the derivatives of G with respect to N and I; ω_0 is the modal frequency of the

slave cavity; ω_1 is the frequency of ML; $N(t)$ is the carrier density; N_0 is the threshold carrier

density; $C(t)$ is the carrier injection rate; ϕ is the phase difference between SL and ML; and τ_s

and τ_i are the spontaneous lifetime of minority carriers and the group round-trip time of SL,

respectively.

If the slave laser is stable locked, the stationary solution from Eq. (3.6) and (3.7) will be

$$\Delta G = -2\rho\cos\phi \tag{3.8}$$

$$\Delta\omega = \rho(\sin\phi - \alpha\cos\phi) \tag{3.9}$$

where $\Delta\omega = \omega_1 - \omega_0$ is the frequency detuning; $\Delta G = G_N\Delta N + G_I\Delta I$, ΔI and ΔN being the

deviations of carrier density and photon density from their free running values; and $\rho = (I_1/I)^{1/2}/\tau_i$ is the normalized optical injection level [6, 20]. Therefore, the static limit of the

injection locking range, as shown in Fig. 3.3, is determined from (3.9) by $\Delta\omega \leq \rho(1+\alpha^2)^{1/2}$,

and corresponding phase tuning range values from $\tan^{-1}(\alpha) - \pi/2$ to $\tan^{-1}(\alpha) + \pi/2$. However,

they further found that all the points inside this static range are not surely stable due to the

intrinsic laser property: relaxation oscillation.

Therefore, the small-signal analysis is provided by linearizing (3.6) and (3.7) in terms of

small deviations around the equilibrium values, that is, $I(t) = I + \delta I(t)$, $\varphi(t) = \varphi + \delta\varphi(t)$, $N(t) = N + \delta N(t)$, $C(t) = C + \delta C(t)$. The small-signal equations are

$$\frac{d\delta I}{dt} = \left(G_I - \frac{R}{I} - \rho\cos\phi\right)\delta I - 2\rho\, I\sin\phi\, \delta\phi + G_N I\delta N \tag{3.9}$$

$$\frac{d\delta\phi}{dt} = \frac{\rho\sin\phi}{2I}\delta I - \rho\cos\phi\, \delta\phi - \frac{\alpha\, G_N}{2}\delta N \tag{3.10}$$

$$\frac{d\delta N}{dt} = -G\delta I - \left(G_N I + \frac{1}{\tau_s}\right)\delta N + \delta C \tag{3.11}$$

It is reasonable that a stable injection locking will be achieved if the system, with slight perturbations of δI, δN, and $\delta\phi$, returns to its equilibrium state through a damped relaxation oscillation. Therefore, following the standard treatment as in [6], the Fourier transformation and Routh-Herqitz criterion were applied to above equation to obtain the damping time of the relaxation oscillation in the following form:

$$\frac{1}{\tau_R} = \frac{1}{\tau_s} + (G_N - G_I)I + \frac{R}{I} + \rho(\sin\phi - \alpha\cos\phi) \tag{3.12}$$

As a result, the dynamic limit of injection locking range is defined by the curve $\tau_R = 0$ illustrated in Fig 3.3. Four different regimes are thus distinguished as a function of injection power ratio: (A) a symmetrical stable locking band; (B) two stable locking bands for positive and negative values of frequency detuning separated by an unstable region; (C) stable locking only for negative values of detuning; and (D) a bistable region [22-24].
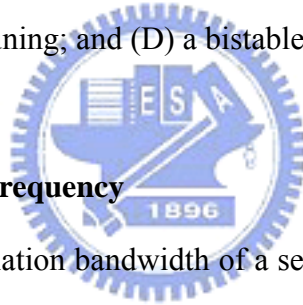
3.2.3 Relaxation Oscillation Frequency

It is known that the modulation bandwidth of a semiconductor laser is proportional to its relaxation oscillation frequency given by the following form [25]:

$$f_r = \frac{1}{2\pi}\sqrt{\upsilon g'\frac{S_0}{\tau_p} - \frac{1}{2}\left(\frac{1}{\tau_s} + \upsilon g' S_0\right)^2} \tag{3.13}$$

where τ_p is the average photon life time in the laser cavity, υ is the group velocity of light, and S_0 is the photon density in steady state which is proportional to $|\beta(t)|^2$. In fact, the second term in (3.13) is relatively small and negligible. Apparently, in order to enhance the relaxation oscillation frequency, we have two choices: reducing the photon life time τ_p, and increasing the photon density S_0. Reducing the photon life time can be achieved by reducing the length of laser active medium and lowering the reflectivity of the end facet. And from above analysis, we know that the injection locking is a useful technique to increase the photon density S_0 in

the laser cavity by stimulated emission, and the relaxation oscillation frequency can thus be effectively enhanced. In addition, the damping time will also be highly reduced as the injection level increase. Therefore, fast signal processing using a stably injection locked semiconductor laser is promising and can be highly expected.

3.2.4 Applications on All-Optical Signal Processing

Semiconductor-based nonlinear element plays an important role in all-optical signal processing. For example, a semiconductor optical amplifier can be used as optical switches and wavelength converters by employing the cross-gain modulation effect, four-wave mixing effect, or the cross-phase modulation effect. Recently, in addition to semiconductor amplifiers, semiconductor lasers have also been viewed as promising candidate for high-speed all-optical signal processing. In that case, the output light, generated within the semiconductor laser, is controlled by the input light via the thresholding effect of injection locking or cross-gain compression. Moreover, the injection-locked laser also can be used for the signal retiming and amplitude regeneration.

Throughout this thesis, we emphasize the all-optical 2R (reamplification and reshaping) regenerating function provided by a cost-effective injection-locked semiconductor laser. Injection-locking is to inject optical power from a master into a slave laser through an optical isolator. If the frequencies of both lasers are within a well-defined range called the locking range, the slave laser is locked to the master laser's frequency as the above analysis. The locking range is determined by the relative injection level and the amplitude-phase coupling coefficient. Figure 3.4 shows the diagram of all-optical 2R regeneration using a injection-locked semiconductor laser. As shown is Fig. 3.4, there exists an injection locking threshold power which can used to judge whether the slave laser is in the locked or unlocked states, and the injection locked slave laser like an binary amplitude quantizer can provide a

step-like transfer function for the signal from master laser. Such thresholding nature and cross-gain compression effect make the injection-locked semiconductor laser a promising device for high-speed all-optical amplitude and waveform regeneration.

3.3 All-Optical 2R Regeneration Using Conventional Injection Locking Techniques

3.3.1 Main-Mode Injection Locking (MMIL)

The concept model of all-optical 2R regeneration using a main-mode injection locked semiconductor laser is illustrated in Fig. 3.5. A distorted signal S_{in} at the center frequency of f_l is injected into a slave laser diode whose free-running lasing frequency is f_{main}. Main-mode Injection locking is achieved when the signal frequency f_l fall within the locking range of the main mode of the slave laser at frequency f_{main}. There exists an injection-locking threshold power between stably locked state and unlocked state. When the injection light power of distorted signal exceeds the threshold power, the slave LD is injection-locked by signal S_{in} and begins to operate at f_l. Another part of signal S_{in} will experience loss in the unlocked state. Therefore, the slave laser is alternatively locked and unlocked by the signal S_{in}. After band-pass filtering, a reshaped signal can be obtained.

In order to test the reshaping ability, in Fig. 3.6, we demonstrated the regeneration waveform of a 100 MHz sinusoidal wave by main mode injection locking technique. A rectangular-like reshaped waveform can be obtained. However, in case of main-mode injection locking, two frequencies f_l and f_{main} are very close, and optical filtering is quite difficult because of close frequency separation (~10 GHz). In addition, the low relaxation oscillation frequency limited the speed of regeneration.

3.3.2 Side-Mode Injection Locking (SMIL)

Figure 3.7 shows the concept model of side-mode injection locking of a semiconductor laser diode for all-optical 2R regeneration. The signal S_{in} at frequency f_I is injected at one side mode of the laser diode rather than the main mode. The free-running side mode is defined as the 0th mode, and the injected side mode is as the mth mode. The mode number m is positive at the higher frequency side from the main mode. Like the mechanism of MMIL 2R technique, the slave LD will be enforced to operate at the side mode if the injected signal power exceeds an injection-locking threshold. Compared with the conventional MMIL, the master and slave laser frequencies can be easily separated by an optical bandpass filter. It is evident that the injection-locking bandwidth and the relaxation oscillation frequency are related to the injection power and the wavelength of the target mode, and are enhanced for positive m [12, 15].
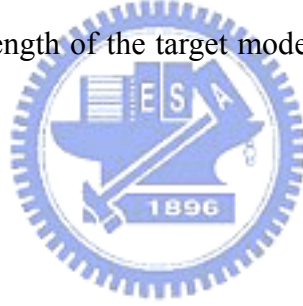
3.3.2.1 Theoretical Model

In order to investigate behavior of the SMIL 2R technique, we follow the theoretical model presented by A. Kuramoto [16]. Four multimode rate equations: two photon equation, one carrier equation, and one phase equation, are shown below

$$\frac{dP_{peak}}{dt} = G_N \cdot \delta n \cdot P_{peak} + C_{sp\text{-}peak} \cdot C_{th} + G_I \cdot P_{Peak}^{3/2} \qquad (3.14)$$

$$\frac{dP_{side}}{dt} = (G_{side} + G_N \cdot \delta n - G)P_{side} + C_{sp\text{-}side} \cdot C_{th}$$
$$+ G_I \cdot P_{side}^{3/2} + \frac{2\sqrt{P_{in} \cdot P_{side}} \cdot \cos\phi_{side}}{\tau_i} \qquad (3.15)$$

$$\frac{d\phi_{side}}{dt} = -p(v - \omega_{th}) + \frac{1}{2}\alpha \cdot G_N \cdot \delta n - \sqrt{\frac{P_{in}}{P_{side}}} \cdot \frac{\sin\phi_{side}}{\tau_i} \qquad (3.16)$$

$$\frac{d\delta n}{dt} = -\{(G + G_N \cdot \delta n)P_{peak} + (G_{side} + G_N \cdot \delta n)P_{side}\}$$
$$+ (C - C_{th}) - \frac{\delta n}{\tau_s} \qquad (3.17)$$

where P_{peak}, P_{side} and P_{in} are the field intensities of the peak (main) mode, of the side (target) mode of the slave LD, and of the input signal, respectively. ϕ_{side} represents the phase difference between the side mode and the input signal, and δn is the deviations of the carrier numbers around the threshold values. G and G_{side} are the temporal gain of the peak and side modes, respectively, and G_N and G_I are the derivatives of G, with respect to carrier numbers and field density, respectively. p is the ratio of the effective mode index to the effective group index. ν and ω_{th} are the angular frequencies of the input signal and the side mode. α is the linewidth broadening factor for the side mode. τ_s is the carrier lifetime and τ_i is the photon lifetime of the save LD. C is the carrier injection rate and C_{th} is that at the lasing threshold. $C_{sp\text{-}peak}$ and $C_{sp\text{-}side}$ are the spontaneous emission rates of the peak and side modes, respectively.

In eq. (3.14), the first and third terms represent increasing rate of the number of photons per unit volume due to stimulated emissions, and the second term reveals the fraction of spontaneous emission entering the lasing mode at the lasing threshold, which is generally very small. In addition, nonlinear gain suppression effects, which may occur at high pumping currents or at high optical injection, are also taken into account by incorporating a photon-density-dependent term G_I in the gain function. In eq. (3.15), the fourth term on the right hand side represents the external light injection at side mode. Without this term, eq. (3.15) is identical to any coherent model of main-mode injection locking like eq. (3.14). However, the magnitude of that term can be much larger for side-mode injection, due to the nature of the gain-curve roll off. It is assumed that the gain function varies linearly with carrier density and parabolically with the wavelength difference between the main and the target modes. Equation (3.16) is the phase equation which displays that the phase difference between the side mode and injection signal can be controlled by the ratio of the field intensity of injection signal to that of the side mode. Therefore, side mode injection locking can be

governed the intensity of input signal as well as the accompanying phase change. The carrier-density-dependent refractive index is included in the linewidth broadening factor, which indicates the spectrum linewidth enhancement due to the coupling between the amplitude and phase fluctuation of the optical field. Finally, in eq. (3.17), the first and second terms represent the carrier loss due to the stimulated emission, the third term is the carrier increase by current injection, and the last term indicates the carrier loss via the carrier recombination.

3.3.2.2 Testing Results

In Fig. 3.8, we demonstrate the injected and regenerated waveforms at 625 MHz for different mode number. When m=2, the regenerated signal had some relaxation oscillation effect at its rising edge. However, when m=10, the regenerated signal was clear. Therefore, the relaxation oscillation can be suppressed if the injection mode number is large, which is totally consistent with both the simulation and experimental results in [16].
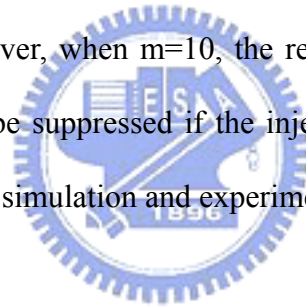
3.3.3 Two-Mode Injection Locking (TMIL)

In order to highly suppress the relaxation oscillation, another CW light (probe laser) was injected at another side mode of the slave LD. The CW light can generate a large number of photon densities by stimulated emission, and thus effectively increase the relaxation oscillation frequency and enhance the modulation bandwidth. Figure 3.9 shows the diagram of two-mode injection locking of a semiconductor laser diode for all-optical 2R regeneration. The signal frequency f_1 and the CW probe frequency f_2 are respectively set to match one of the side modes of the slave LD, separated from the free-running frequency f_{main}. Without the injection signal, the slave LD is initially injection-locked by the probe laser and operates at f_2. When the signal is injected and has a peak power exceeds the injection-locking threshold, the

slave LD will be injection-locked by injection signal and begins to operate at f_1. Thus, owing to the thresholding nature of the injection locking mechanism and cross-gain compression effect, the slave LD will alternatively be injection-locked by the injection signal at f_1 and probe laser at f_2, and thus the distorted and noisy intensity-modulated signal can be converted into a regenerated and noise-suppressed frequency-modulated signal. By using a BPF to filter out f_2, a regenerated intensity-modulated signal with noise suppression over zeros and ones can be obtained.

3.3.3.1 Theoretical Model

In order to investigate the behavior of the TMIL 2R technique, we follow the theoretical model presented by A. Kuramoto [16], which uses the Van der Pol equations and rate equations of the carrier number and photon number in the salve LD, as shown below

$$\frac{d\beta_k}{dt} = \left[-ip \cdot \Delta\omega_k + \frac{1-i\alpha}{2} G_N \cdot \delta n + \frac{1}{2} G_I |\beta_k|^2 \right] \cdot \beta_k + \frac{1}{\tau_i} \beta_k^{\ in} \tag{3.18}$$

$$\frac{d\delta n}{dt} = (C - C_{th}) - \frac{\delta n}{\tau_s} - (G + G_N \cdot \delta n) \times (|\beta_1|^2 + |\beta_2|^2 + P_{peak}) \tag{3.19}$$

$$\frac{dP_{peak}}{dt} = G_N \cdot \delta n \cdot P_{peak} + C_{sp\text{-}peak} \cdot C_{th} + G_I \cdot P_{peak}^{\ 3/2} \tag{3.20}$$

where $k = 1$ denotes the signal mode, $k = 2$ represent the probe mode, and superscript "*in*" stands for the input signal. β_k is the slowly varying field envelope of the locked mode, $\beta_k^{\ in}$ is the injected field, and other symbols are in common with (3.14)–(3.17).

Figure 3.10 shows the diagram of the theoretical model for a semiconductor laser with external light injection. Because the slave LD is injection-locked by an additional external light, the dynamics of the injected modes can not be described alone by the photon rate equation, and field differential equation should be included. The so-called Van der Pol equation is a model of an electronic circuit that appeared around 1920 in the vacuum tubes of a triode electronic oscillator in very early radios. The main feature is that electrical circuits

that contain these elements pump up small oscillations due to a negative resistance when currents are small, but drag down large amplitude oscillations due to positive resistance when the currents are large. Such behavior is known as a relaxation oscillation. Therefore, the dynamic of the optical fields in the TMIL slave LD can be well described by eq. (3.18), which is the Van Der Pol equation for both the signal and probe modes, and can be viewed as a stiff type ordinary differential equation (ODE). In eq. (3.18), $1/\tau_i$ is the proportionality constant, and stands for the time interval at which the injected field adds β_k^{in} to the amplitude of the propagating field β_k every time it hits the irradiated facet. Equation (3.19) defines the rate of carrier deviation. The field intensity at the probe mode β_2 will change with the amplitude variation of the injected signal field β_1 due to the gain change in the second term of eq. (3.18), which is closely related with eq. (3.19). In addition, the term P_{peak} is quite small and negligible since the slave LD is injection-locked by either the injected signal or the external probe laser during the whole time.
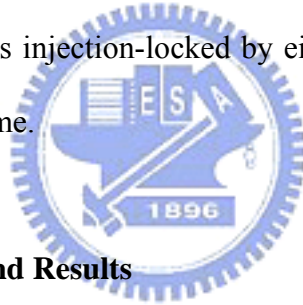
3.3.3.2 Experimental Setup and Results

The experimental setup for the conventional all-optical 2R regeneration using TMIL is illustrated in Fig. 3.11. A probe light source at 1556.8 nm was injected into the slave Fabry-Perot laser diode (FP-LD) at the mode number of 12. The FP-LD was bias at 40.8mA and 23.22^{o}C. Then, a 1.25 GHz sinusoidal wave was injected into the +10 mode of FP-LD with an average peak power of –4.12 dBm. Figure 3.12(a) shows the optical spectra of the TMIL FP-LD, and both the waveforms of the regenerated signal and the input distorted signal are illustrated in Fig 3.12(b). Obviously, a rectangular-like regenerated waveform can be obtained by using the TMIL 2R technique.

3.3.3.3 Operating Ranges

To have a better knowledge of the TMIL semiconductor laser, the operating ranges for this 2R device should be identified. We investigated the relationship between the wavelength range of the injection signal and mode number of probe laser, and also observed the input dynamic ranges at different injection modes.

In Fig 3.13, the power of the probe laser was kept at -6 dBm, and we observe the range of signal mode as a function of the probe modes when all-optical 2R regeneration was achieved. The bias current of FP-LD was 26 mA. The injection signals was a 625 MHz sinusoidal waves with different injection powers at different modes to achieve waveform reshaping. As shown is Fig. 3.13, the signal mode ranges from -10 to +12 for each probe mode, which means, at the data rate of 625 MHz, the operation range of signal mode is independent of the chosen probe mode number. The corresponding input and output waveforms are illustrated in Fig. 3.14. Figure 3.15 shows the testing results with the same condition in Fig. 3.13 except for the decrease bias current of 16 mA. As shown in Fig. 3.15, the range of signal mode will be a little wider since injection locking threshold power was reduced, and a fixed injection power can lock the mode with larger mode number. The corresponding input and output waveforms are illustrated in Fig. 3.16.

In addition, Figure 3.17 depicts the power dynamic range of the injection signal at different mode when the probe mode number is 0, and all-optical 2R regeneration is achieved as well. As displayed in Fig 3.17, the injection power level is lower around the probe mode, and will be higher as the mode number increase. Moreover, a narrower dynamic range can be observed at +12 mode due to the deficit of a high injection power for far side mode injection locking. The corresponding regenerated waveforms for max and min input signals at different signal modes are illustrated in Fig. 3.18. Moreover, the same measurement was performed when the probe mode number changed to +8. Figure 3.19 shows the same trend as Fig 3.17, that is, the power level is still low around mode number 0 and the dynamic range is small with

large injection mode number. Moreover, the dynamic ranges at different mode in Fig. 3.19 is larger than those in Fig 3.17. The corresponding regenerated waveforms for max and min input signals at -4 and +12 signal modes are illustrated in Fig. 3.20.

In Table 3.1, we compare three types of semiconductor-laser-based 2R techniques: MMIL, SMIL, and TMIL. Only the MMIL needs narrow-band filtering, which is not easy to execute. As the injection mode number increase, modulation bandwidth and the relaxation oscillation frequency could be the improved in SMIL technique, and could be highly enhanced by introducing an external probe laser in the TMIL technique. However, such additional light sources at each 2R regeneration stage will make the entire optical communication system more complex and expensive.

3.4 All-Optical 2R Regeneration Using New TMIL Techniques

In last section, we concluded that the most promising candidate for high-speed semiconductor-laser-based all-optical 2R regeneration is two-mode injection locking (TMIL). However, some disadvantages of the conventional TMIL method, such as increasing the system complex by introducing additional outside probe light sources, should be improved before being used for future field deployment. Therefore, based on the conventional TMIL technique, we proposed four new TMIL schemes to execute all-optical 2R regeneration up to 10 Gb/s in a simple and effective fashion.

3.4.1 Simplified TMIL Technique without External Probe Lasers

The characteristic of this simplified TMIL 2R technique is to create a compound cavity of a semiconductor laser. An optical feedback light can be automatically generated to injection-locked the semiconductor laser, and the external probe light sources used in

conventional scheme are not required. Therefore, to the best of our knowledge, a compact self-seeded Fabry-Pérot laser diode (SSFP-LD) with a 10mm-long embedded fiber Bragg grating cavity was fabricated and proposed for the first time to execute all-optical 2R regeneration up to 10 Gb/s, and experimentally compared with the performance of the traditional TMIL scheme. The proposed self-seeded semiconductor laser is expected to have equivalent BER performance as the traditional TMIL one, which will be demonstrated in the next chapter.

On the other hand, in formal TMIL scheme, EDFAs are indispensable, and are usually placed at the input and output ports of a TMIL semiconductor laser to provide high power level for side-mode injection locking and compensate the signal loss after waveform reshaping, respectively. In addition, optical bandpass filters for ASE reduction of input and output EDFAs are also required. Apparently, the complication and price of entire transmission system will rise with the number of EDFAs and corresponding optical filters at each 2R stages. Therefore, we came up with another idea to present an all-optical 2R regenerator, which combine the compact self-seeded Fabry-Pérot laser diode (SSFP-LD) with a 10mm-long embedded fiber Bragg grating cavity and a bidirectional EDFA with short EDF. The bidirectional EDFA with low pump power can offer proper amplification for both the injected and the regenerated signals, and thus the total number of EDFAs in our system becomes half the conventional one.

3.4.2 Novel Amplifier-Free TMIL Technique

As mentioned above, the reason why the outside EDFAs are needed is mainly because the injected signal requires high peak power for stable side mode injection locking, and signal gain is hardly obtained. Such phenomenon makes neither the proposed self-seeded semiconductor laser nor traditional TMIL one a real 2R regenerator since a qualified 2R

device should provide both reamplifying and reshaping capabilities simultaneously. Therefore, by analyzing the relationship between the injection mode number, signal gain, and regeneration quality, we find that TMIL semiconductor laser will have a good change to become a real 2R device if the signal was injected around the main mode rather than side mode. That is, under this situation, the enhanced relaxation oscillation frequency of the semiconductor laser, primarily contributed by a strong side mode injection of the CW or self-seed lights, is sufficient to cover the whole modulation bandwidth. As a result, we presents an EDFA-free all-optical 2R regeneration scheme based on a compact self-seeded Fabry-Pérot laser diode (SSFP-LD). Device characteristics such as data-rate transparency, input dynamic range, amplified gain, and 2R regeneration performance are investigated experimentally.

On the other hand, based on concept given above, a novel and cost-effective 1.3 μm all-optical 2R regenerator using a two-mode injection-locked distributed feedback laser diode (TMIL DFB-LD) is proposed for simultaneously all-optical reamplification and reshaping in the second window. So far as we know, optical telecommunication using standard single mode fiber experiences large signal loss in 1.3 μm operation window, and there is no suitable amplification technique in this optical spectrum. Therefore, the proposed all-optical 2R regenerator based on TMIL DFB-LD provide a low-cost solution for 1.3 μm amplification. The detail description will given is chapter 5.

References for Chapter 3

[1] G. P. Agrawal, "Suppression of Mode Partition Noise by Laser Diode Light Injection," *IEEE Trans. Microw. Theory Tech.*, vol. 82, pp. 1657-1662, Oct. 1982.

[2] S. E. Miller, "On the injection laser contribution to mode partition noise in fiber telecommunication systems," *IEEE J. Quantum Electron.*, vol. 25, no. 8, pp.1771-1781, Aug. 1989.

[3] J. Wang, M. K. Haldar, L. Li, and F. V. C. Mendis, "Enhancement of modulation bandwidth of laser diodes by injection lcoking," *IEEE Photon. Technol. Lett.*, vol. 8, pp. 34-36, Jan. 1996.

[4] T. B. Simpson, J. M. Liu, and A. Gavrielides "Bandwidth enhancement and broadband noise reduction in injection-locked semiconductor laser," *IEEE Photon. Technol. Lett.*, vol. 7, pp. 709-711, Jul. 1995.

[5] J. M. Luo and M.Osinski, "Multimode small-signal analysis of side-mode injection-locked semiconductor laser," *Jpn. J. Appl. Phys.*, vol. 31, No. 6A, pp. 685-688, 1992.

[6] I. Petitbon, P. Gallion, G. Debarge, and C. Chabran, "Locking bandwidth and relaxation oscillations of an injection-locked semiconductor laser," *IEEE J. Quantum Electron.*, vol. 24, pp. 148-154, Feb 1988.

[7] G. P. Agrawal., "Intensity dependence of the linewidth enhancement factor and its implications for semiconductor laser," *IEEE Photon. Technol. Lett.*, vol. 1, pp. 212-214, Aug. 1989.

[8] G. Liu, X. Jin, and S. L. Chuang, "Measurement of linewidth enhancement factor of semiconductor lasers using an injection-locking technique," *IEEE Photon. Technol. Lett.*,

vol. 13, pp. 430-432, May. 2001.

[9] M. P. van Exter and J. P. Woerdman, "Determination of α factor of fabry-perot-type semiconductor laser by injection locking," *Electron. Lett.*, vol. 28, No. 17, pp. 1607-1608, 1992.

[10] R. J. Jones, P. S. Spencer, and K. A. Shore, "Influence of amplitude-phase coupling on the dynamics of semiconductor lasers subject to optical feedback," *Phys. Rev. A*, vol. 60, No. 1, pp. 634-641, 1999.

[11] S. Piazzolla, P. Spano, M. Tamburrini, and F. Bordoni, "Small signal analysis of frequency chirping in injection-locked semiconductor lasers," *IEEE J. Quantum Electron.*, vol. 12, pp. 2219- 2223, Feb 1988.

[12] J. Hörer and E. Patzak, "Large-signal analysis of all-optical wavelength conversion using two-mode injection-locking in semiconductor lasers," *IEEE J. Quantum Electron.*, vol. 33, pp. 596-608, Apr. 1997.

[13] S. Yamashita and D. Matsumoto, "Waveform reshaping based on injection locking of a distributed-feedback semiconductor laser," *IEEE Photon. Technol. Lett.*, vol. 12, pp. 1388-1390, Oct. 2000.

[14] K. Inoue and M. Yoshino, "Bistability and waveform reshaping in a DFB-LD with side-mode light injection," *IEEE Photon. Technol. Lett.*, vol. 7, pp. 164-166, Feb. 1995.

[15] Y. Hong and K. A. Shore, "Locking characteristics of a side-mode injected semiconductor laser," *IEEE J. Quantum Electron.*, vol. 35, pp. 1713-1717, Nov. 1999.

[16] A. Kuramoto and S. Yamashita, "All-optical regeneration using a side-mode injection-locked semiconductor laser," *IEEE J. Select. Topics Quantum Electron.*, vol. 9, pp. 1283-1287, Sept./Oct. 2003.

[17] C. W. Chow, C. S. Wong, H. K. Tsang, "All-optical data format and wavelength conversion in two-wavelength injection-locked slave Fabry-Perot laser diodes," *Electron.*

Lett., vol. 22, No. 11, pp. 2386- 2392, 2004.

[18] K.Weich, E. Patzak, and J. Hörer, "Fast all-optical switching using two-section injection-locked semiconductor lasers," *Electron. Lett.*, vol. 30, pp. 493-494, 1994.

[19] P. C. Ku, C. J. Chang-Hasnain, S. L. Chuang, "Variable semiconductor all-optical buffer," *Electron. Lett.*, vol. 38, pp. 1581- 1583, 2002.

[20] A. E. Siegman, *Lasers*, University Science Books, Mill Valley, CA, 1986

[21] R. Hui, A. D'Ottavi, A. Mecozzi, and P. Spano, "Injection locking in distributed feedback semiconductor lasers," *IEEE J. Quantum Electron.*, vol. 27, pp. 1688-1695, Jun 1991.

[22] R. Hui, S. Benedetto, and I. Montrosset, "Optical bistability in diode-laser amplifiers and injection-locked laser diodes," *Electron. Lett.*, vol. 18, No. 4, pp. 287-289, 1993.

[23] R. Hui, "Static and dynamical properties of dispersive optical bistability in semiconductor laser," *IEEE J. lightwave Technol.*, vol. 13, No. 1, pp. 42-48, 1995.

[24] R. Hui, A. Paradisi, S. Benedetto, and I. Montrosset, "Dynamics of optically switched bistable laser diodes in the injection-locked state," *Optics. Lett.*, vol. 18, No. 20, pp. 1733-1735, 1993.

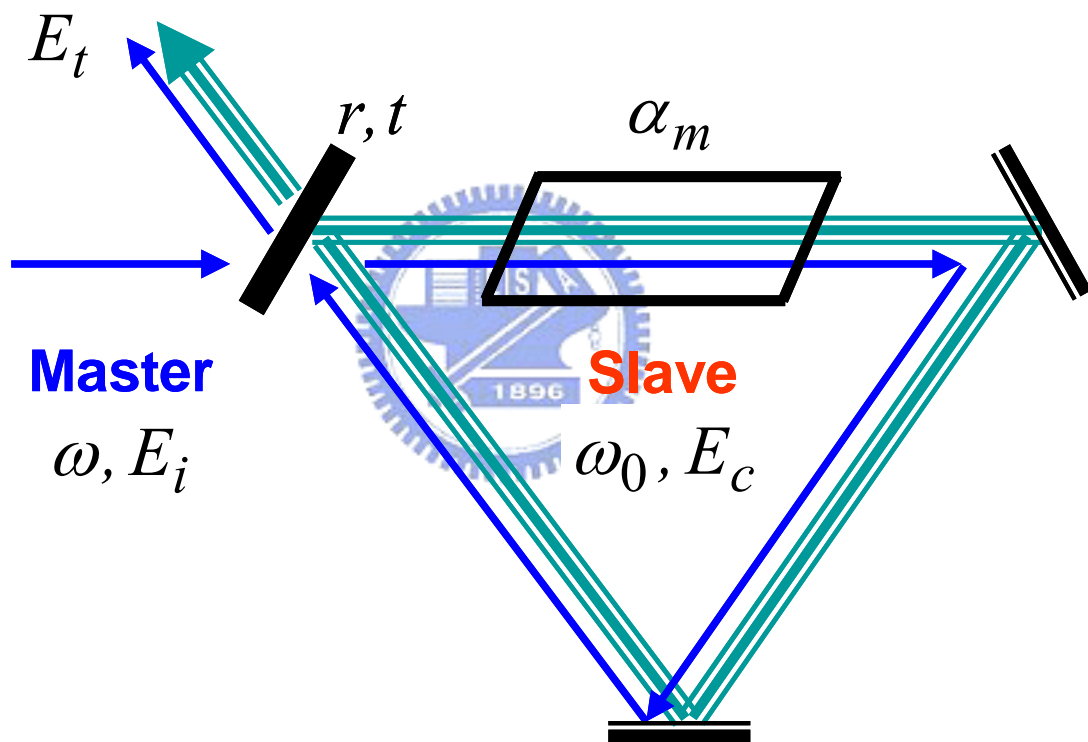[25] S. L. Chuang, *Physics of Optoelectronics Devices* New York: Wiley, 1995.

Fig. 3.1 Conceptual model of ring laser oscillator with simultaneous injected and free-running signals
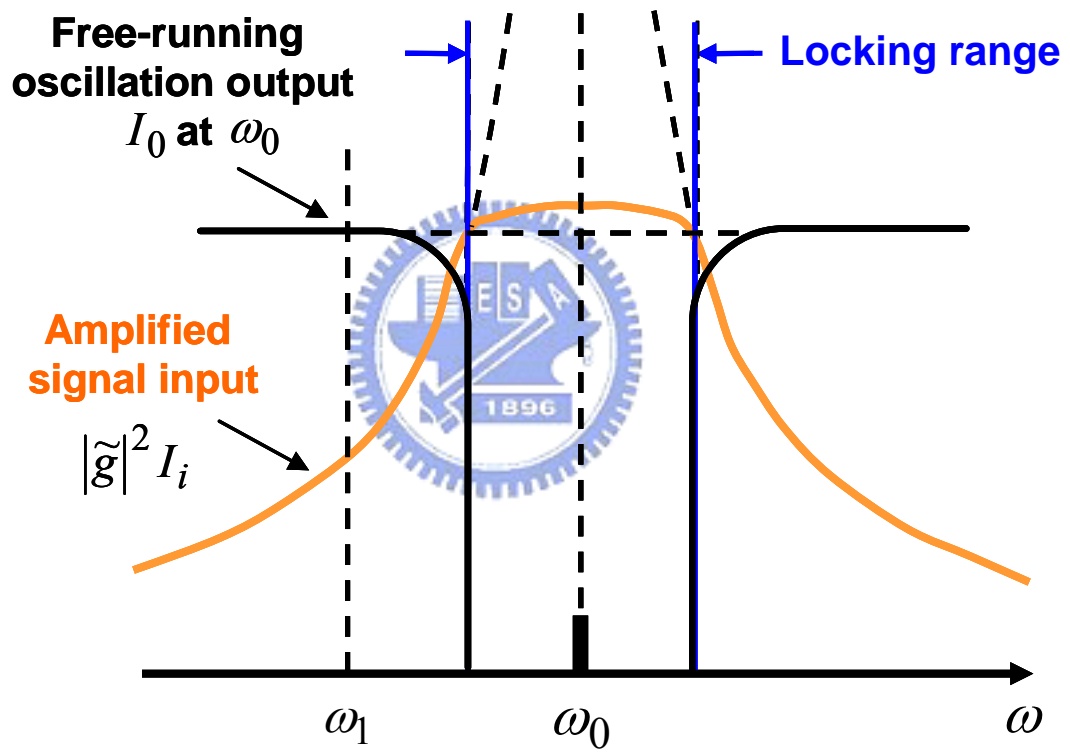
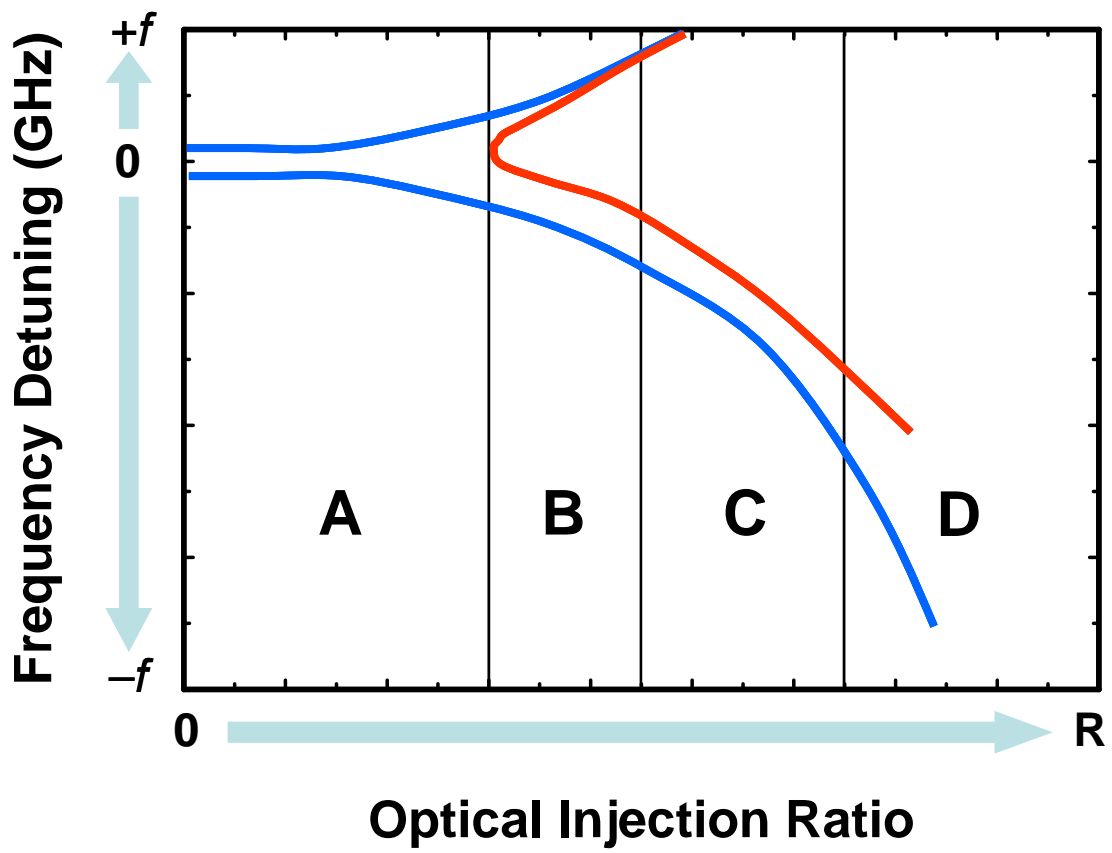**Fig. 3.2** Suppression of free-running oscillation by injection locking

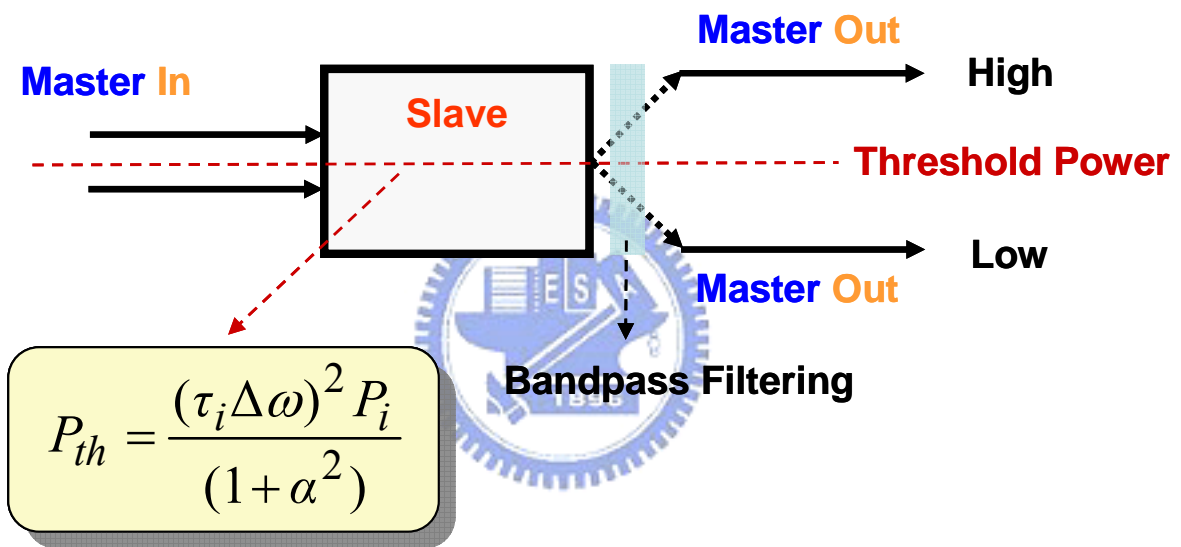**Fig. 3.3** Locking bandwidth against optical injection power ratio

Fig. 3.4 Diagram of an injection-locked semiconductor laser as a binary

amplitude quantizer for all-optical 2R regeneration.

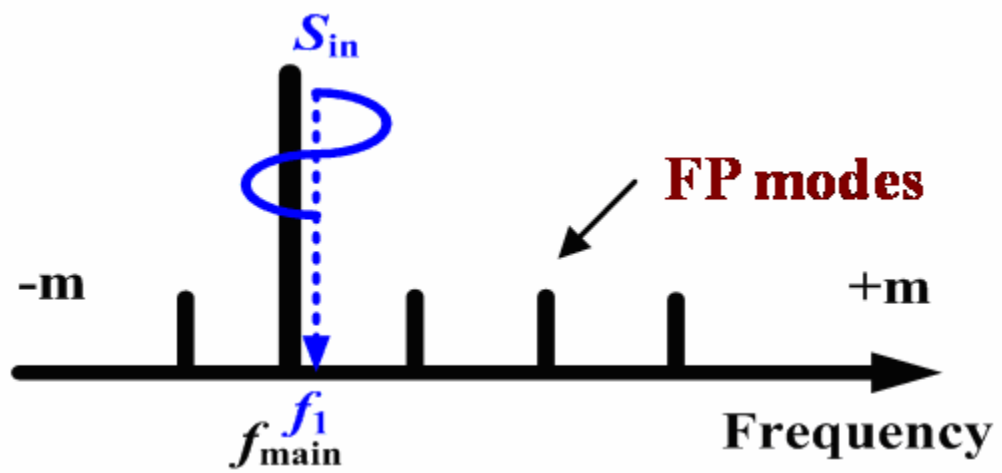**Fig. 3.5** Conceptual diagram of the main-mode injection locking technique.
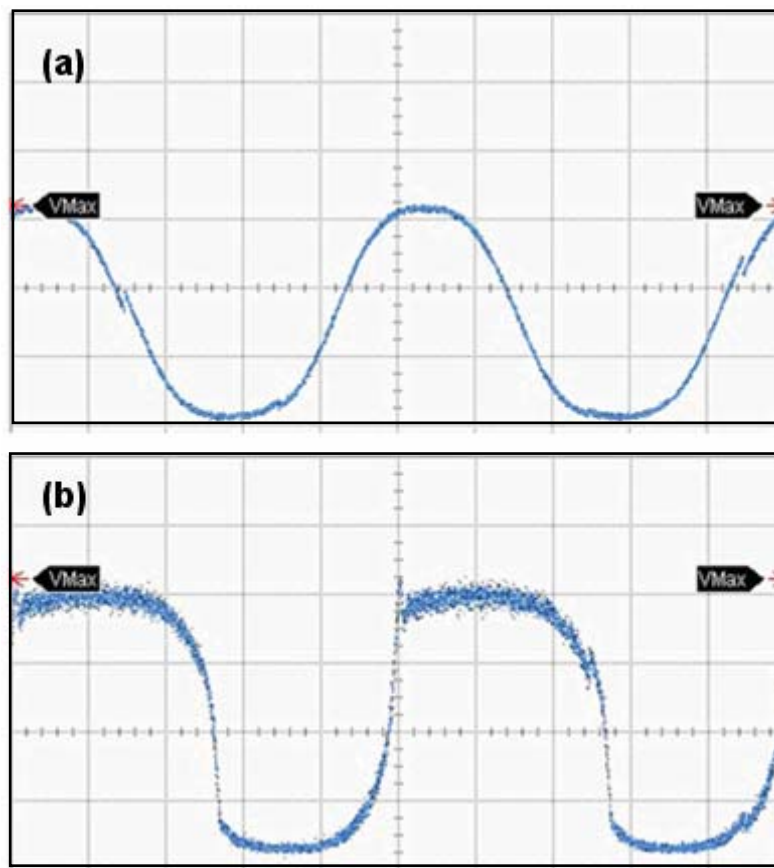
Fig. 3.6 (a) the input sinusoidal wave and (b) the regenerated signal at 100 MHz.
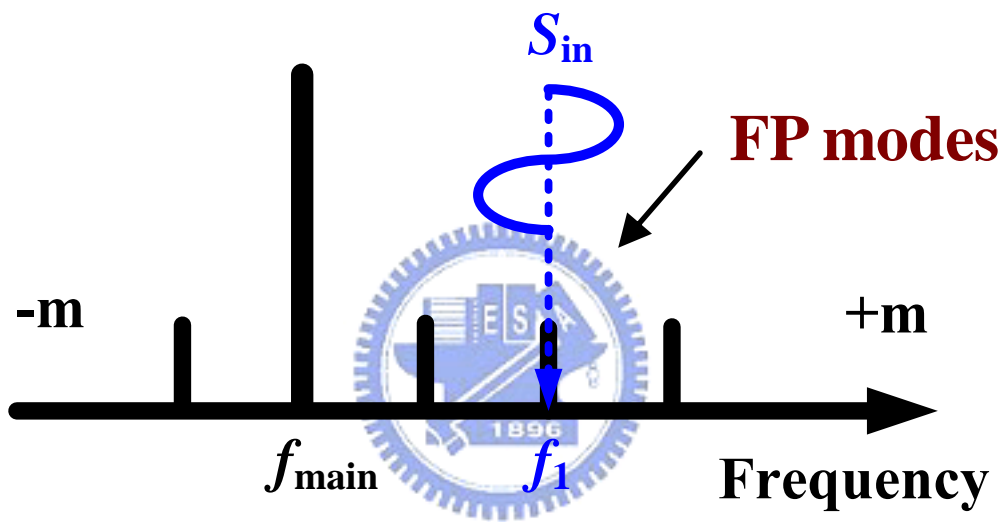
Fig. 3.7 Conceptual diagram of the side-mode injection locking technique.
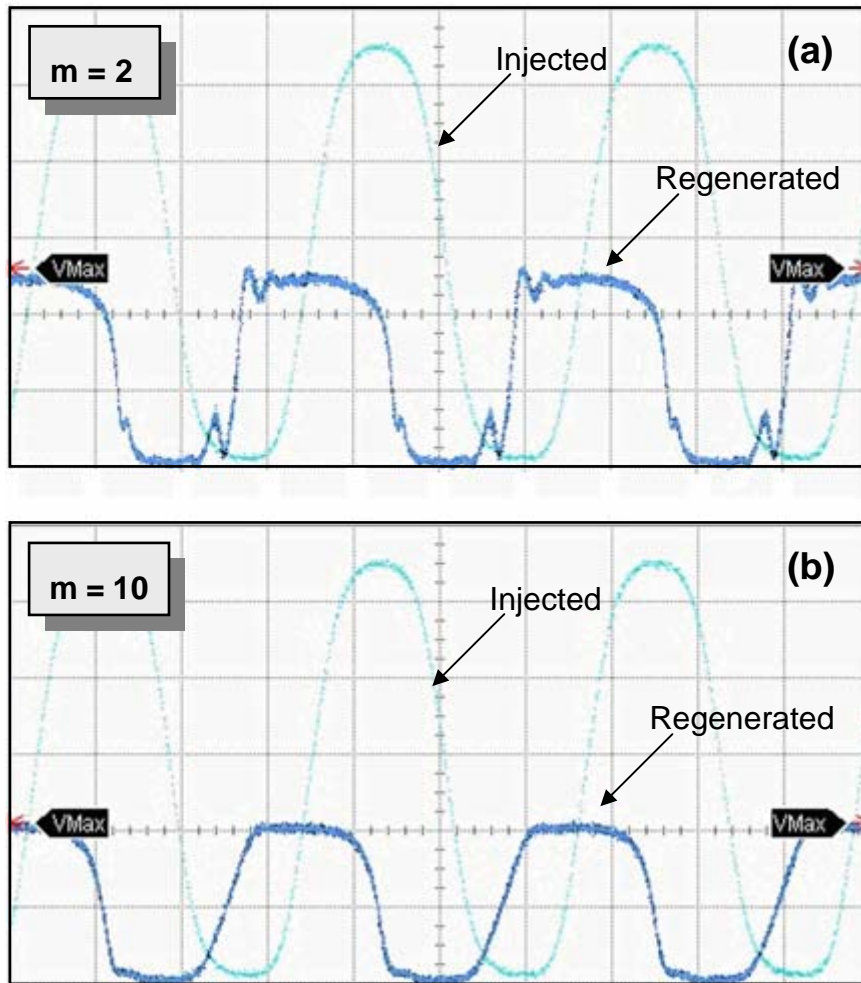
Fig. 3.8 The injected and regenerated waveforms at 625 MHz for mode number (a) m=2 and (b) m=10.
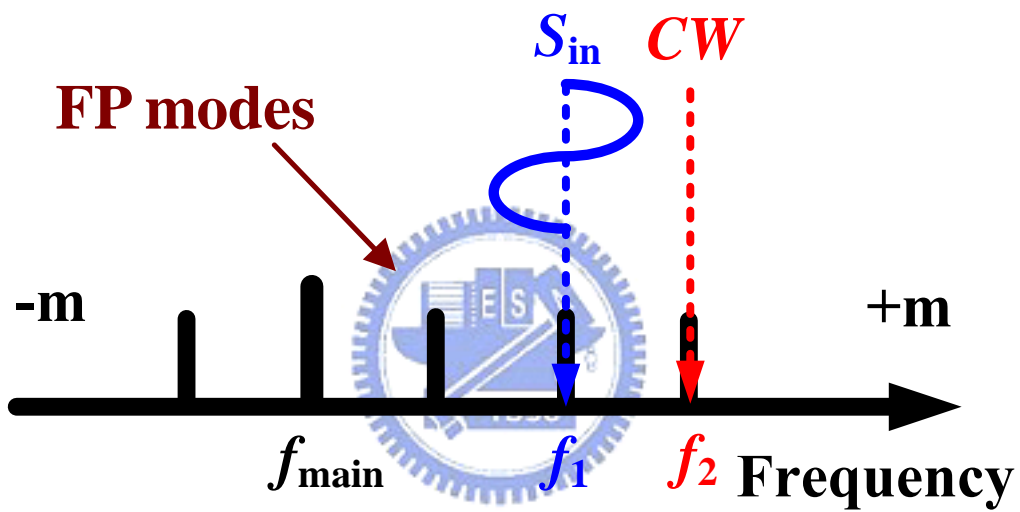
Fig. 3.9 Conceptual diagram of the two-mode injection locking technique
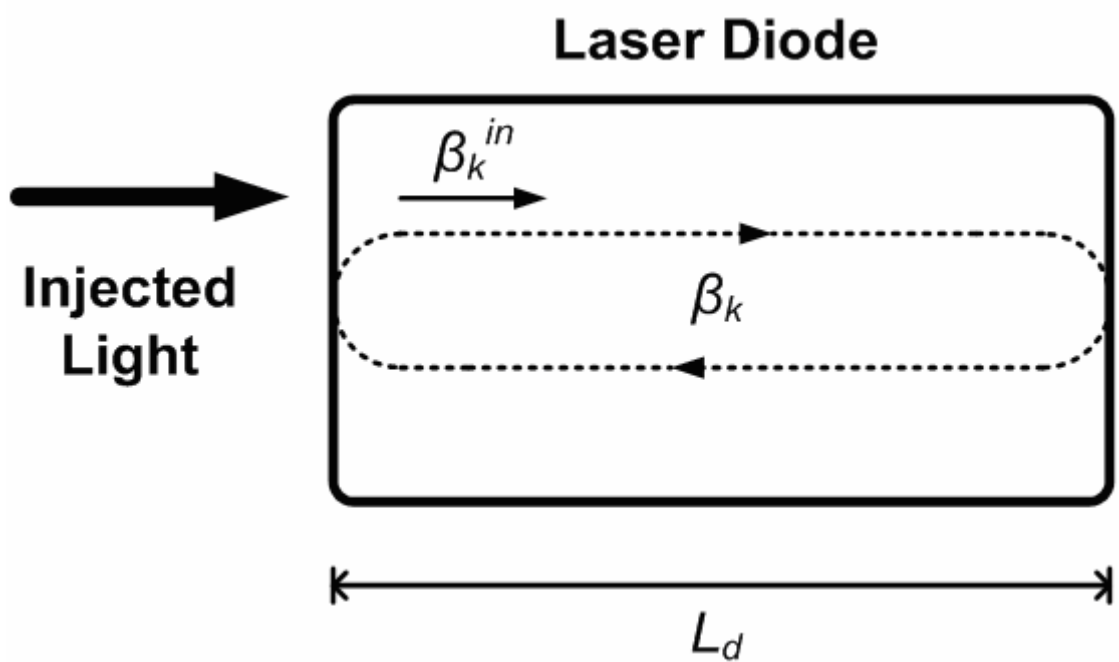
Fig. 3.10 Diagram of the theoretical model for a semiconductor laser with external light injection.
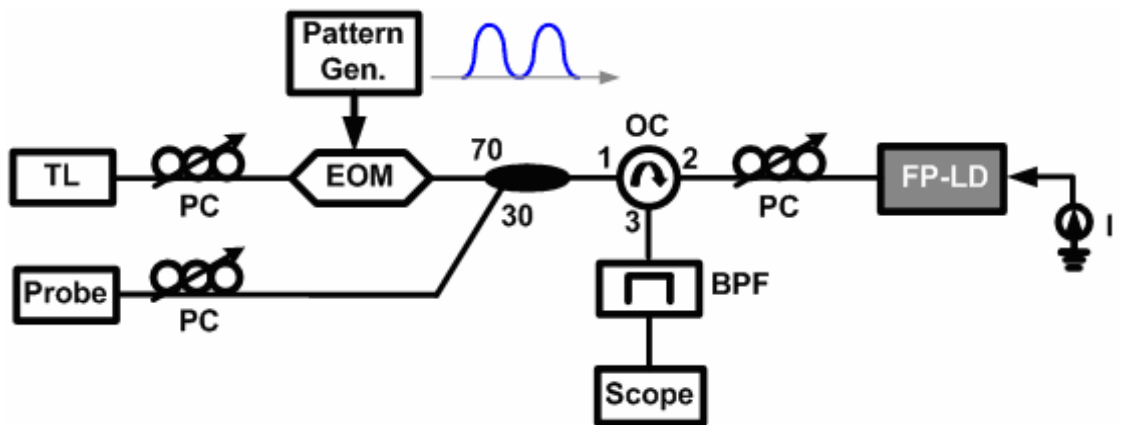
Fig. 3.11 Experimental setup for conventional all-optical 2R regeneration using two-mode injection locking.
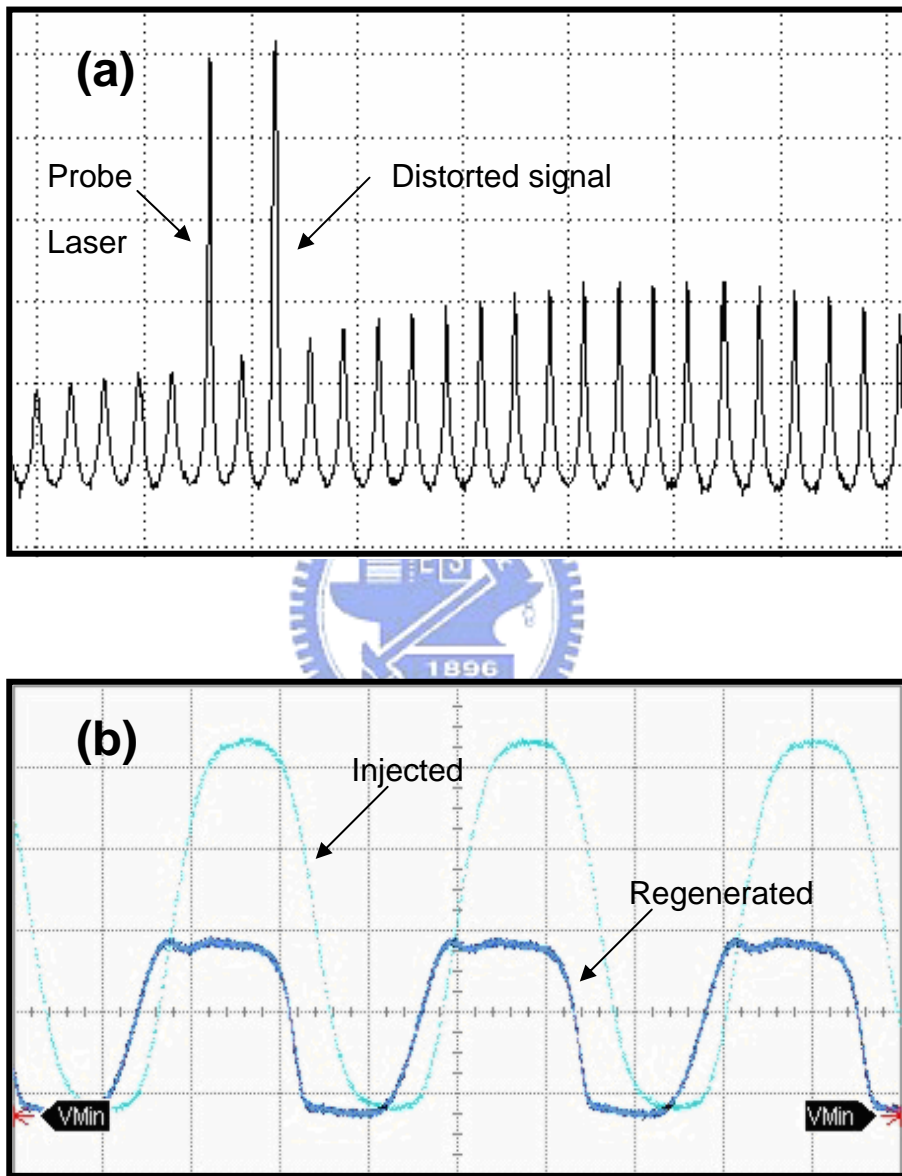
Fig. 3.12 (a) The optical spectra of the TMIL FP-LD and (b) the waveforms of

the regenerated signal and the input distorted signal.
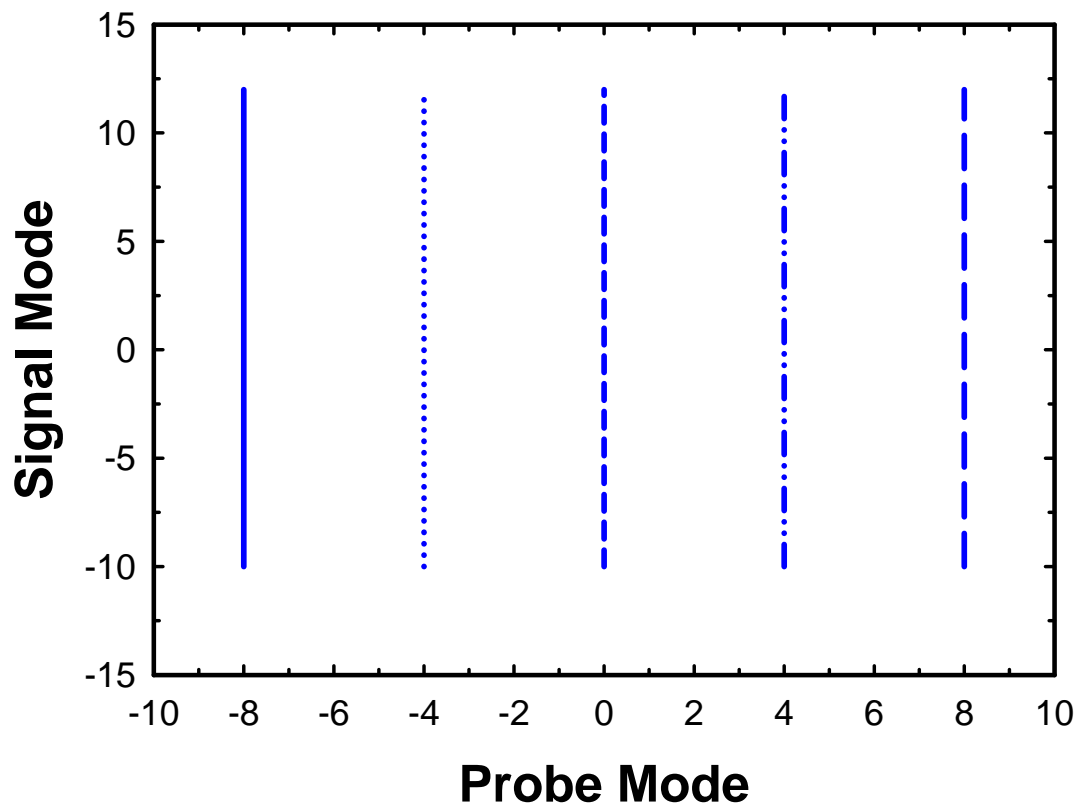
Fig. 3.13 The operation range of signal mode as a function of the probe modes when all-optical 2R regeneration was achieved. (FP-LD was biased at 26 mA)

(a) probe mode -8

signal mode +12   signal mode -10

(b) probe mode +8
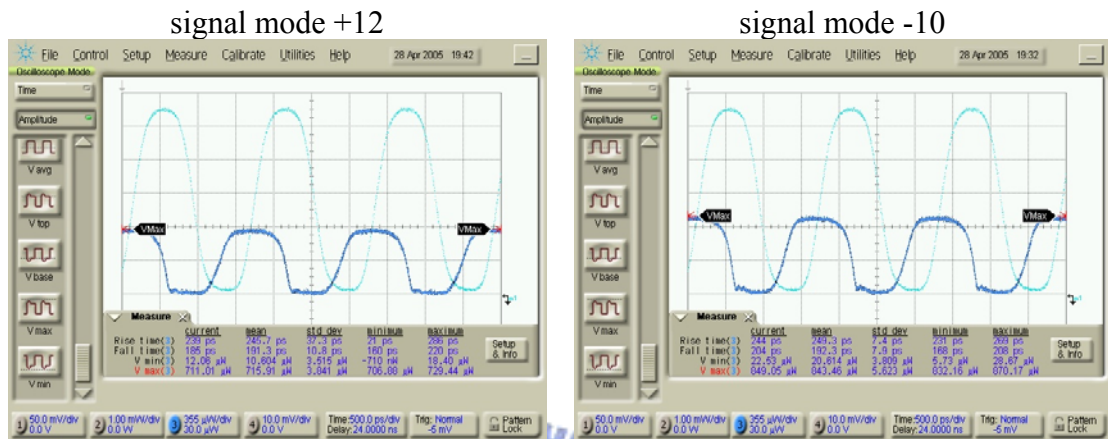
signal mode +12   signal mode -10
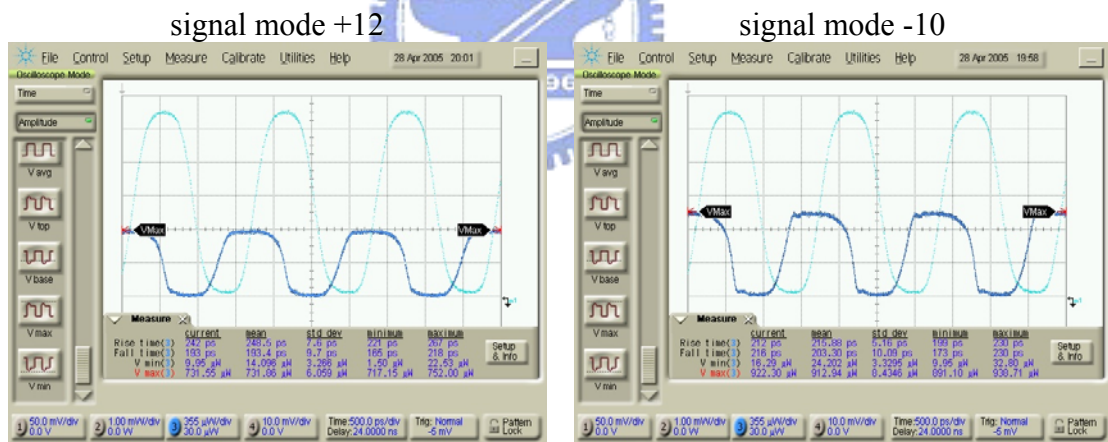
Fig. 3.14 The regenerated waveforms when the signal modes are at +12 and -10, and the probe modes are at -8 and +8, respectively.
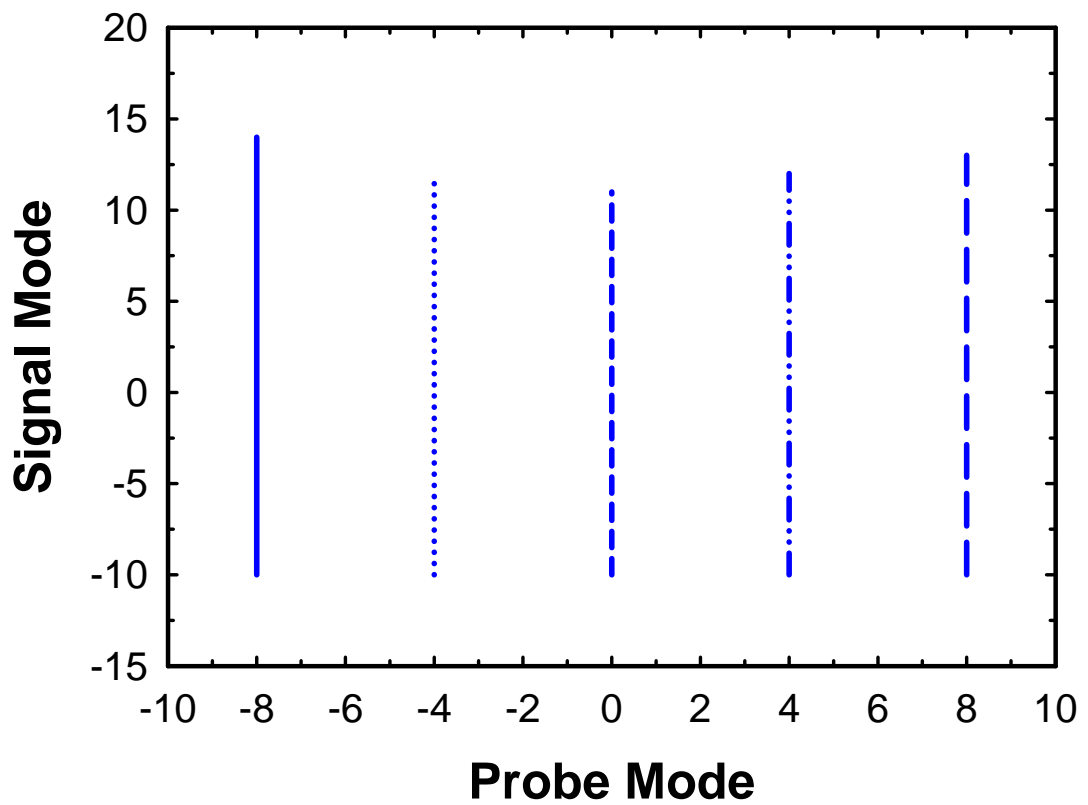
Fig. 3.15 The operation range of signal mode as a function of the probe modes when all-optical 2R regeneration was achieved. (FP-LD was biased at 16 mA)

(a) probe mode -8

signal mode +14   signal mode -10

(b) probe mode +8
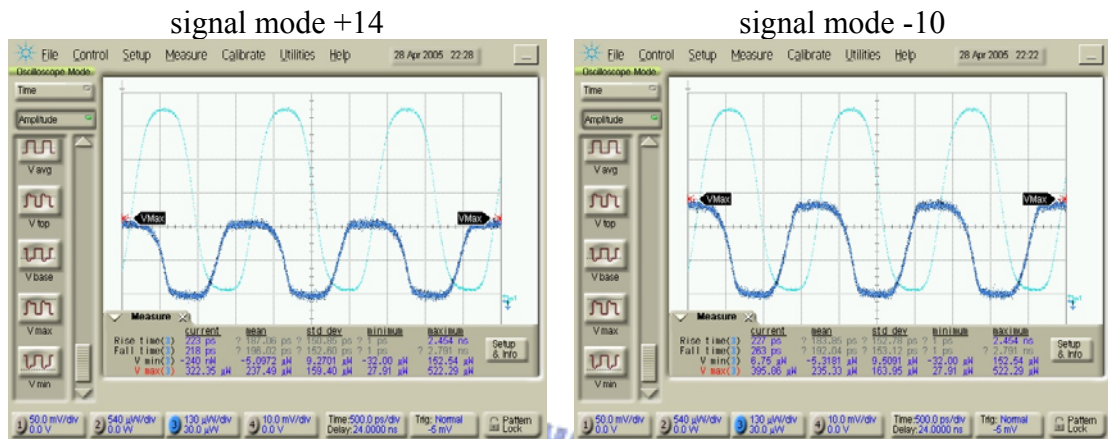
signal mode +13   signal mode -10
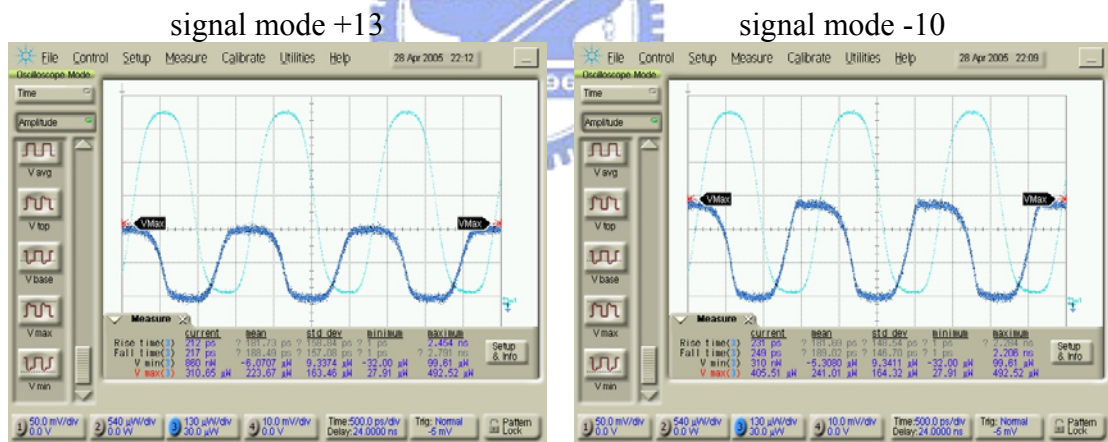
Fig. 3.16 The regenerated waveforms when the signal modes are at +14, +13, and -10, and the probe modes are at -8 and +8, respectively.
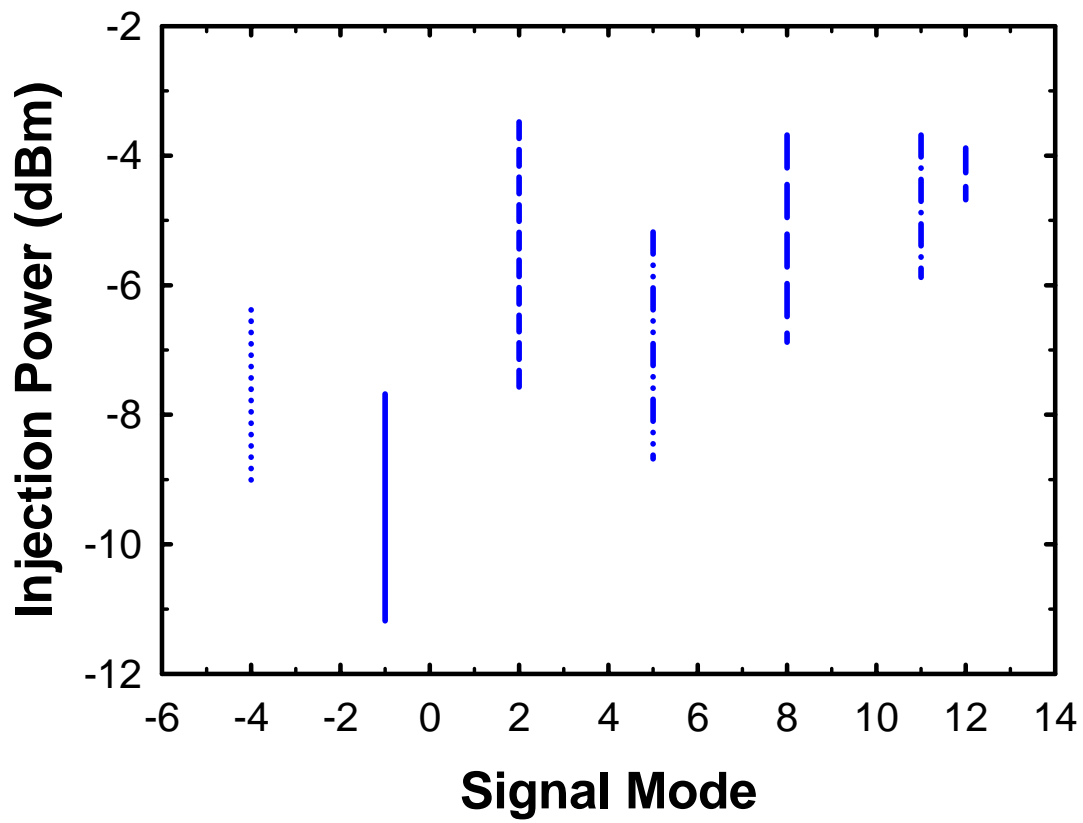
Fig. 3.17 The power dynamic range of the injection signal at different modes when all-optical 2R regeneration is achieved. (probe mode: 0)

(a) signal mode -4

Max   Min

(b) signal mode +12

Max   Min
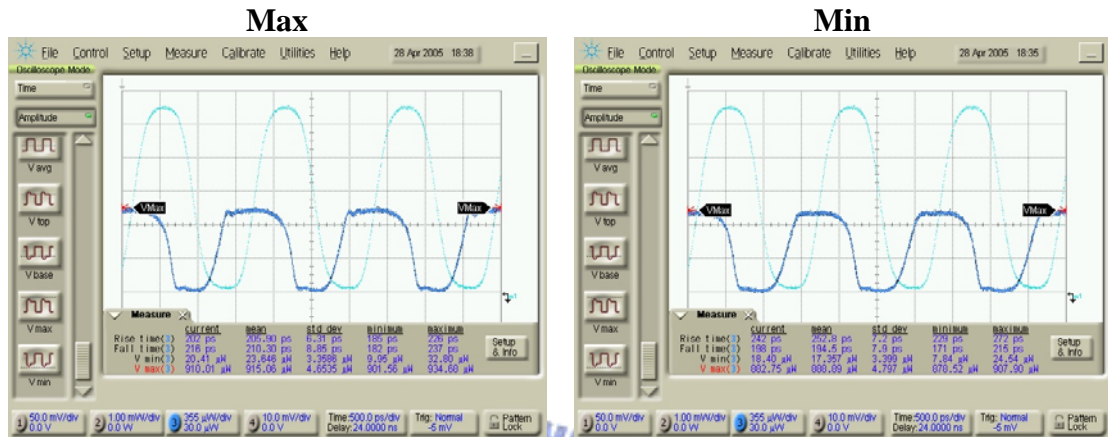
Fig. 3.18 The regenerated waveforms for max and min input signals at -4 and +12 signal modes, respectively. (probe mode: 0)
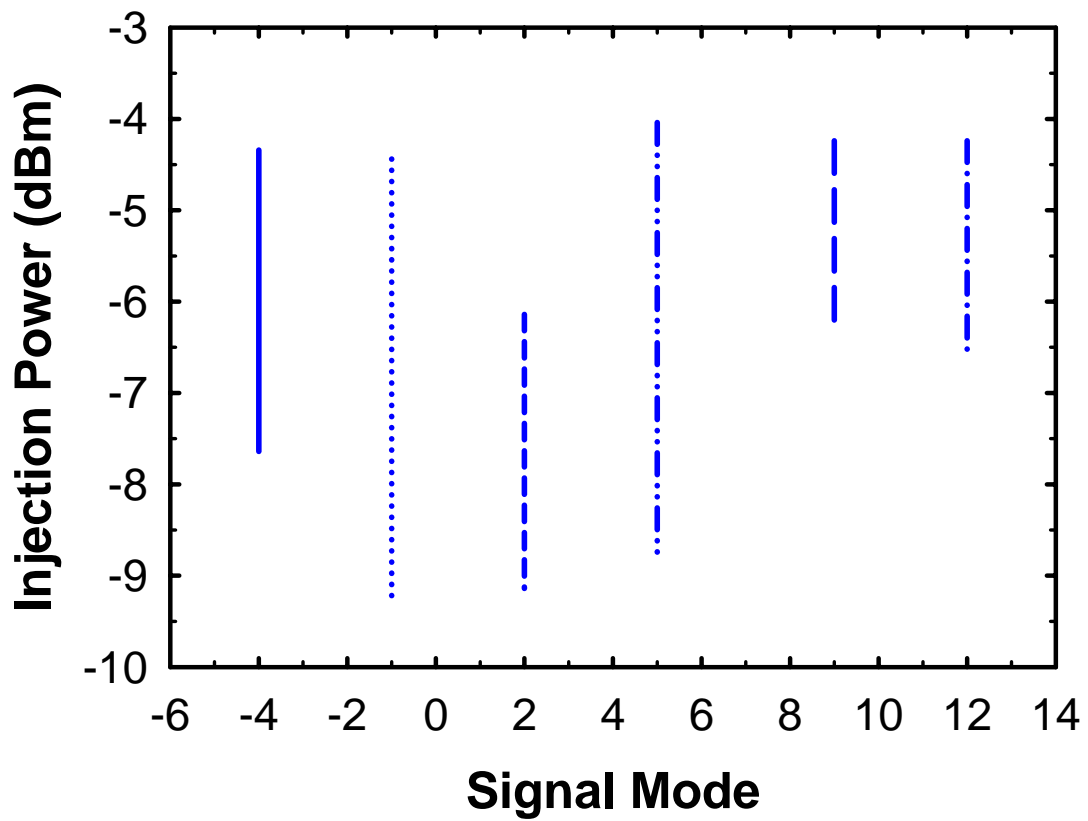
Fig. 3.19 The power dynamic range of the injection signal at different modes when all-optical 2R regeneration is achieved. (probe mode: +8)

(a) signal mode -4
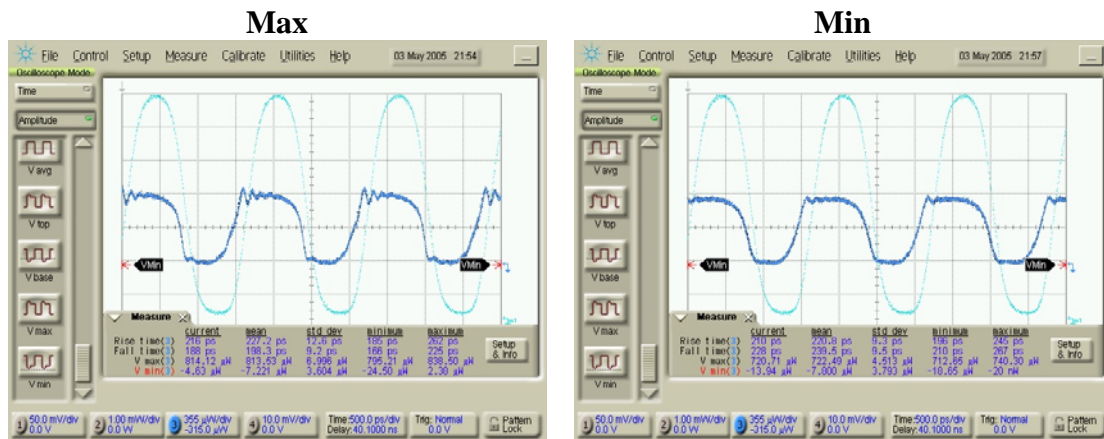
(b) signal mode +12
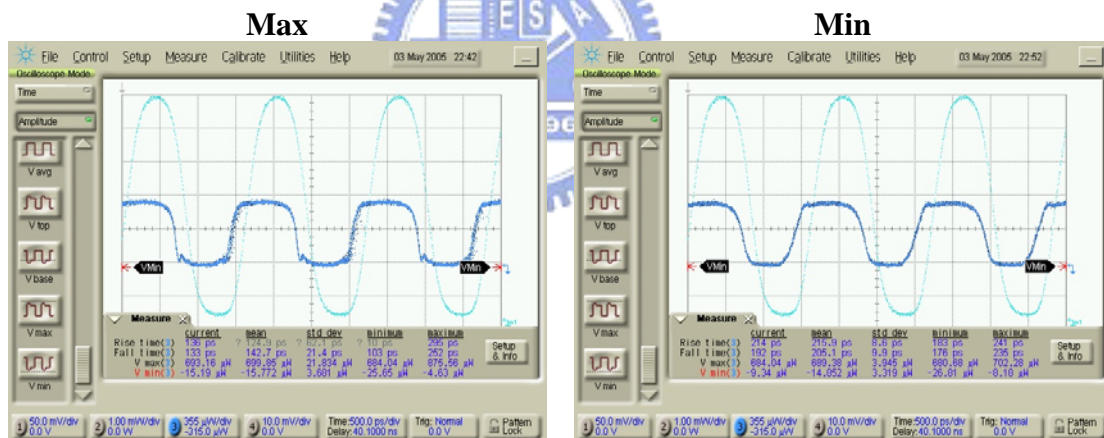
Fig. 3.20 The regenerated waveforms for max and min input signals at -4 and +12 signal modes, respectively. (probe mode: +8)

Table 3.1 Comparison of MMIL, SMIL, TMIL schemes
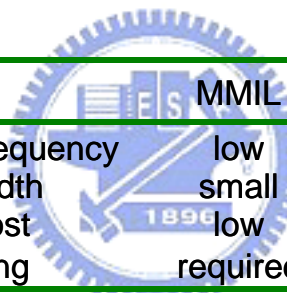
	MMIL	SMIL	TMIL
Relaxation oscillation frequency	low	medium	high
Modulation bandwidth	small	medium	large
Complexity and cost	low	low	high
Narrowband filtering	required	✗	✗

Chapter 4

All-Optical 2R Regeneration Using Simplified TMIL Scheme

4.1 Introduction

In this chapter, two simplified TMIL schemes for all-optical 2R regeneration are presented. In section 4.2, a cost-effective method, based on the injection locking technique of a compact self-seeded Fabry-Pérot laser diode (SSFP-LD) with a 10mm-long embedded fiber Bragg grating cavity, is proposed and experimentally compared with the traditional two-mode injection locked scheme for all-optical 2R regeneration at 10 Gb/s. Placing the presented all-optical 2R regenerator after a 50 km fiber significantly improves the transmission performance of a signal over 50 km and 100 km fiber links. The power penalties at BER = 10^{-9} are similar to those of the traditional two-mode injection locked scheme. Therefore, it's evident that the external probe lasers, which are required in conventional TMIL scheme, are not necessary in our simplified scheme using a compact SSFP-LD.

In conventional TMIL scheme, EDFAs are usually arranged at the input and output ports of a TMIL semiconductor laser for power-level adjustment. However, the cost of a long-haul system will increase with the number of EDFAs using at each 2R stages. Therefore, in section 4.3, an all-optical 2R regenerator, based on a compact self-seeded Fabry-Pérot laser diode (SSFP-LD) with a 10mm-long embedded fiber Bragg grating cavity, and a bidirectional EDFA, is proposed and experimentally demonstrated to execute all-optical 2R regeneration at 10 Gb/s. Compared with the conventional 1R regeneration, the proposed scheme has achieved significant 6.4 dB improvement of power penalty at BER = 10^{-9} in the transmission experiment over 100 km standard single-mode fiber, and significantly reduced the total number of EDFAs.

4.2 All-Optical 2R Regeneration Using a Compact Self-Seeded Fabry-Perot Laser Diode (SSFP-LD)

All-optical regeneration, a highly promising technology for all-optical networks, can restore signals degraded by the combined effects of noise accumulation, fiber dispersion and fiber nonlinearities. The injection-locked semiconductor laser has attracted much attention as a 2R device with reamplification and regeneration capabilities [1-4]. Additionally, all-optical 2R regeneration based on a side-mode injection-locked semiconductor laser has been analyzed. The relaxation oscillation frequency and injection-locking bandwidth [5-18] can be enhanced by a stronger injected power required for a stable side-mode injection due to an increased threshold gain deficit, but they remain insufficient to meet the current needs of high-speed regeneration. All-optical 2R regeneration at 10 Gb/s, using a two-mode injection-locked Fabry-Pérot laser diode (FP-LD), has been recently presented [19-21]: an external probe laser was introduced to suppress the effect of relaxation oscillation. However, the complexity will increase for the two-mode injection-locked method. Therefore, this study demonstrates a new and economical technique for executing all-optical 2R regeneration at 10 Gb/s using a compact self-seeded FP-LD with an embedded fiber Bragg grating (FBG).

4.2.1 Operation Principle

Figure 4.1 depicts the operating principle of the proposed waveform reshaping scheme, which is based on the injection-locking technique using a self-seeded Fabry-Pérot laser diode (FP-LD). In the absence of the injected signal, the FP-LD is stable-locked by the self-seeded tone generated by the FBG cavity, and has a single-longitudinal-mode operation at frequency f_2. When an injected signal S_{in} at frequency f_1 has a power that exceeds the injection-locking threshold, which produces enough locking bandwidth to cover f_1, the FP-LD is injection locked and begins to operate at f_1 with a constant power. The induced red-shift of the FP mode

comb would lead to a frequency misalignment between the reflectivity maximum of the FBG and the closest FP longitudinal mode and help to quench the self-seeded tone [22]. The injection locking mechanism is characterized by an on-off threshold that can be exploited to reduce and compress the noise over the zeros and ones. The schematic diagram of the proposed self-seeded FP-LD is illustrated in Fig. 4.2. To achieve higher modulation bandwidth and lower polarization effect, a short FBG cavity length is needed. A 2.5 GHz commercial high-power FP-LD without an output isolator is employed. A fiber Bragg grating (FBG) is directly integrated into a FP-LD with a ~10mm-long feedback cavity.

4.2.2 Static Characteristics

Figure 4.3 shows the output power of the self-seeded tone varies with the signal injection power at different bias currents. As shown in Fig 4.3, step-like transfer functions can be observed. The peak power of self-seeded tone increase with the bias current, and require more signal injection power to compete with it. In addition, Figure 4.4 displays the output power of the self-seeded tone varies with the signal injection power at different injection mode numbers. As indicated in Fig 4.4, with larger injection mode number +8, the injection locking threshold power is higher and the injection signal requires more peak power to suppress the self-seeded tone.

4.2.3 Experimental Setup

Figure 4.5 displays the experimental setup for this proposed all-optical 2R regeneration at 10 Gb/s (with block A). A self-seeded FP-LD for all-optical waveform reshaping was placed between two 50 km standard single-mode fiber (Corning SMF-28) spans. A 1548.39 nm transmission signal, generated from a tunable laser (TL), was externally modulated by an electro-optic modulator (EOM) with a 2^{31}-1 PRBS data stream at 10 Gb/s. The modulated

signal was propagated through the first 50 km fiber span, and was then injected into the self-seeded FP-LD via an optical circulator (OC) and a polarization controller (PC). The self-seeded FP-LD was biased at 3.14 times the threshold current and the temperature was controlled at 19.76℃ to generate a self-seeded tone at 1546.26 nm with a side mode suppression ratio (SMSR) larger than 30 dB. Moreover, an FBG with a central wavelength of 1546.1 nm, a grating reflection of 9 dB, and a bandwidth of 0.2 nm, was packaged inside the FP-LD. After filtered out by a bandpass filter (BPF) with a 3 dB bandwidth of 0.8 nm, the regenerated signal was propagated through another 50 km fiber span and transmitted to a clock and data receiver (CDR) to generate electrical clock and data for performance evaluation in a bit-error-ratio tester (BERT). A variable optical attenuator (VOA1) was used to adjust the input signal power at FP-LD, and VOA2 was employed to set the average powers at each input port of 50km spans to 1 dBm to prevent fiber nonlinearity. Moreover, the functional block B represents the all-optical waveform regenerator for the two-mode injection locked method [6-7]. In this case, a 1547.08 nm external probe laser with 0 dBm power and a 1549.28 nm transmission signal with -1.7 dBm average power were injected into the FP-LD via a 70:30 coupler, an OC and PCs for all-optical reshaping.

4.2.4 Result and Discussion

Figures 4.6(a) and (b) show the optical spectra of the self-seeded FP-LD without and with the injection signal at 10 Gb/s, respectively. As shown in Fig. 4.6(b), a 1548.39 nm injection signal results in gain competition with the self-seeded tone at 1546.24 nm, and induces two four wave mixing (FWM) tones. Such FWM tones can be negligible since they'll be filtered out by the optical band-pass filter. The insert is the optical reflection and transmission spectra of the FBG. Figure 4.7 illustrates the received eye diagrams at 10 Gb/s with and without 2R regeneration. The average injection power into the FP-LD was kept at

1.3 dBm, and the distorted signal was injected at a frequency in one of the FP modes with a slight detuning of +0.05 nm from the central frequency in this mode. As a result, with regeneration, the eye diagram was still wide-open after 100 km propagation, while the signal without regeneration was seriously distorted by the accumulation of chromatic dispersion. Figure 4.8 shows the bit error rate (BER) performance of the proposed (P) scheme and that of the two-mode injection locked (T) method. The BER performance without using optical regenerators is also indicated in Figure 4.8. For fair comparison, the same FP-LD without an embedded FBG was employed as the slave laser and was driven under the same condition. When the proposed method was used, the power penalties, compared with the back-to-back case, are 1.3 and 2.5 dB after transmission over 50 km and 100 km, respectively, at BER = 10^{-9}. Futhermore, with the two-mode injection locked scheme, the power penalties are 1.1 and 2.6 dB after transmission over 50 km and 100 km, respectively, at BER = 10^{-9}.

4.3 All-Optical 2R Regenerator Using Compact SSFP-LD Incorporated in a Bidirectional EDFA

All-optical 2R regeneration (reamplification and reshaping) plays an important role in future all-optical network due to its outstanding ability for the high-speed restoration of signals degraded by the noise accumulation, fiber dispersion and nonlinearities. All-optical 2R regeneration based on a side-mode injection-locked semiconductor laser has been analyzed [3-6]. These studies show that the operating bit rate has a limitation caused by the carrier-induced relaxation oscillation frequency. Recently, several researches [19-21] of using a two-side-mode injection-locked Fabry-Pérot laser diode (FP-LD) to execute 10 Gb/s all-optical 2R regeneration have been presented. The relaxation oscillation frequency was dramatically increased by introducing an external probe laser in this method. However, an extra probe laser is needed for this scheme. Besides, a stronger injection power for a stable two-side-mode injection locking, and a high output level for fiber-link loss compensation will require two Erbium-doped fiber amplifiers (EDFA's) placed at input and output sides of the FP-LD. Therefore, this study proposes and demonstrates a new and cost-effective 10 Gb/s all-optical 2R regenerator by using a compact self-seeded FP-LD incorporated in a bidirectional EDFA.

4.3.1 Operation Principle

Fig. 4.9 illustrates the schematic diagram of this proposed 2R regenerator. A compact self-seeded Fabry-Pérot laser diode (SSFP-LD), which is composed of a 2.5 GHz commercial FP-LD without output isolator, and a integrated fiber Bragg grating (FBG), is combined with a bidirectional EDFA to form the new 2R regenerator. To achieve higher modulation

bandwidth and lower polarization effect, the external feedback cavity of less than 10 mm is used. In addition, an EDFA with short Erbium-doped fiber is placed in front of this SSFP-LD to provide adequate bidirectional amplification for both the injected and reshaped signals. The operating principle is based on the on-off thresholding nature of an injection-locked SSFP-LD to compress the accumulated noise over the zeros and ones. In the beginning, the SSFP-LD, stable-locked by the FBG-reflected light, has single-longitudinal-mode (SLM) operation at frequency f_2. Then a distorted signal S_{in} at frequency f_1 is injected. When the amplified power level of S_{in} exceeds the injection-locking threshold, a sufficient locking bandwidth can be obtained to cover f_1, and the induced red shift of the FP mode comb would also help to quench the self-seeded tone at frequency f_2. Thus, at this moment, the SSFP-LD is stable-locked at f_1 with a constant output power. After passing through the amplified SSFP-LD and filtered out by an optical bandpass filter (OBPF), a wavelength-preserved and 2R-regenerated signal S_{reg} can be obtained.
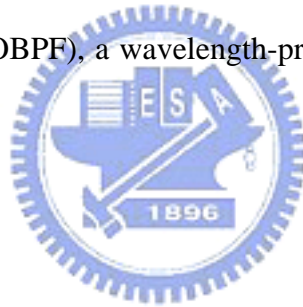
4.3.2 Experimental Setup

Fig. 4.10 illustrates the setups of transmission experiments for the proposed all-optical 2R (block A) and the traditional amplifier modules (1R, block B). The proposed 2R regenerator, comprising an optical circulator (OC), a 3 m Erbium-doped fiber (EDF) with absorption of 4.5 – 5.5 dB/m at 980 nm, a 980 / 1550 nm wavelength division multiplexer, a 980 nm pump laser operated at 14.6 mW, and a SSFP-LD, was placed between two 50 km standard single-mode fiber (SSMF) spans. This SSFP-LD, composed of a commercial 2.5 GHz FP-LD and an embedded FBG, was biased at 4.28 times its threshold current and controlled at 16.67 $^{\circ}$C to emit a self-seeded tone at 1550.76 nm with a side mode suppression ratio (SMSR) larger than 40 dB. The embedded FBG has a central wavelength of 1550.68 nm, a grating reflectivity of 70 %, and a bandwidth of 0.2 nm. A tunable laser (TL) was externally

modulated via an electro-optic modulator (EOM) with a $2^{31}-1$ PRBS data format to generate a 10 Gb/s testing signal at 1555.32 nm. Such signal was transmitted over the first fiber span of 50 km, and then was injected into block A or B through a polarization controller (PC). The transmission performance at 50 km can be measured right after the point b. To measure the performance of 100 km transmission, the regenerated signal, after filtered out by an OBPF with the 3 dB bandwidth of 0.8 nm, was propagated through another 50 km fiber span and into a receiving module. This module includes a variable optical attenuator (VOA), an optical preamplifier, an OBPF, and an optical-to-electrical (O/E) module. A 20 Gb/s digital scope for eye diagram measurement or a bit-error-ratio tester (BERT) with a clock and data receiver (CDR) for bit-error-ratio (BER) measurement is utilized after this receiving module. To prevent from causing fiber nonlinearity, the average powers at each input port of 50 km spans were set at –8 dBm.

4.3.3 Result and Discussion

Fig. 4.11 shows the output spectra of the proposed 2R regenerator when the testing signal is injected. As shown in Fig. 4.11, the injected signal of 1555.32 nm is located in the fourth longitudinal mode counting from the self-seeded tone in the long wavelength direction. In order to optimize the regenerated signal, the average injection power into the proposed 2R regenerator is kept at –18.2 dBm with a slight wavelength detuning of +0.03 nm from the central frequency of targeted mode. The input power dynamic range of the proposed 2R regenerator ranges between –16.2 and –21.8 dBm, and the total signal gain provided by this proposed 2R module is about 10.2 dB. Moreover, two four wave mixing (FWM) tones generated by the injected signal and the self-seeded tone are observed in Fig. 4.11. The inset in Fig. 4.11 indicates the optical spectra of the embedded FBG for reflection and transmission. Figure 4.12 shows that the measured input and output optical signal to noise ratio (OSNR) of

the proposed 2R regenerator are 22.64 and 35.41 dB/0.1nm, respectively. The minimum required OSNR is about 21 dB/0.1nm. ASE noise accumulated in mark and space of the incoming signal could be obviously suppressed due to the thresholding characteristic of the proposed 2R device. Figure 4.13 performs a back-to-back testing that puts signal from transmitter directly into the 2R regenerator and measure the BER penalty in this situation. The input and output eye patterns are measured. The power penalty at 10^{-9} BER in that situation is about 0.5 dB, which is the regenerating limitation for the proposed 2R module. Fig. 4.14 illustrates the received eye diagrams at 10 Gb/s using proposed 2R and traditional 1R regenerations for 50 and 100 km fiber link transmissions. As shown in Fig. 4.14, the proposed 2R regeneration can provide a wide-opened eye after 100 km propagation, while the signal using 1R-only regeneration was seriously distorted by the accumulated chromatic dispersion over 100 km transmission. In addition, Figure 4.15 shows the BER performances of the proposed 2R regenerator and the conventional 1R module for 50 and 100 km fiber transmissions. For the proposed 2R regenerator, the power penalties of BER = 10^{-9}, referring to the back-to-back case, are 1.9 and 2.5 dB after 50 and 100 km transmissions, respectively. However, larger power penalties of 3 and 8.9 dB are observed for 1R-only regeneration after transmitting over 50 km and 100 km. Therefore, compared with conventional 1R regeneration, this proposed 2R regeneration can obtain 6.4 dB improvement of power penalty at BER = 10^{-9} for 100 km SSMF propagation.

4.4 Summary

In this chapter, we present and experimentally demonstrates the feasibility of 10 Gb/s all-optical 2R regeneration via the injection locking of a compact self-seeded FP-LD with an ultrashort feedback cavity of ~10 mm. In our experiments, it is proven that, by using the proposed self-seeded method, the BER performances can compete with those of the

traditional two-mode injection locked scheme. Also, we further propose a new and economic

10 Gb/s all-optical 2R regenerator consisting of a compact SSFP-LD with an ultrashort

feedback cavity of ~10 mm, and a bidirectional EDFA. The BER performances of using the

proposed scheme, compared with the one of 1R-only regeneration, can be significantly

improved. The elimination of external probe laser and utilization of a bidirectional EDFA can

highly simplify the all-optical 2R regeneration. Both simplified TMIL schemes are promising

on the applications of future optical networks.

References for Chapter 4

[1] R. Lang, "Injection locking properties of a semiconductor laser," *IEEE J. Quantum Electron.*, vol. QE-18, pp. 976-983, June 1982.

[2] K.Weich, E. Patzak, and J. Hörer, "Fast all-optical switching using two-section injection-locked semiconductor lasers," *Electron. Lett.*, vol. 30, pp. 493-494, 1994.

[3] S. Yamashita and D. Matsumoto, "Waveform reshaping based on injection locking of a distributed-feedback semiconductor laser," *IEEE Photon. Technol. Lett.*, vol. 12, pp. 1388-1390, Oct. 2000.

[4] K. Inoue and M. Yoshino, "Bistability and waveform reshaping in a DFB-LD with side-mode light injection," *IEEE Photon. Technol. Lett.*, vol. 7, pp. 164-166, Feb. 1995.

[5] Y. Hong and K. A. Shore, "Locking characteristics of a side-mode injected semiconductor laser," *IEEE J. Quantum Electron.*, vol. 35, pp. 1713-1717, Nov. 1999.

[6] A. Kuramoto and S. Yamashita, "All-optical regeneration using a side-mode injection-locked semiconductor laser," *IEEE J. Select. Topics Quantum Electron.*, vol. 9, pp. 1283-1287, Sept./Oct. 2003.

[7] R. J. Jones, P. S. Spencer, and K. A. Shore, "Detuned side-mode injection for enhancing oscillation frequency of a semiconductor laser," *IEEE Proceedings*, vol. 148, No. 1, pp. 35-39, 2001.

[8] J. M. Luo and M.Osinski, "Stable-locking bandwidth in sidemode injection locked semiconductor lasers," *Electron. Lett.*, vol. 27, No. 19, pp. 1737-1738, 1991.

[9] J. M. Luo, "Side-mode injection locking of semiconductor lasers," *IEEE Proceedings*, vol. 136, No. 1, pp. 33-37, 1989.

[10] Y. Hong, K. A. Shore, J. S. Lawrence, and D. M. Kane, "Wavelength switching by

positively detuned side-mode injection in semiconductor laser," *Appl. Phys. Lett.*, vol. 76, No. 22, pp. 3170-3172, 2000.

[11] T. B. Simpson and J. M. Liu, "Enhanced modulation bandwidth in injection-locked semiconductor laser," *IEEE Photon. Technol. Lett.*, vol. 9, pp. 1322-1324, Oct. 1997.

[12] J. M. Liu, H. F. Chen, X. J. Meng, and T. B. Simpson, "Modulation bandwidth , noise, and stability of a semiconductor laser subject to strong injection locking," *IEEE Photon. Technol. Lett.*, vol. 9, pp. 1325-1327, Oct. 1997.

[13] J. Wang, M. K. Haldar, L. Li, and F. V. C. Mendis, "Enhancement of modulation bandwidth of laser diodes by injection lcoking," *IEEE Photon. Technol. Lett.*, vol. 8, pp. 34-36, Jan. 1996.

[14] T. B. Simpson, J. M. Liu, and A. Gavrielides "Bandwidth enhancement and broadband noise reduction in injection-locked semiconductor laser," *IEEE Photon. Technol. Lett.*, vol. 7, pp. 709-711, Jul. 1995.

[15] J. K. White, J. V. Moloney, A. Gavrielides, V. Kovanis, A. Hohl, and R. Kalmus, "Multilingitudinal-mode dynamics in a semiconductor laser subject to optical injection," *IEEE J. Quantum Electron.*, vol. 34, pp. 1469-1473, Aug 1998.

[16] R. Hui, A. D'Ottavi, A. Mecozzi, and P. Spano, "Injection locking in distributed feedback semiconductor lasers," *IEEE J. Quantum Electron.*, vol. 27, pp. 1688-1695, Jun 1991.

[17] I. Petitbon, P. Gallion, G. Debarge, and C. Chabran, "Locking bandwidth and relaxation oscillations of an injection-locked semiconductor laser," *IEEE J. Quantum Electron.*, vol. 24, pp. 148-154, Feb 1988.

[18] J. M. Luo and M.Osinski, "Multimode small-signal analysis of side-mode injection-locked semiconductor laser," *Jpn. J. Appl. Phys.*, vol. 31, No. 6A, pp. 685-688, 1992.

[19] J. Hörer and E. Patzak, "Large-signal analysis of all-optical wavelength conversion using

two-mode injection-locking in semiconductor lasers," *IEEE J. Quantum Electron.*, vol. 33, pp. 596-608, Apr. 1997.

[20] L. Xu, W. H. Chung, L. Y. Chan, L. F. K. Lui, P. K. A. Wai, and H. Y. Tam, "Simultaneous all-optical waveform reshaping of two 10-Gb/s signals using a single injection-locked fabry-pérot laser diode," *IEEE Photon. Technol. Lett.*, vol. 16, pp. 1537-1539, June 2004.

[21] S. Yamashita and J. Suzuki, "All-optical 2R regeneration using a two-mode injection-locked fabry-pérot laser diode," *IEEE Photon. Technol. Lett.*, vol. 16, pp. 1176-1178, Apr. 2004.

[22] A. Murakami, K. Kawashima, and K. Atsuki, "Cavity resonance shift and baidwidth enhancement in semiconductor lasers with strong light injection," *IEEE J. Quantum Electron.*, vol. 39, pp. 1196-1204, Oct 2003.
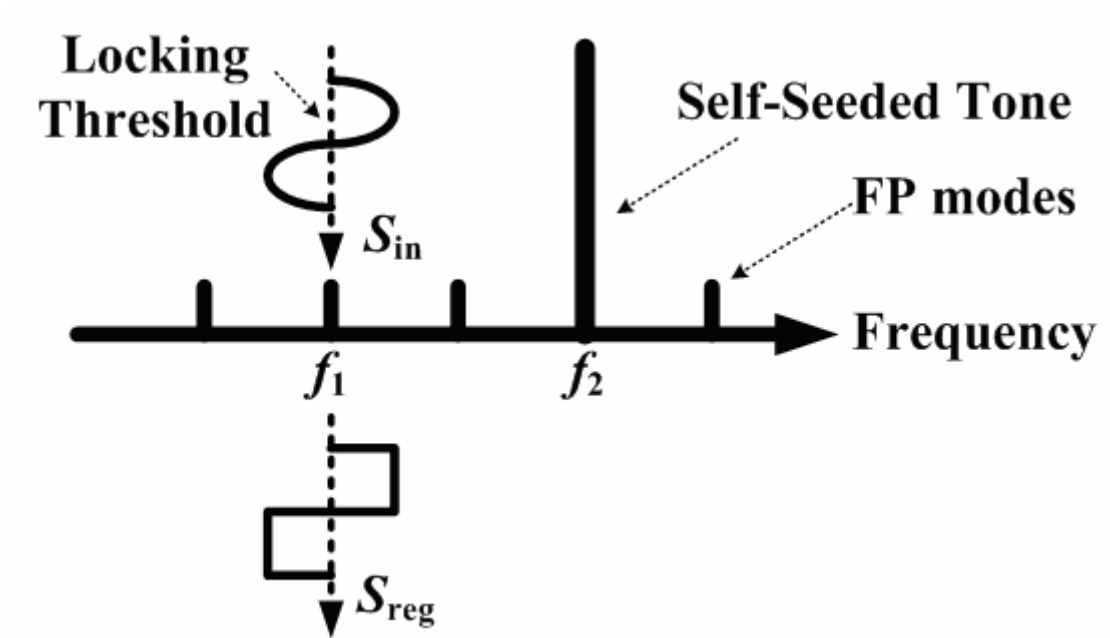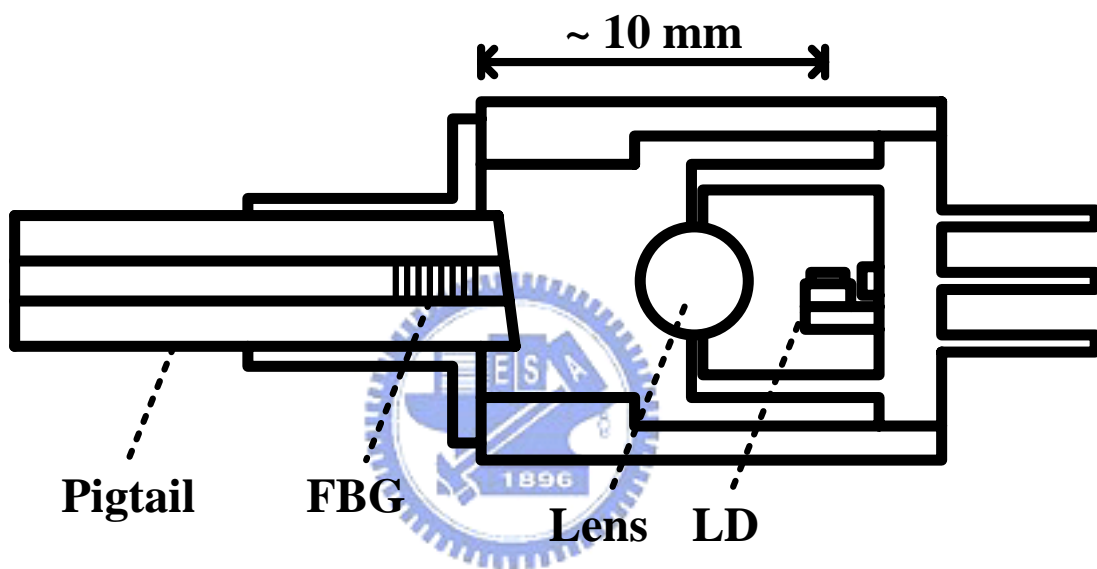
Fig. 4.1 Principle of the proposed 2R regeneration.

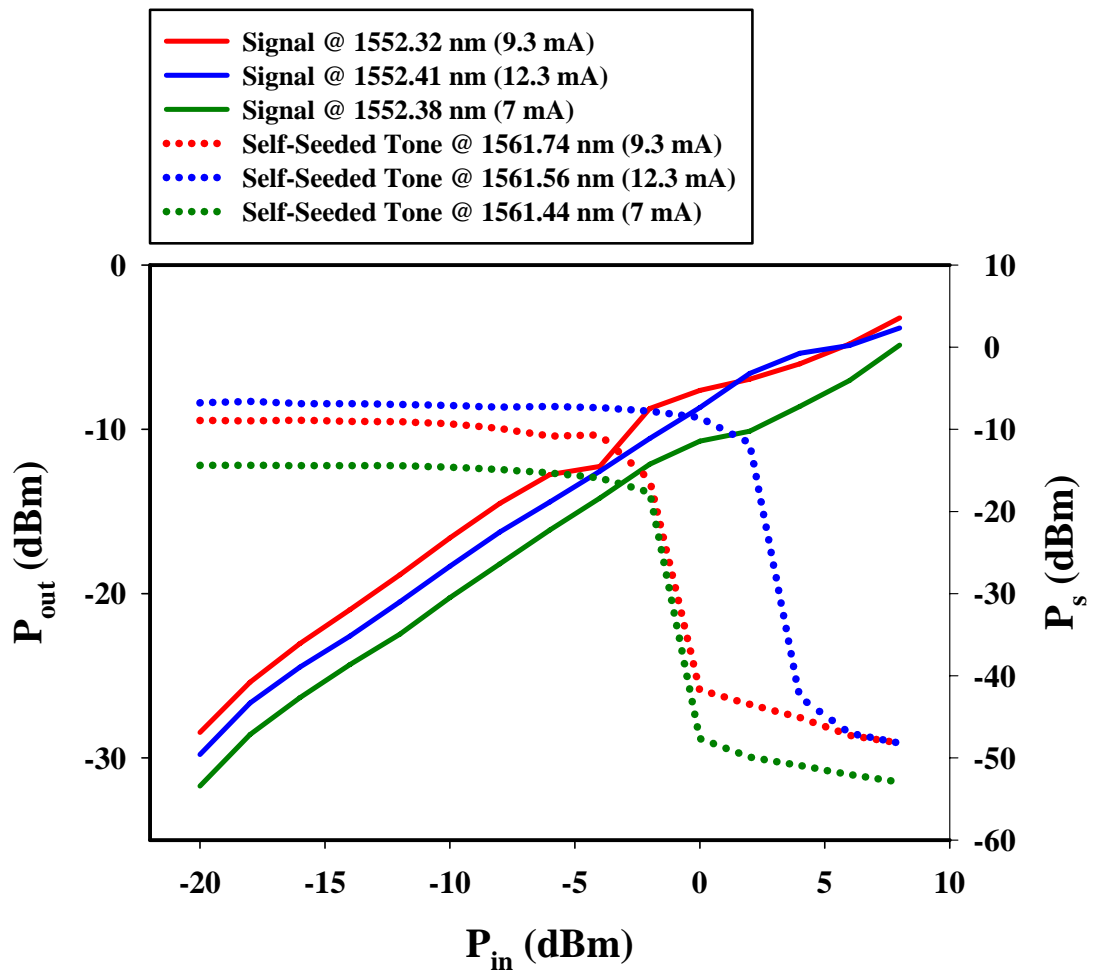**Fig. 4.2** Schematic diagram of the proposed self-seeded FP-LD.

Fig. 4.3 The output power of the self-seeded tone varies with the signal injection power at different bias currents.
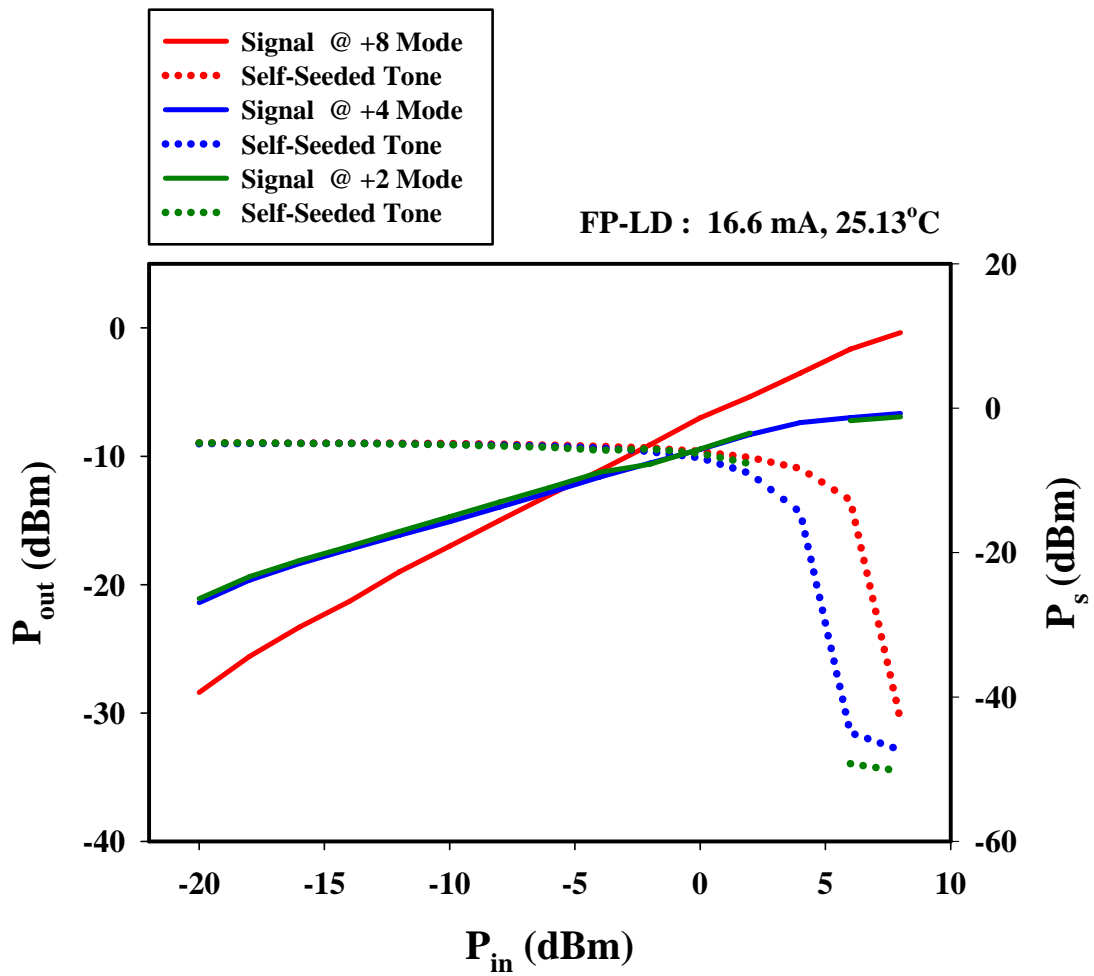
Fig. 4.4 The output power of the self-seeded tone varies with the signal injection

power at different injection mode numbers.
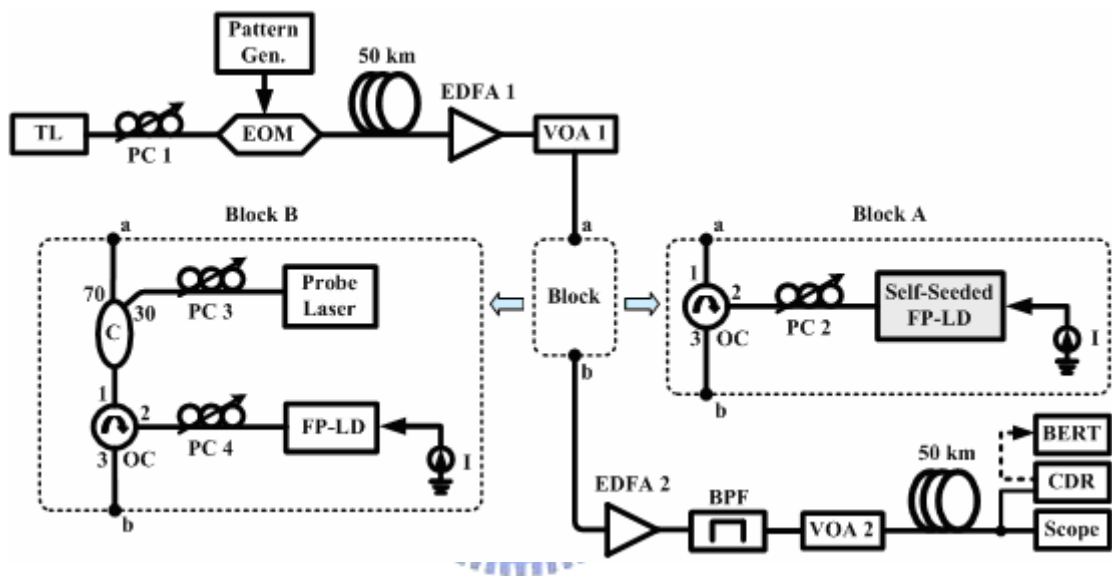
Fig. 4.5 Experimental setups for all-optical waveform regeneration of a distorted signal at 10 Gb/s.
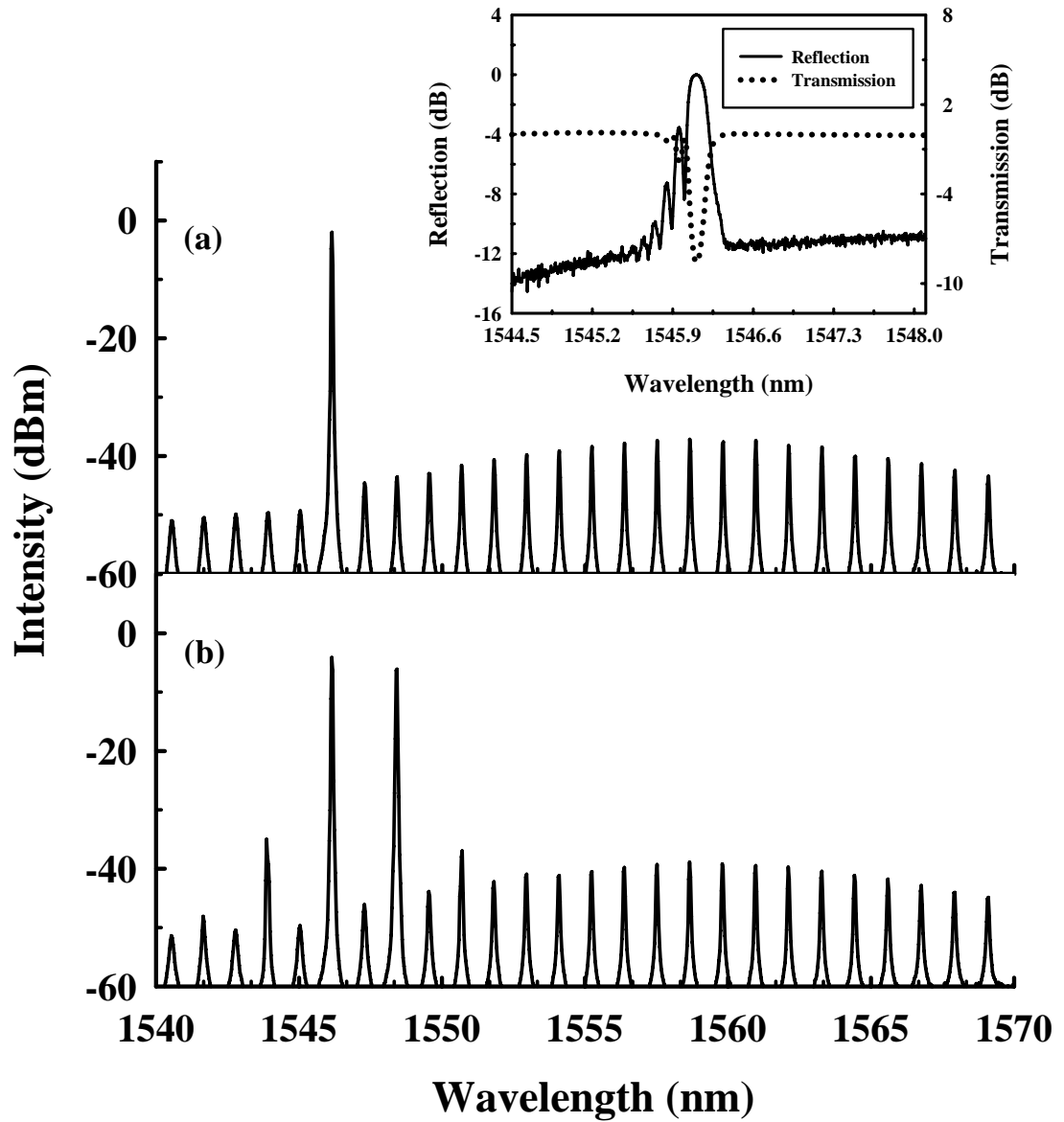
Fig. 4.6 Measured optical spectra of the self-seeded FP-LD (a) without, and (b) with the injection signal at 10 Gb/s.
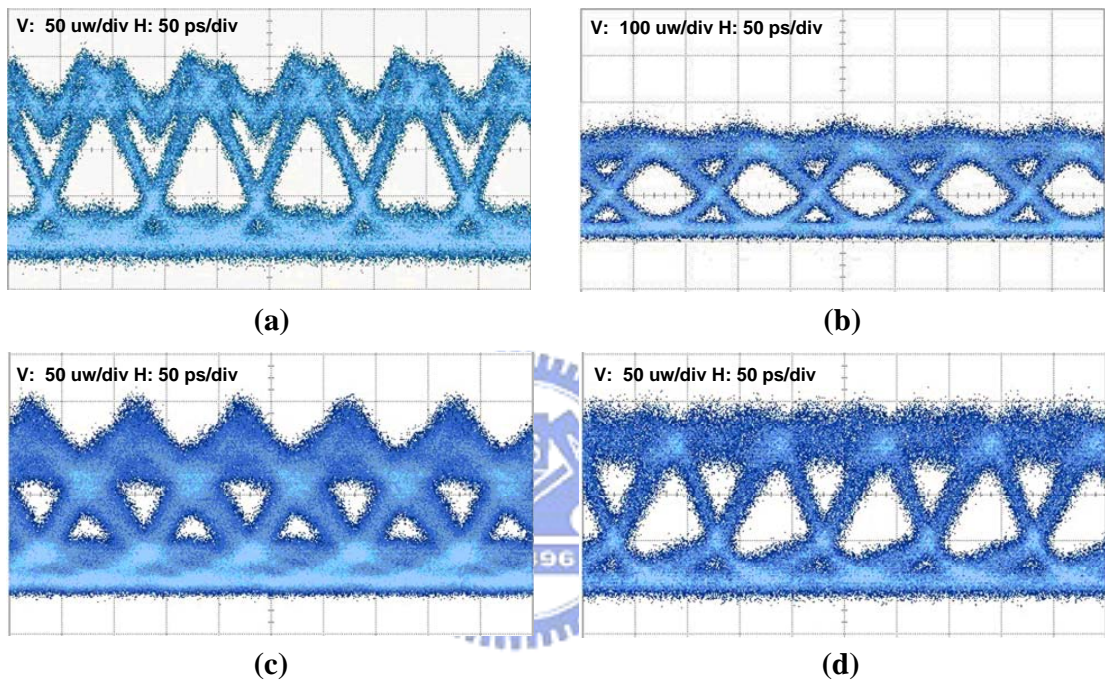
Fig. 4.7 Measured eye diagrams of the signal (a) after 50-km propagation without regeneration, (b) regenerated at 50 km, (c) after 100-km propagation without regeneration, and (d) after 100-km propagation with regeneration.
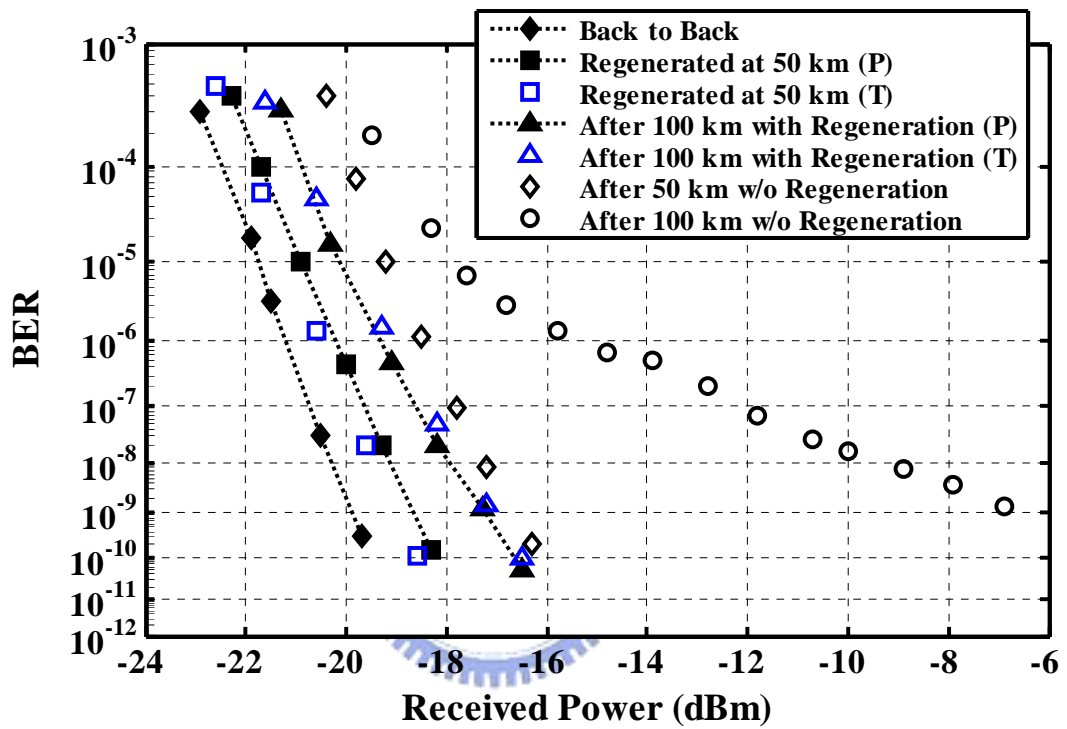
Fig. 4.8 BER performances with, and without the proposed (P) and the two-mode injection locked (T) regeneration schemes, respectively.
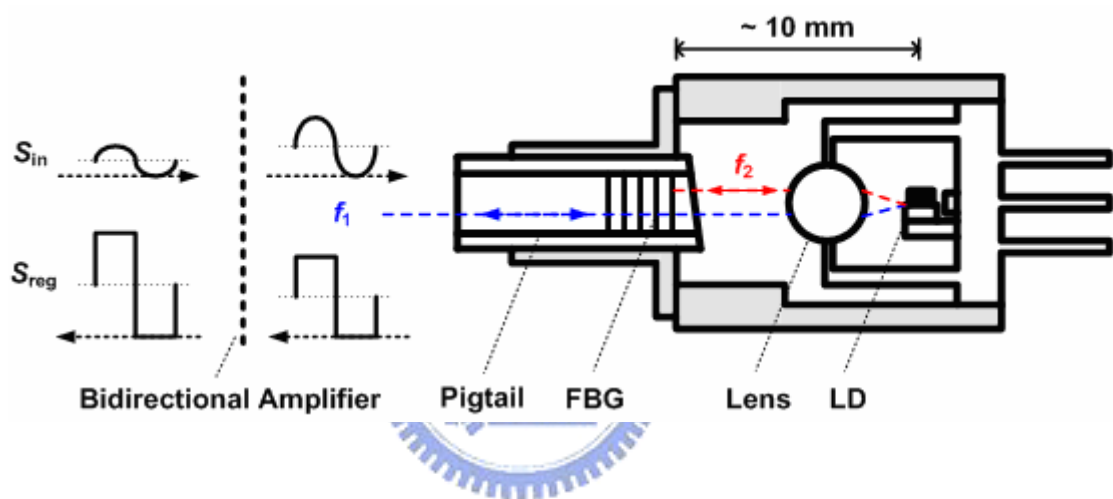
Fig. 4.9 Schematic diagram of the proposed 2R regenerator.
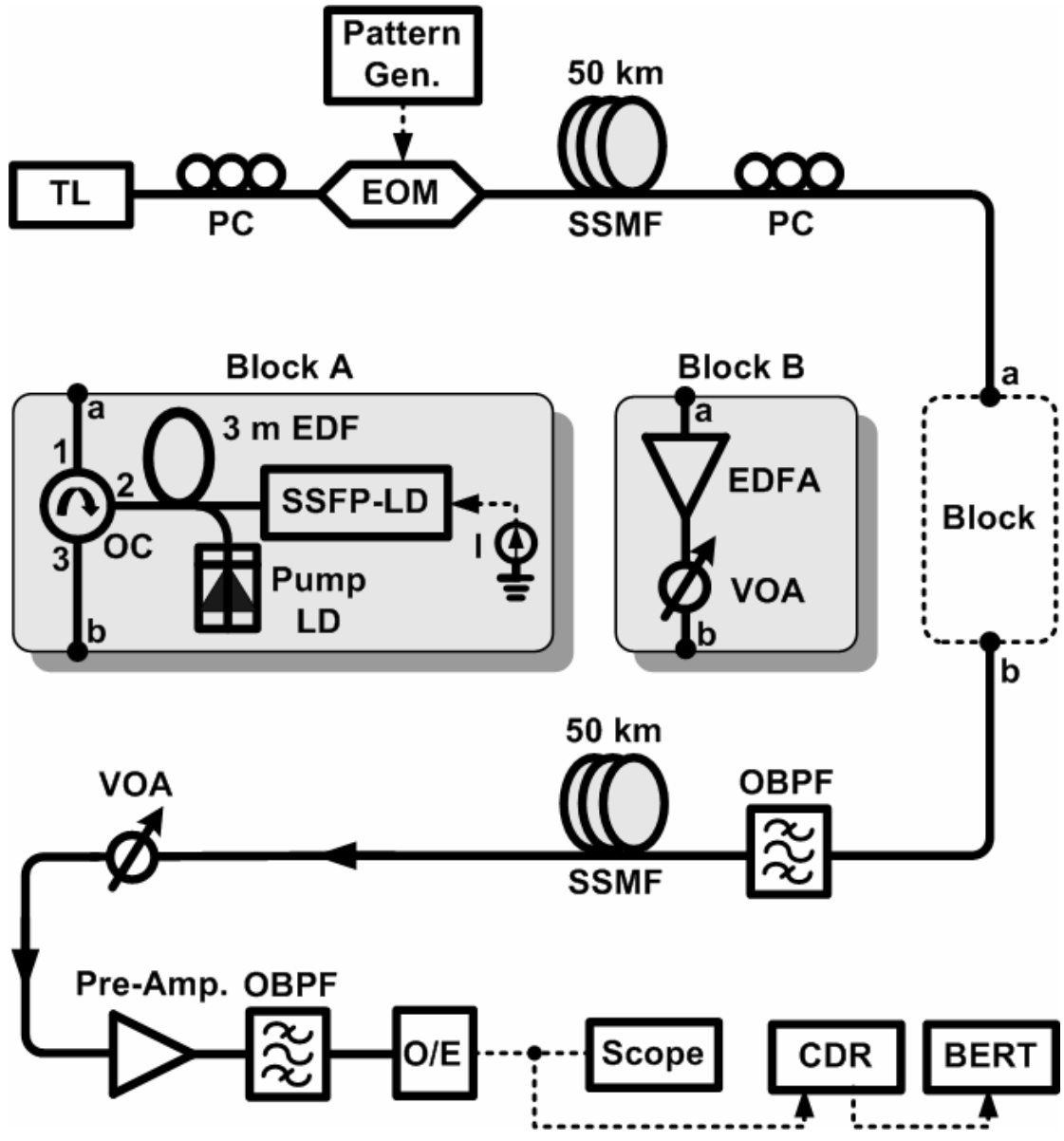
Fig. 4.10 The experimental setups for the proposed all-optical 2R (block A) and the traditional 1R modules (block B).
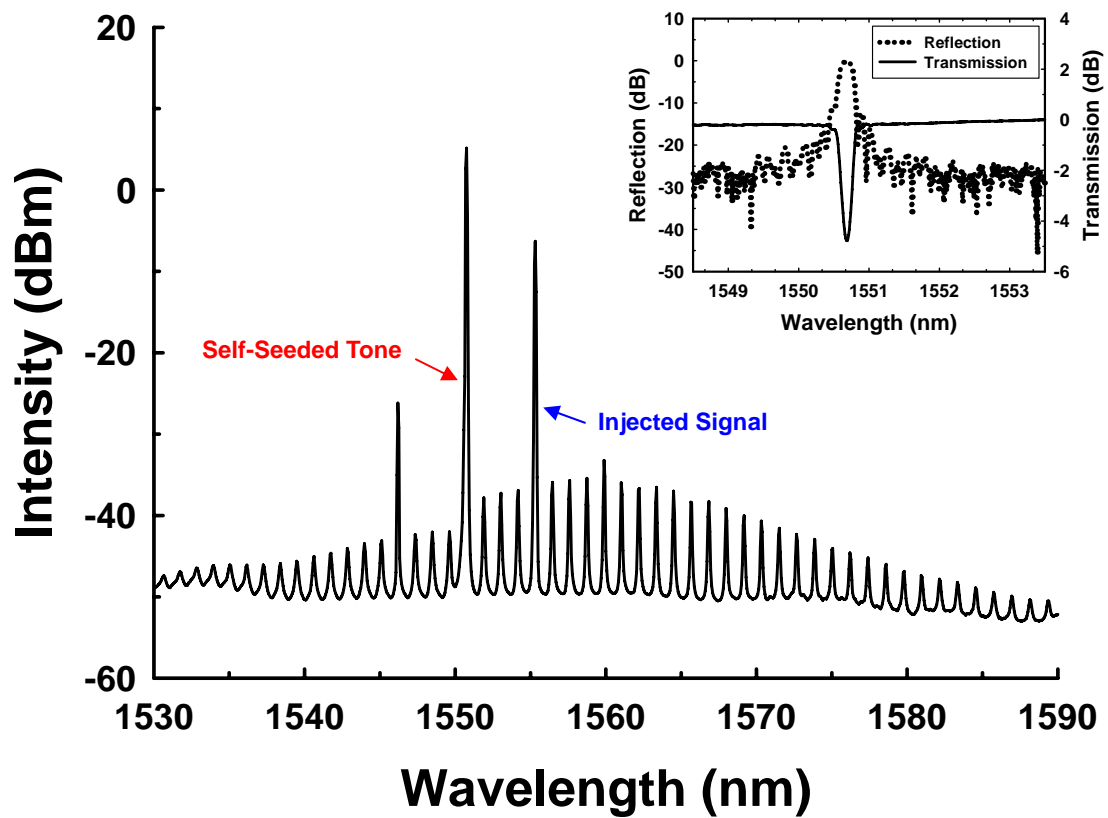
Fig. 4.11 The output spectra of the proposed 2R regenerator when a testing signal is injected. The inset is the optical spectra of the embedded FBG for the reflection and transmission.
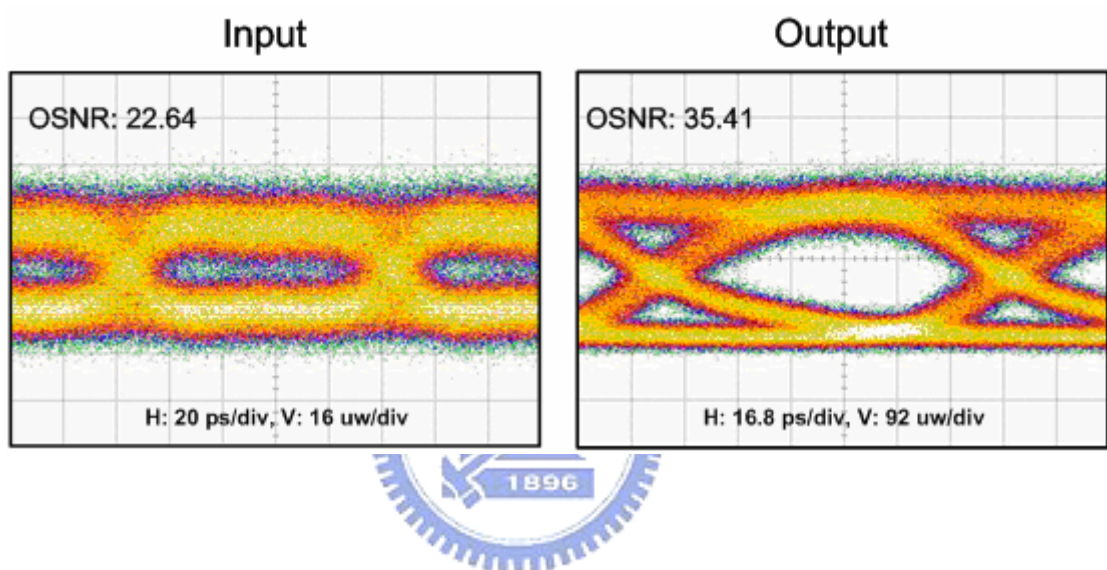
Fig. 4.12 Measured optical signal to noise ratios (OSNRs) of the input and output signals.
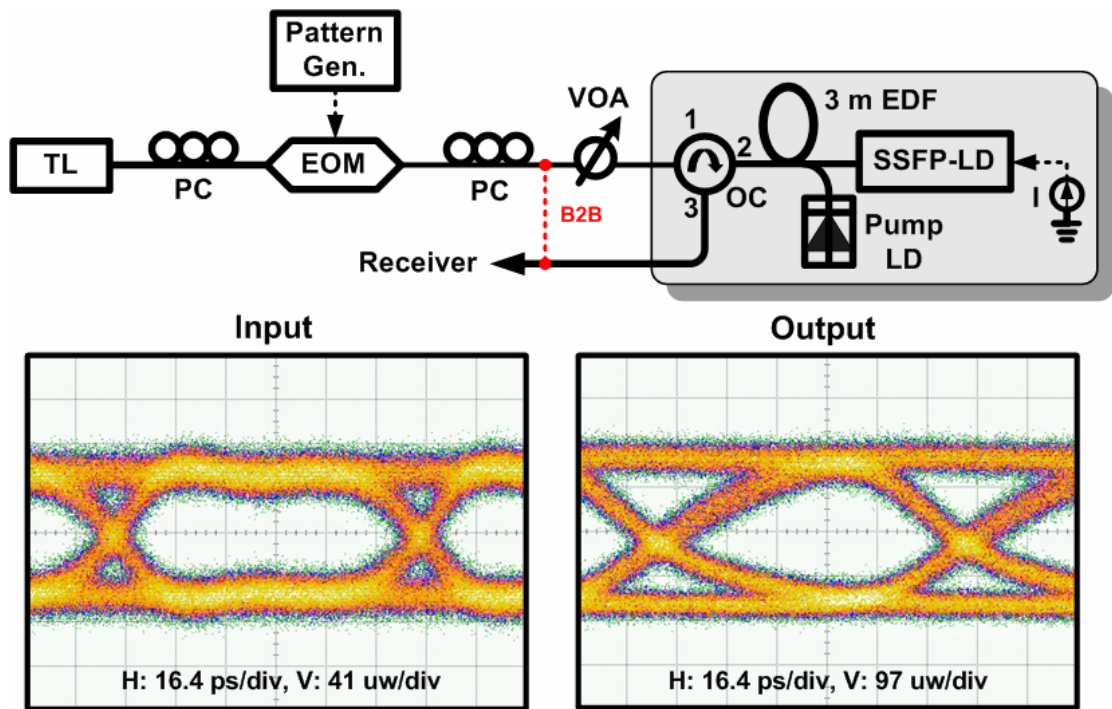
Fig. 4.13 Regenerating limit testing of the proposed all-optical 2R regenerator.
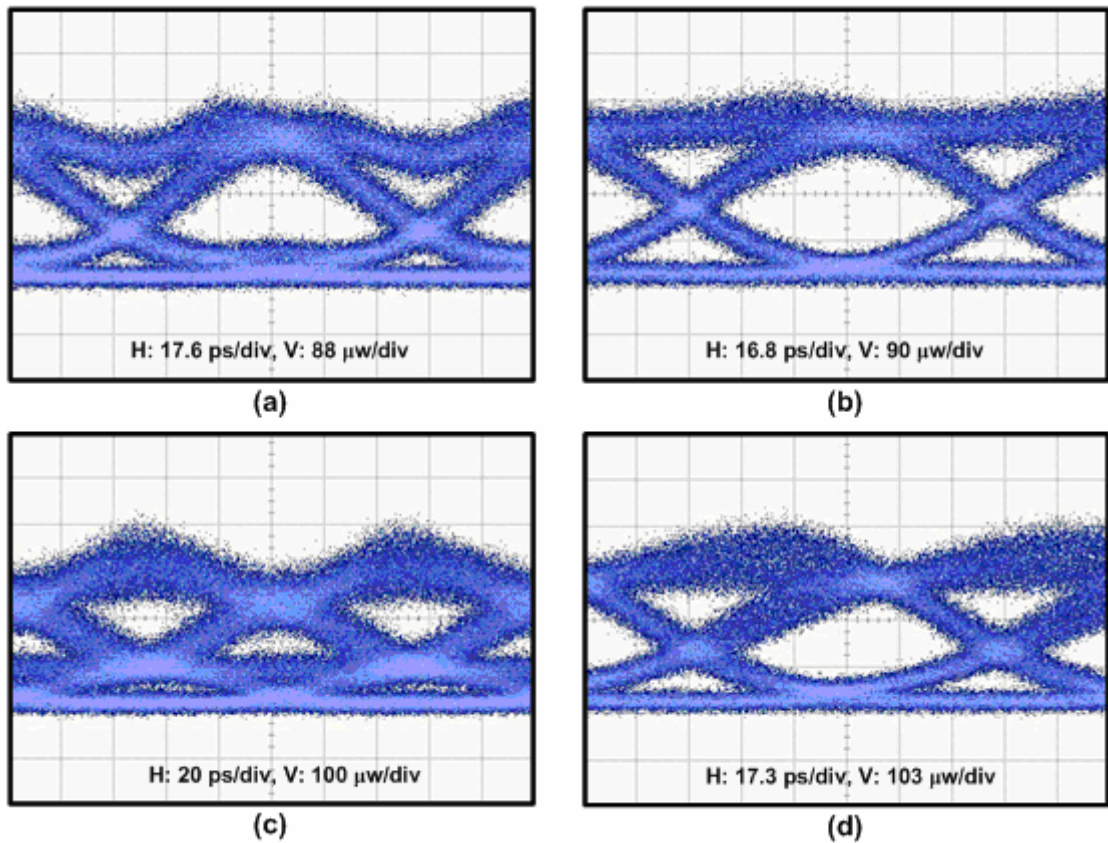
Fig. 4.14 Received eye diagrams of the 10 Gb/s testing signal for (a) 1R-regenerated at 50 km, (b) 2R-regenerated at 50 km, (c) 100 km propagation with 1R regeneration at 50 km, and (d) 100 km propagation with 2R regeneration at 50 km.
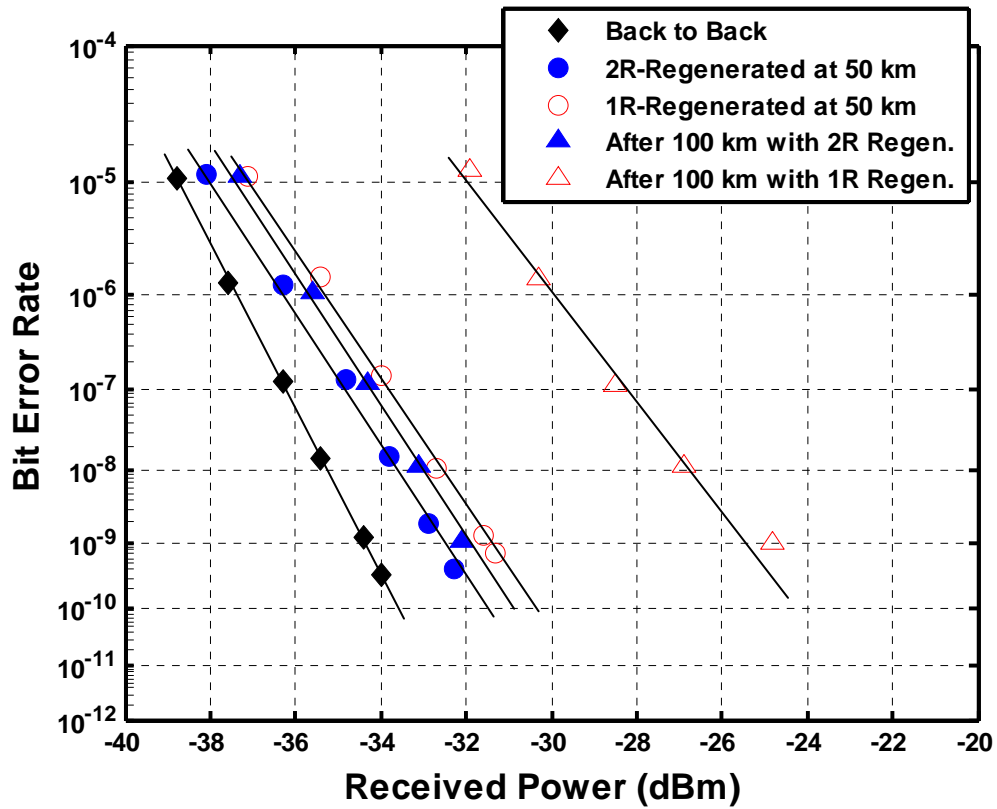
Fig. 4.15 The BER performances of the proposed 2R regenerator and the conventional 1R module for 50 and 100 km fiber transmissions.

Chapter 5

Amplifier-Free All-Optical 2R Regeneration

5.1 Introduction

This chapter presents an EDFA-free all-optical 2R regeneration scheme based on a compact self-seeded Fabry-Pérot laser diode (SSFP-LD). The proposed 2R regenerator achieves a straight line transmission at 10 Gb/s over 76 km without either the EDFA or the external probe laser, both of which are traditionally required. Additionally, device characteristics such as data-rate transparency, input dynamic range, amplified gain, and 2R regeneration performance are investigated experimentally. On the other hand, a novel and cost-effective 1.3 μm all-optical 2R regenerator based on a two-mode injection-locked distributed feedback laser diode (TMIL DFB-LD) is also proposed to provide adequate all-optical reamplification and reshaping in the second window. The proposed 2R regenerator, with 14.13 dB small signal gain, has achieved a 10 Gb/s straight line transmission over 60 km while keeping the power penalty less than 0.84 dB at bit-error-rate=10^{-9}. In addition, properties like bit-error-rate degradation, output extinction ratio, gain, and data-rate transparency are also experimentally investigated.

5.2 EDFA-Free All-Optical 2R Regenerator Using Compact SSFP-LD

All-optical 2R regeneration (re-amplification and re-shaping), which can restore the signal degradation caused by the combined effects of noise accumulation, fiber dispersion and nonlinearities, is a highly promising technique for future all-optical networks. Several techniques, including a side-mode injection-locked semiconductor laser [1-18] and a two-mode injection-locked Fabry-Pérot laser diode (FP-LD) [19-21], have recently been

reported. Although the two-mode injection-locked method has significantly better re-shaping and relaxation frequency performances than the one-side-mode scheme [5-18], it also has a higher device cost and complexity due to the introduction of an external probe laser. In addition, extra optical amplifiers, such as the Erbium-doped fiber amplifier (EDFA), are needed to re-amplify the signal and to compensate the loss of re-shaping. In this paper, we propose and demonstrate a new and cost-effective technique to simultaneously execute all-optical 2R regeneration without the need for optical amplifiers by using a compact self-seeded FP-LD with an embedded fiber Bragg grating (FBG).

5.2.1 Operation Principle

Figure 5.1 illustrates a schematic diagram of the proposed self-seeded FP-LD (SSFP-LD). An FBG is directly integrated into a 2.5 GHz commercial FP-LD without an optical isolator to form a ~10mm-long feedback cavity. This FBG has a 70 % reflectivity at central wavelength of 1550.8 nm, a bandwidth of 0.25 nm, and a grating length of 1 cm. In the absence of the injected signal, the FP-LD, which is self-seeded and stable-locked by the reflection tone at wavelength λ_2 generated by the FBG, has a single-longitudinal-mode operation. When a degraded signal S_{in} at wavelength λ_1, which has a power exceeding the injection-locking threshold, is injected into this SSFP-LD, the FP-LD is injection-locked and begins to operate at λ_1 with a constant power. The induced red-shift of the FP mode comb would lead to a wavelength misalignment between the reflectivity maximum of the FBG and the closest FP longitudinal mode, and helps to quench the self-seeded tone [22]. The injection-locking mechanism is characterized by an on-off threshold that can be exploited to reduce and compress the noise over the zeros and ones. In addition, the regeneratively amplified gain of injected signal S_{in} is limited by the spectral profile of the FP-LD. A positive gain of input signal can be achieved by arranging the signal wavelength in the main-peak mode area and

the self-seeded tone far from the main-peak mode.

5.2.2 Experimental Setup

Figure 5.2 indicates experimental setups for 10 Gb/s all-optical transmissions with the proposed 2R regenerator (block A) and a conventional EDFA module (1R device, block B). To provide an EDFA-free transmission, a self-seeded FP-LD, which can provide 8.3 dB gain at 1560.12 nm, was placed between two 38 km standard single-mode fiber (SSMF) spans. A signal at 1560.12 nm, generated from a tunable laser (TL), was externally modulated by an electro-optic modulator (EOM) with $2^{31}-1$ PRBS data stream at 10 Gb/s. The modulated signal propagated through the first 38 km fiber span, and then was injected into the SSFP-LD via an optical circulator (OC) and a polarization controller (PC). The SSFP-LD was biased at 4.6 times its threshold current (10 mA) and had its temperature controlled at 17.35℃ to generate a self-seeded tone at 1551 nm with a side mode suppression ratio (SMSR) larger than 40 dB. After filtered out by a bandpass filter (BPF) with a 3 dB bandwidth of 0.8 nm, the regenerated signal was propagated through another 38 km fiber span, and transmitted to an optical receiver to investigate the bit error rate (BER) performance and the eye diagram. Average input powers of around −8 dBm were set at two 38 km spans to avoid or decrease the nonlinear effects such as self phase modulation (SPM) of fiber and four wave mixing (FWM) of SSFP-LD.

5.2.3 Result and Discussion

Figure 5.3(a) and (b) illustrate the optical spectra of the SSFP-LD without, and with the injection signal, respectively. As shown in Fig. 5.3(a), the free-running SSFP-LD have a 1551 nm self-seed tone with side-mode suppression ratio (SMSR) over 40 dB. In Fig. 5.3(b), when a 1560.12 nm degraded signal at 10 Gb/s was injected, the beating between the injection

signal and the self-seeded tone led to two FWM tones at 1541.94 and 1569.42 nm, respectively. However, such redundant components can be eliminated by an OBPF before being transmitted to the next span. Figure 5.4 shows the testing results of data-rate transparency up to 10 GHz. The noisy signals at bit rates of 155 MHz, 2.5 GHz and 10 GHz were input into the proposed 2R regenerator, and the outputs with clear eye diagrams come out. The data-rate transparency of the proposed scheme has been successfully proven.

Figure 5.5 depicts the dynamic range and amplified gain of the injection signal for the proposed SSFP-LD as a function of the operating wavelengths to achieve successful waveform reshaping. Clearly, a higher signal gain and lower injection power level can be obtained if the operating wavelength approaches the free-running main mode of the FP-LD (~1562 nm). Figure 5.6 depicts the measured sensitivity of the reamplified and reshaped signal from SSFP-LD as a function of the injection power. As shown in Fig. 5.6, in order to maintain the sensitivity of -18.5 dBm, the injection power ranges from -10.2 dBm to 17.3 dBm, which match well with the results in Fig. 5.5. However, when the sensitivity of -19 dBm is required, there exists a dip around injection power of -15 dBm, and the dynamic range is reduced to about 1 dB.

Figure 5.7 shows the 10 Gb/s bit error rate (BER) performance of the proposed 2R regenerator and the 1R EDFA module in the setup of Fig. 5.2. The insets show the measured eye diagrams of the signal: (a) 2R-regenerated at 38 km; (b) 1R-regenerated at 38 km; (c) after 76 km propagation with 2R regeneration; and (d) after 76 km propagation with 1R regeneration. By using the proposed method, the power penalties, compared with the back-to-back case, were 0.65 and 0.9 dB after transmission over 38 km and 76 km, respectively, at BER = 10^{-9}. However, the 1R-only transmission has larger power penalties of 1.5 and 3.4 dB after transmitting over 38 km and 76 km, respectively, at BER = 10^{-9}. To optimize the regenerated signal, the average injection power into the FP-LD was kept at

−14.58 dBm, and the degraded signal was injected at the wavelength which is located within one of the FP modes and has a slight detuning of +0.04 nm from the central wavelength of this mode. As a result, by using this proposed SSFP-LD, a distorted signal was successfully re-amplified and re-shaped, and the eye diagram was still wide open after 76 km propagation without the assistance of an EDFA. On the contrary, the signal in 1R-only transmission was seriously distorted due to the accumulation of chromatic dispersion.

On the other hand, to verify the cascadability of the proposed 2R device, a re-circulating loop was employed. As illustrated in Fig. 5.8, the performance of the SSFP-LD was also compared with that of the 1R EDFA module (block B) and a dispersion-compensated EDFA module (block C). The bias condition of the SSFP-LD and average power at points "a" and "b" are kept the same with those in Fig. 5.2 setup. In the functional block C, an 8.031 km long Corning DCF with 86.3 ps/nm/km dispersion at 193.0 THz was utilized to compensate the accumulated chromatic dispersion in the 38 km SSMF. Moreover, $EDFA_l$ in re-circulating loop was used to compensate the loop loss except for SSMF. Fig. 5.9 presents the BER performances of the re-circulating loop experiments with three functional blocks, as shown in the setup of Fig. 5.2, for cascadability verification. The inserts are the corresponding eye diagrams. Due to the poor performance limitation of this re-circulating loop, only 2 laps were demonstrated, which means the signal will propagate over 76 km and passing through 2R or 1R regeneration twice. As can be seen in Fig. 5.9, after 2 laps, the measured power penalties of blocks A, B, and C at 10^{-9} BER are 1.05 dB, 1.5 dB and 3 dB, respectively. Therefore, the results reveal that the proposed 2R regeneration can be insensitive to the accumulated dispersion and two times of 2R regeneration.

5.3 1.3 μm Amplifier-Free All-Optical 2R Regeneration Using TMIL

Distributed Feedback Laser Diode

High-speed transmission system in 1.3 μm operation window features zero dispersion, but suffers from link-length obstacle due to the intrinsic attenuation limit of a single-mode fiber (SMF). Such limitation is expected to be eliminated by all-optical amplification. Several 1.3 μm amplification techniques have been presented, such as praseodymium doped-fiber amplifier (PDFA) [23-25], Raman amplifier (RA) [26-28], and semiconductor optical amplifier (SOA) [29-31], to provide a supplementary transmission window for the present EDFA-dominant system. However, owing to the issues of device cost and stability, it is still doubtful that whether these methods will meet the requirement for field deployment in local/metropolitan area networks (LANs/MANs). Recently, 1.5 μm all-optical 2R regeneration (re-amplification and re-shaping) modules based on two-mode injection-locked (TMIL) semiconductor laser diodes [19-21] have been intensively studied. This type of regenerator usually requires extra optical amplifiers to re-amplify the signal and to compensate the loss of re-shaping. However, we find that optical amplifiers are not necessities since the TMIL semiconductor laser itself, in principle, can simultaneously act as a regenerative laser amplifier and a waveform re-shaper. Therefore, in this paper, we propose and demonstrate the feasibility of a new and cost-effective 1.3 μm all-optical 2R regenerator using a two-mode injection-locked distributed feedback laser diode (TMIL DFB-LD). This new regenerator can offer a promising alternative for short and middle haul applications.

5.3.1 Operation Principle

Figure 5.10 depicts the conceptual diagram of the proposed 1.3 μm all-optical 2R regenerator. A DFB-LD, which is side-mode injection-locked (SMIL) by a CW signal at λ_p, can provide all-optical 2R regeneration by highly suppressing its free-running main mode and enhancing its relaxation oscillation frequency (ROF). When a degraded signal S_{in} at wavelength λ_s,

which has a power level exceeding the injection-locking threshold, is injected into this DFB-LD and its wavelength is fit into the locking range of the main mode, the S_{in} will be regeneratively amplified after passing through this DFB-LD. In the mean time, the mode frequencies of the DFB-LD will be red-shifted due to the carrier-induced refractive index change, which can help to pull the CW light out of the locking range and relieve the suppressing strength. If the S_{in} has the power level fallen below the injection-locking criterion, it will experience nature loss when going through this DFB-LD. As a result, the DFB-LD by using a two-mode injection-locked (TMIL) technique can reduce the accumulated noise over one and zero levels and achieve the signal regeneration.

5.3.2 Experimental Setup

Figure 5.11 illustrates the experimental setup for a 10 Gb/s straight line link with the proposed 1.3 μm all-optical 2R regenerator. As shown in Fig. 5.11, the proposed 2R regenerator was placed between two 30 km standard single-mode fiber (SSMF) spans. An optical transmitter, composed of a tunable laser (TL), a PC and a Mach-Zehnder Modulator (MZM), can emit a 10 Gb/s signal with $2^{31}-1$ PRBS test pattern at 1307.9 nm. After being transmitted over a 30 km SSMF span, the degraded signal was then fed into the proposed regenerator. This regenerator comprises an optical circulator (OC), a 60:40 coupler, a polarization controller (PC), and two DBF-LDs: DFB-LD$_p$, and DFB-LD$_r$. The DFB-LD$_r$ was biased at 23.6 mA and had its temperature controlled at 13.64℃ to generate a main mode wavelength at 1307.9 nm. In addition, the DFB-LD$_p$, serving as an external probe light source, was biased at 141 mA and 10.42℃ to generate a CW light of 8 mW at 1300.8 nm. This CW signal was combined with the input signal by a 60:40 coupler and injected into DFB-LD$_r$ through OC. A thin-film CWDM bandpass filter (BPF), which has a 3 dB bandwidth of 10 nm, a central wavelength of 1311 nm, and an insertion loss of 0.35 dB, was employed at the output

port of the regenerator to filter out the wanted signal. After 2R regeneration, the regenerated signal was propagated through another 30 km SSMF span, and transmitted to an optical receiver. To evaluate the performance of bit error rate (BER), an error detector is used after the optical receiver.

5.3.3 Result and Discussion

Figure 5.12 shows the optical spectra of the DFB-LD$_r$ at the port 3 of OC in Figure 5.11 for free-run, side-mode injection-locked (SMIL) and two-mode injection-locked (TMIL) operations. As shown in Fig. 5.12, the free-running DFB-LD$_r$ had an output power of 3.91 dBm at 1307.9 nm, and a side-mode suppression ratio (SMSR) over 46.0 dB. When the SMIL is operated by injecting a 1300.8 nm CW light, which has 4.8 dBm power at port 1 of OC, the main mode peak was highly suppressed by 34.9 dB. When a 1307.9 nm signal with average power of –20.3 dBm was injected at the port 1 of OC, it was resonantly amplified up to –6.17 dBm with a reshaped waveform at port 3 of OC. This small signal gain of 14.13 dB from the port 1 to the port 3 of OC can compensate the losses of a 30 km SSMF and a 60:40 coupler. A small four-wave mixing spike at 1293.72 nm, resulting from the beating of two mode signals, was also observed in Figure 4.12 for TMIL operation. Figure 5.13 demonstrates the data-rate transparency characteristic of the proposed 1.3 μm all-optical 2R regenerator. The measured results indicate that the proposed regenerator can restore the eye patterns to wide-open from seriously distorted input ones for data rates from 155 MHz to 10 GHz. Figure 5.14 shows the 10 Gb/s bit error rate (BER) performance of the proposed 1.3 μm 2R regenerator for the experimental setup in Figure 5.11. The power penalties at BER = 10^{-9}, compared with back-to-back case, were 0.47 and 0.84 dB after transmission over 30 km and 60 km, respectively. The insets illustrate the measured eye diagrams of the signal for (a) back to back, and (b) 2R-regenerated at 30 km. The inset (b) shows that the regenerated signals have

extinction ratio (ER) of 10.19 dB.

5.4 Summary

This chapter demonstrates the feasibility of an EDFA-free and all-optical 2R regeneration by using a compact self-seeded FP-LD with an ultra short feedback cavity of ~10 mm. The experiments reveal that external probe lasers and additional EDFAs for the traditional two-mode injection locked scheme are not required when utilizing the proposed approach. This self-seeding method is promising for the future applications on amplifier-free high-speed all-optical 2R regeneration. Besides, a 1.3 μm all-optical 2R regenerator by using the two-mode injection-locked distributed feedback laser diode (TMIL DFB-LD) have been proposed. 1.3 μm regenerative amplification of 14.13 dB gain and the data-rate transparency up to 10 Gb/s have been achieved. In addition, a 10 Gb/s transmission link over 60 km with power penalty < 0.84 dB has also been demonstrated. This 2R regenerator is useful for the future applications on short and middle haul networks.
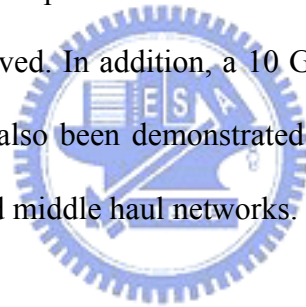
Reference for Chapter 5

[1] R. Lang, "Injection locking properties of a semiconductor laser," *IEEE J. Quantum Electron.*, vol. QE-18, pp. 976-983, June 1982.

[2] K.Weich, E. Patzak, and J. Hörer, "Fast all-optical switching using two-section injection-locked semiconductor lasers," *Electron. Lett.*, vol. 30, pp. 493-494, 1994.

[3] S. Yamashita and D. Matsumoto, "Waveform reshaping based on injection locking of a distributed-feedback semiconductor laser," *IEEE Photon. Technol. Lett.*, vol. 12, pp. 1388-1390, Oct. 2000.

[4] K. Inoue and M. Yoshino, "Bistability and waveform reshaping in a DFB-LD with side-mode light injection," *IEEE Photon. Technol. Lett.*, vol. 7, pp. 164-166, Feb. 1995.

[5] Y. Hong and K. A. Shore, "Locking characteristics of a side-mode injected semiconductor laser," *IEEE J. Quantum Electron.*, vol. 35, pp. 1713-1717, Nov. 1999.

[6] A. Kuramoto and S. Yamashita, "All-optical regeneration using a side-mode injection-locked semiconductor laser," *IEEE J. Select. Topics Quantum Electron.*, vol. 9, pp. 1283-1287, Sept./Oct. 2003.

[7] R. J. Jones, P. S. Spencer, and K. A. Shore, "Detuned side-mode injection for enhancing oscillation frequency of a semiconductor laser," *IEEE Proceedings*, vol. 148, No. 1, pp. 35-39, 2001.

[8] J. M. Luo and M.Osinski, "Stable-locking bandwidth in sidemode injection locked semiconductor lasers," *Electron. Lett.*, vol. 27, No. 19, pp. 1737-1738, 1991.

[9] J. M. Luo, "Side-mode injection locking of semiconductor lasers," *IEEE Proceedings*, vol. 136, No. 1, pp. 33-37, 1989.

[10] Y. Hong, K. A. Shore, J. S. Lawrence, and D. M. Kane, "Wavelength switching by positively detuned side-mode injection in semiconductor laser," *Appl. Phys. Lett.*, vol. 76,

No. 22, pp. 3170-3172, 2000.

[11] T. B. Simpson and J. M. Liu, "Enhanced modulation bandwidth in injection-locked semiconductor laser," *IEEE Photon. Technol. Lett.*, vol. 9, pp. 1322-1324, Oct. 1997.

[12] J. M. Liu, H. F. Chen, X. J. Meng, and T. B. Simpson, "Modulation bandwidth , noise, and stability of a semiconductor laser subject to strong injection locking," *IEEE Photon. Technol. Lett.*, vol. 9, pp. 1325-1327, Oct. 1997.

[13] J. Wang, M. K. Haldar, L. Li, and F. V. C. Mendis, "Enhancement of modulation bandwidth of laser diodes by injection lcoking," *IEEE Photon. Technol. Lett.*, vol. 8, pp. 34-36, Jan. 1996.

[14] T. B. Simpson, J. M. Liu, and A. Gavrielides "Bandwidth enhancement and broadband noise reduction in injection-locked semiconductor laser," *IEEE Photon. Technol. Lett.*, vol. 7, pp. 709-711, Jul. 1995.

[15] J. K. White, J. V. Moloney, A. Gavrielides, V. Kovanis, A. Hohl, and R. Kalmus, "Multilingitudinal-mode dynamics in a semiconductor laser subject to optical injection," *IEEE J. Quantum Electron.*, vol. 34, pp. 1469-1473, Aug 1998.

[16] R. Hui, A. D'Ottavi, A. Mecozzi, and P. Spano, "Injection locking in distributed feedback semiconductor lasers," *IEEE J. Quantum Electron.*, vol. 27, pp. 1688-1695, Jun 1991.

[17] I. Petitbon, P. Gallion, G. Debarge, and C. Chabran, "Locking bandwidth and relaxation oscillations of an injection-locked semiconductor laser," *IEEE J. Quantum Electron.*, vol. 24, pp. 148-154, Feb 1988.

[18] J. M. Luo and M.Osinski, "Multimode small-signal analysis of side-mode injection-locked semiconductor laser," *Jpn. J. Appl. Phys.*, vol. 31, No. 6A, pp. 685-688, 1992.

[19] J. Hörer and E. Patzak, "Large-signal analysis of all-optical wavelength conversion using two-mode injection-locking in semiconductor lasers," *IEEE J. Quantum Electron.*, vol.

33, pp. 596-608, Apr. 1997.

[20] L. Xu, W. H. Chung, L. Y. Chan, L. F. K. Lui, P. K. A. Wai, and H. Y. Tam, "Simultaneous all-optical waveform reshaping of two 10-Gb/s signals using a single injection-locked fabry-pérot laser diode," *IEEE Photon. Technol. Lett.*, vol. 16, pp. 1537-1539, June 2004.

[21] S. Yamashita and J. Suzuki, "All-optical 2R regeneration using a two-mode injection-locked fabry-pérot laser diode," *IEEE Photon. Technol. Lett.*, vol. 16, pp. 1176-1178, Apr. 2004.

[22] A. Murakami, K. Kawashima, and K. Atsuki, "Cavity resonance shift and baidwidth enhancement in semiconductor lasers with strong light injection," *IEEE J. Quantum Electron.*, vol. 39, pp. 1196-1204, Oct 2003.

[23] Y. Nishida, M. Yamada, T. Kanamori, K. Kobayashi, J. Temmyo, S. Sudo, and Y. Ohishi, "Development of an efficient praseodymium-doped fiber amplifier," *IEEE J. Quantum Electron.*, vol. 34, no. 8, pp.1332-1339, Aug. 1998.

[24] K. Kikushima, M. Yamada, M. Shimizu, and J Temmyo, "Distortion and noise properties of a praseodymium-doped fluoridefiber amplifier in 1.3 μm AM-SCM video transmission systems," *IEEE Photon. Technol. Lett.*, vol. 6, pp. 440-442, Apr. 1994.

[25] T. J. Whitley, "A review of recent system demonstrations incorporating 1.3-μm praseodymium-doped fluoride fiber amplifiers," *J. Lightwave Technol.*, vol. 13, no. 5, pp. 744-760, May. 1995.

[26] A. G. Okhrimchuk, G. Onishchukov, F. Lederer, "Long-haul soliton transmission at 1.3 μm using distributed Raman amplification," *J. Lightwave Technol.*, vol. 19, no. 6, pp. 837-841, Jun. 2001.

[27] E. M. Dianov, M. V. Grekov, I. A. Bufetov, V. M. Mashinsky, et al, "Highly efficient 1.3 μm Raman fibre amplifier," *Electron. Lett.*, vol. 34, pp. 669-670, 1998.

[28] S. V. Chernikov, Y. Zhu, R. Kashyap, J. R. Taylor, "High-gain, monolithic, cascaded fibre Raman amplifier operating at 1.3 μm," *Electron. Lett.*, vol. 31, pp. 472-473, 1995.

[29] C. Holtmann, P. A. Besse, T. Brenner, H. Melchior, "Polarization independent bulk active region semiconductor optical amplifiers for 1.3 μm wavelengths," *IEEE Photon. Technol. Lett.*, vol. 8, pp. 343-345, Apr. 1996.

[30] Y. Zhang, P. P. Ruden, "1.3-μm polarization-insensitive optical amplifier structurebased on coupled quantum wells," *IEEE J. Quantum Electron.*, vol. 35, no. 10, pp.1509-1514, Oct. 1999.

[31] B. H. Verbeek, L. H. Spiekman, "Semiconductor optical amplifiers for all transmission wavelength bands," *Conference on Lasers and Electro-Optics (CLEO)*, pp. 421, May 2000.
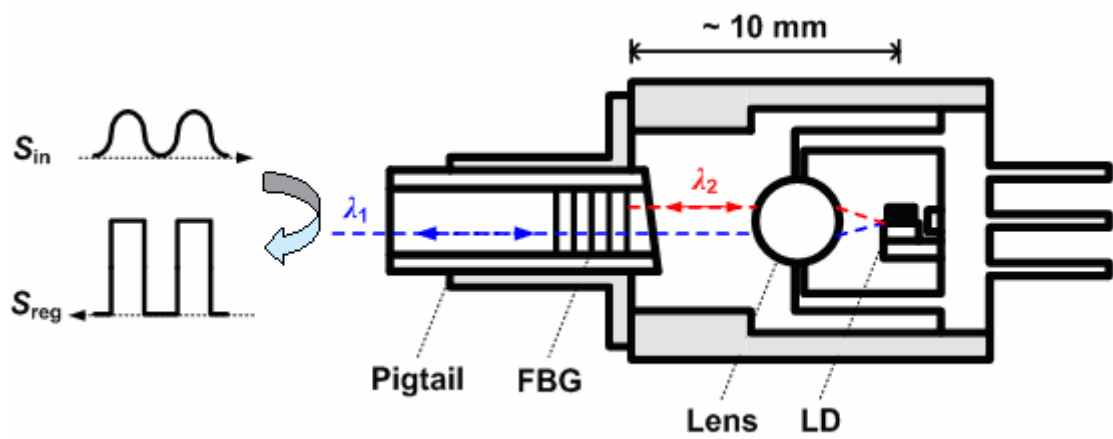
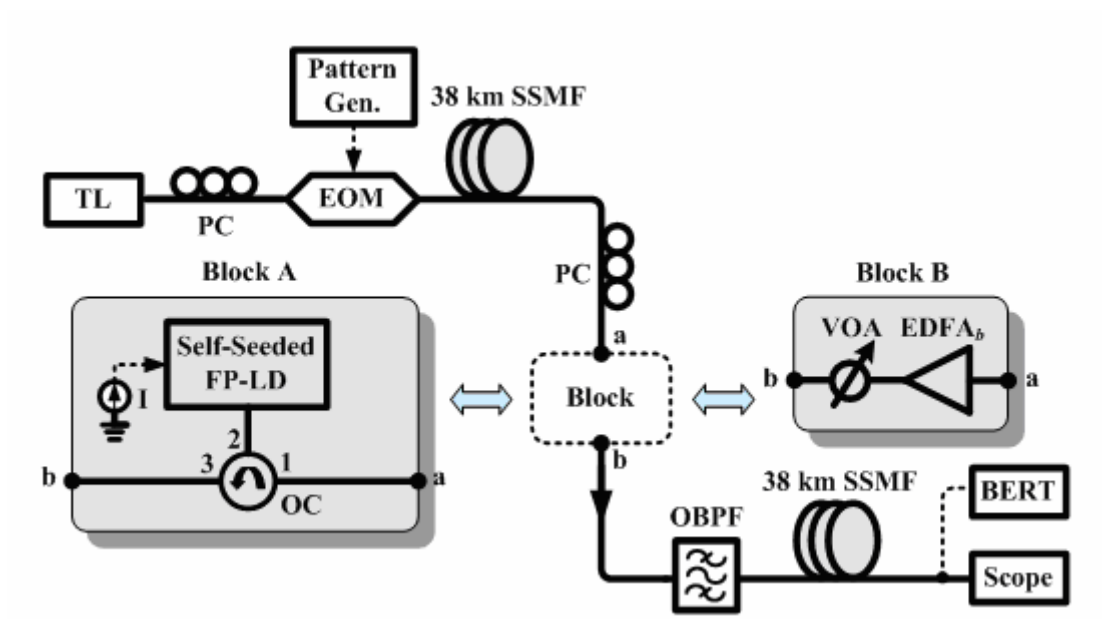**Fig. 5.1** Schematic diagram of the proposed compact self-seeded FP-LD.

Fig. 5.2 Experimental setup for the proposed 10 Gb/s all-optical 2R regenerator in the transmission link.
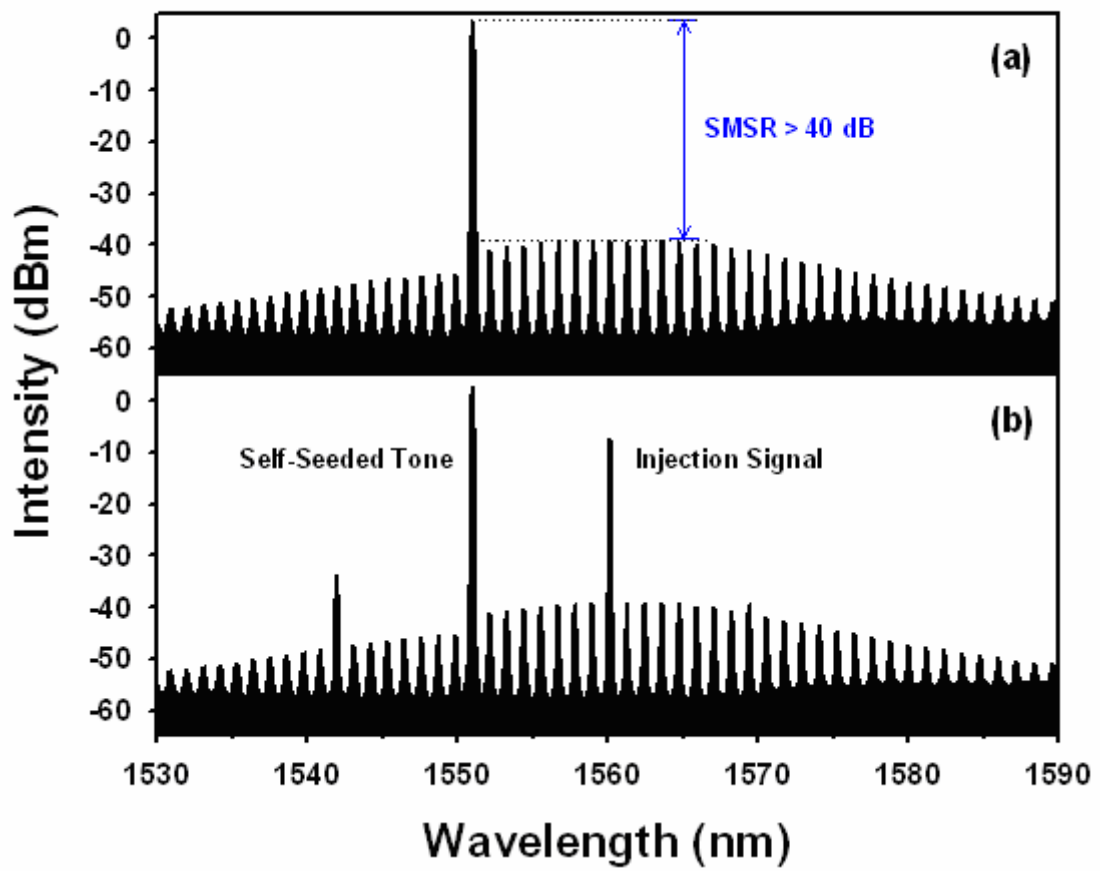
Fig. 5.3 Measured optical spectra of the SSFP-LD (a) without, and (b) with the
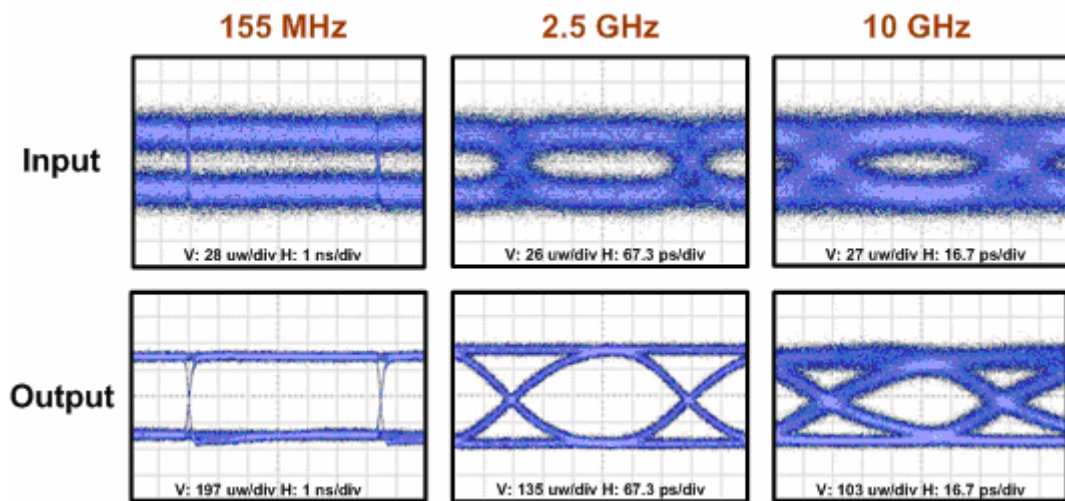
10 Gb/s injection signal.

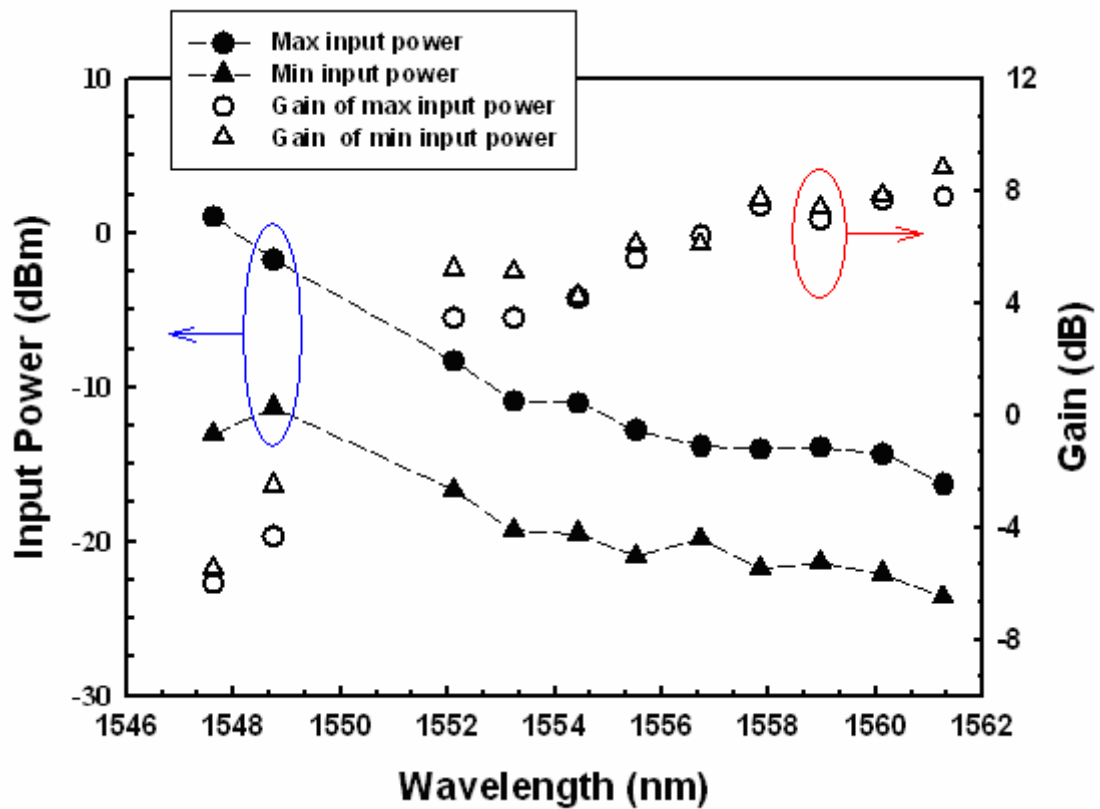**Fig. 5.4** Data-rate transparency up to 10 GHz of the proposed 2R regenerator.

Fig. 5.5 Dynamic range and gain of the injection signal for the proposed SSFP-LD as a function of operating wavelengths. The main mode of SSFP-LD is at about 1560 nm.
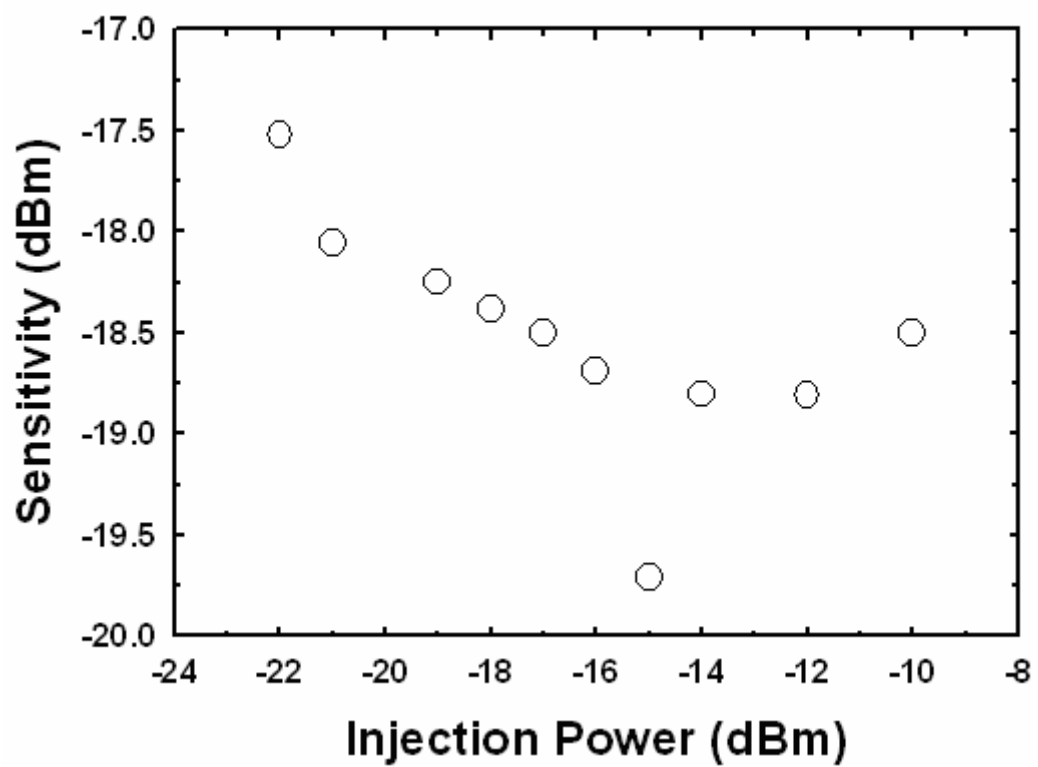
Fig. 5.6 Sensitivity of the regenerated signal as a function of injection power.
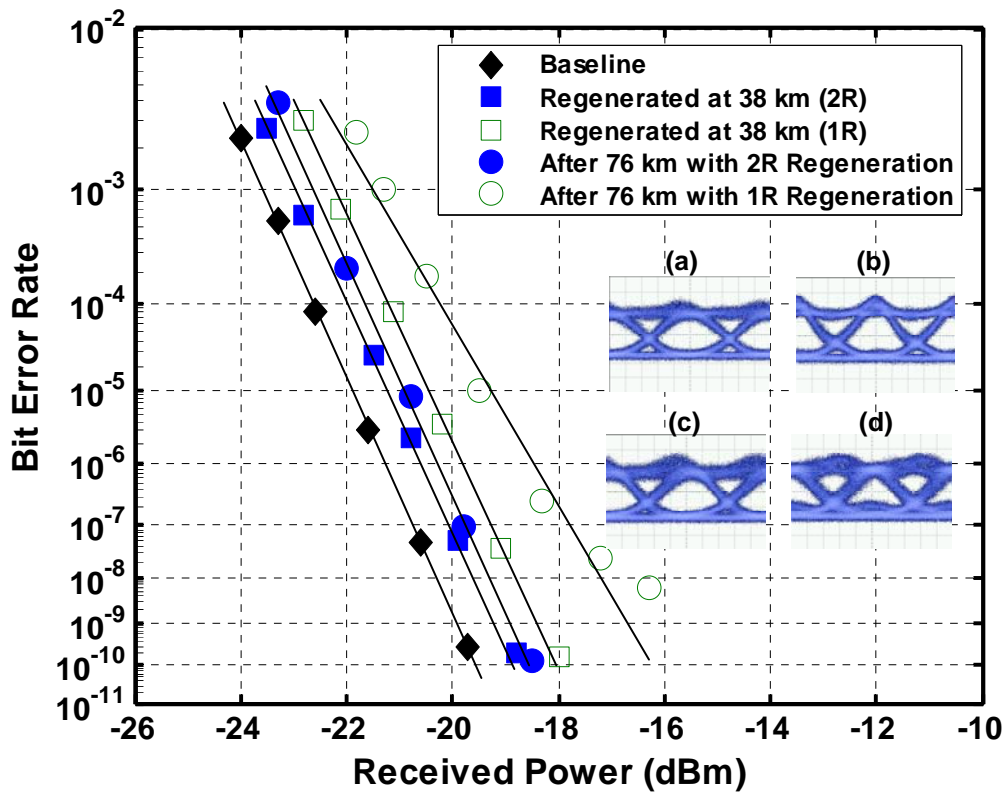
Fig. 5.7 BER performances and eye diagrams of the proposed 2R, and 1R regenerations at 10 Gb/s in a transmission link, respectively.
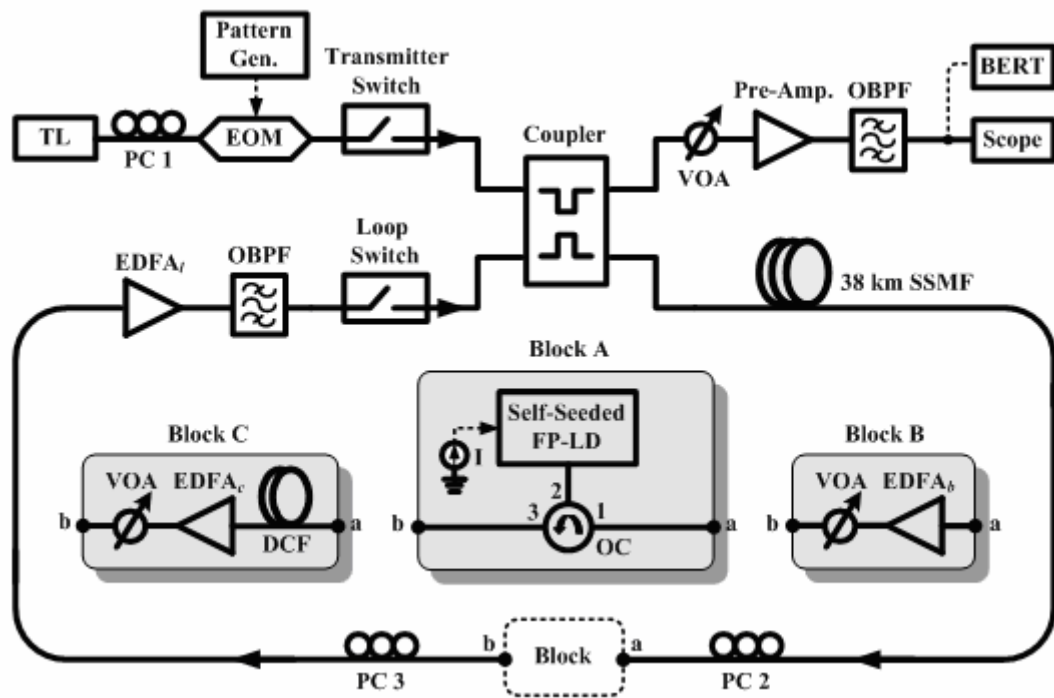
Fig. 5.8 Experimental setups for the proposed 10 Gb/s all-optical 2-R regenerator in the re-circulating loop
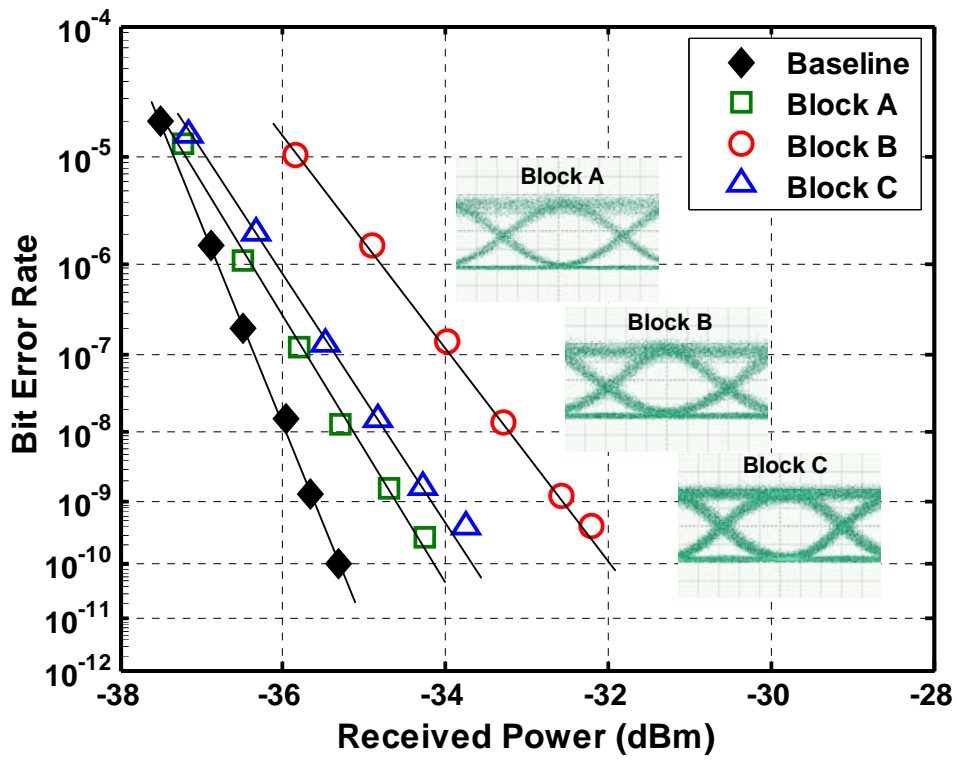
Fig. 5.9 BER performances and eye diagrams of the re-circulating loop experiments with functional block A, B, and C, respectively
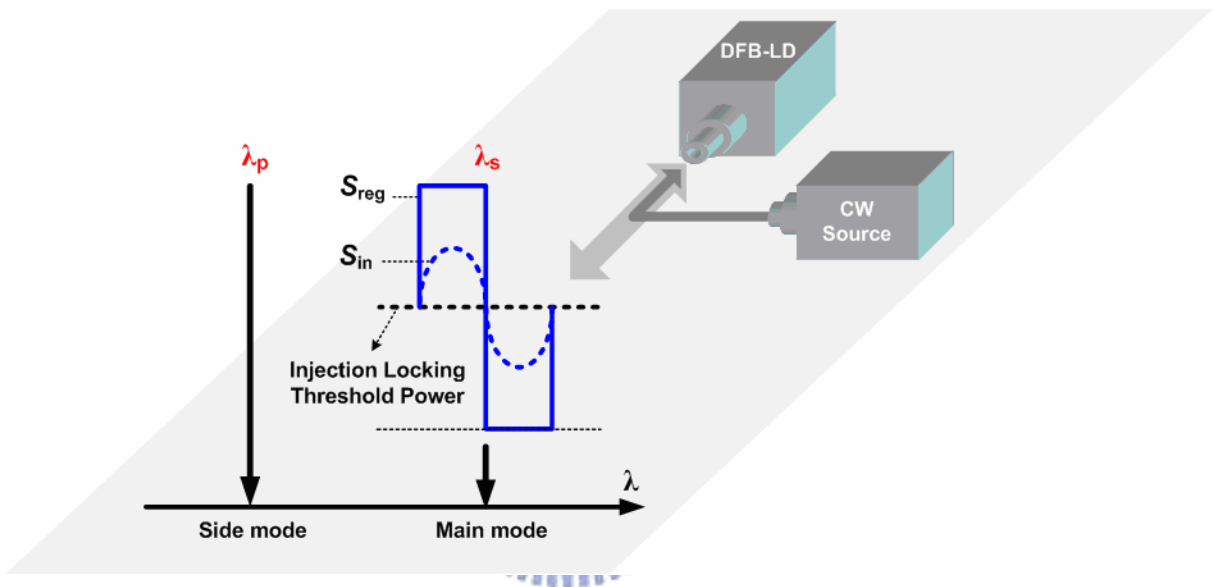
Fig. 5.10 Conceptual diagram of the proposed 1.3 μm all-optical 2R regeneration technique using a TMIL DFB-LD.
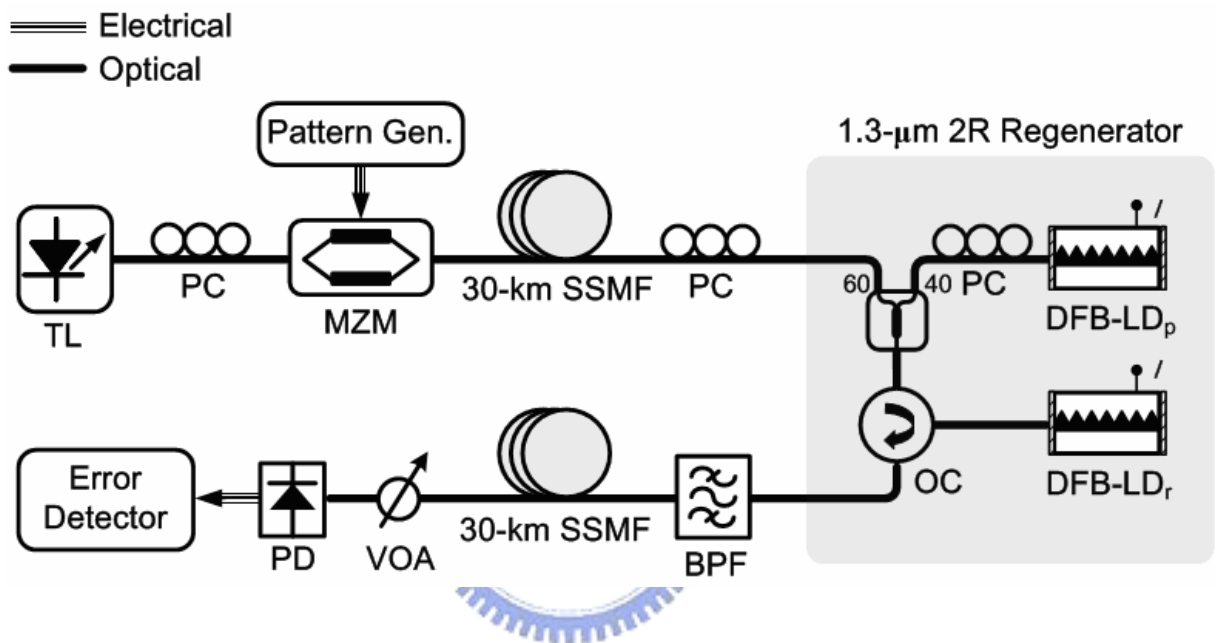
Fig. 5.11 The experimental setup for a 10 Gb/s straight line link over 60 km with

the proposed 1.3 μm all-optical 2R regenerator.

Fig. 5.12 The measured optical spectra of the DFB-LD$_r$ at the port 3 of OC in Figure 5.11 for free-run, SMIL and TMIL operations.

Fig. 5.13 Data-rate transparency up to 10 GHz of the proposed 1.3 μm 2R regenerator.

Fig. 5.14 BER performance of the 1.3 μm proposed 2R regenerator at 10 Gb/s.

The insets are the measured eye diagrams of the signal for (a) back to back, and

(b) 2R-regenerated at 30 km.

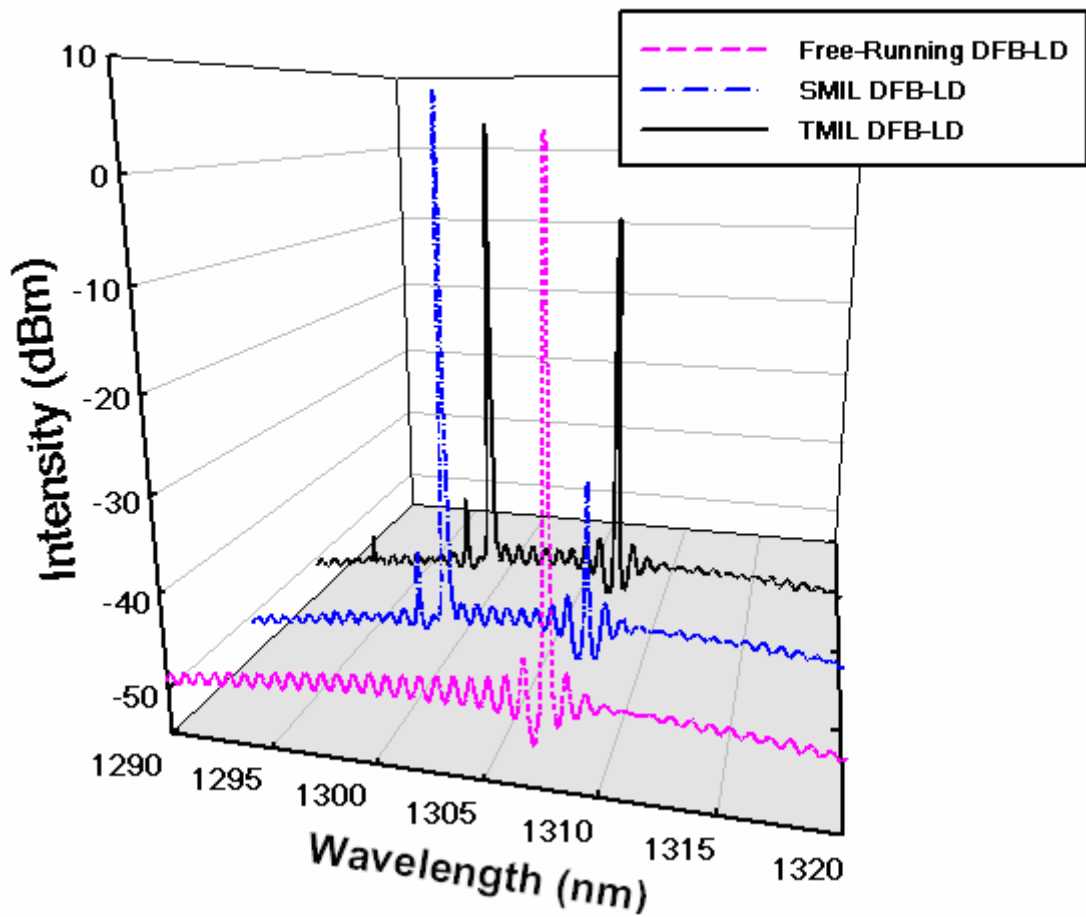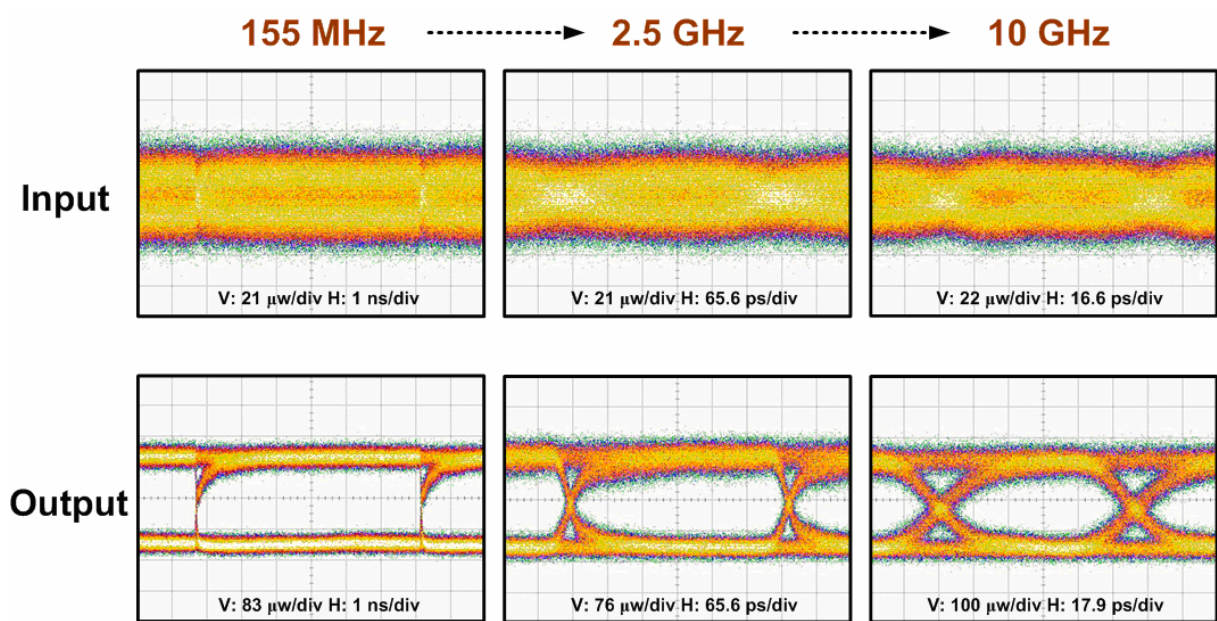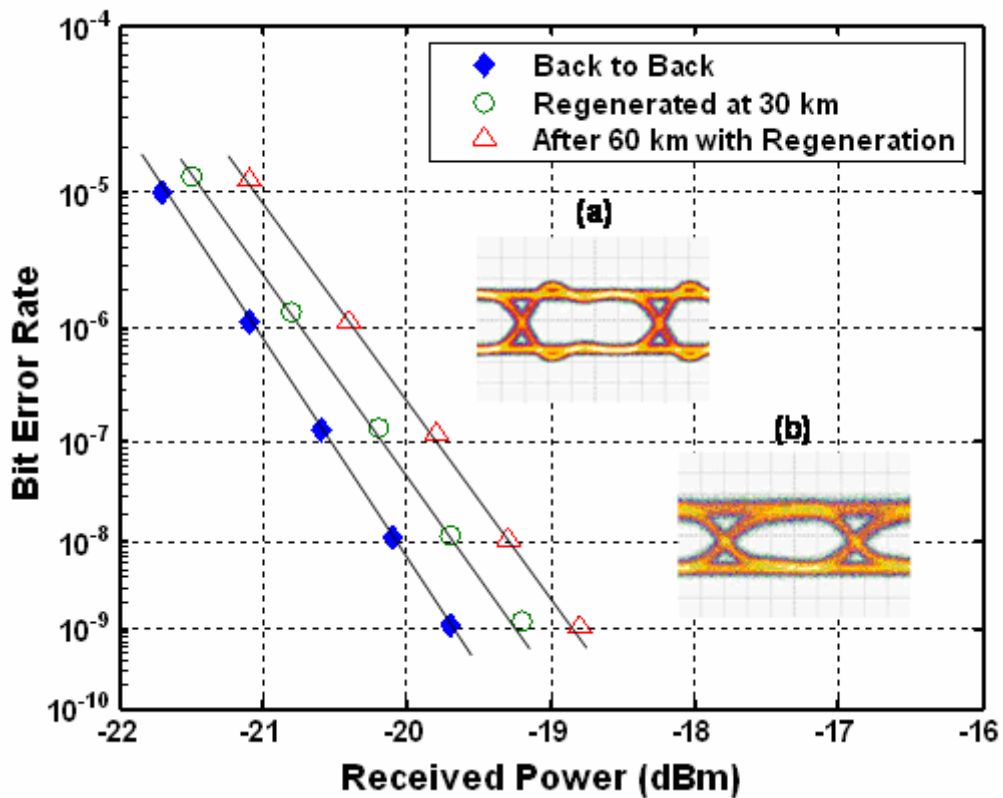# Chapter 6

Conclusions and Future Work

6.1 Conclusions

Fiber-optic communication system is sensitive to several impairments like amplifier noise accumulation, fiber dispersion, fiber nonlinearity, and inter/intrachannel interactions as the channel capacity increases. The resulting signal degradation requires efficient all-optical regenerating scheme or device to overcome the transmission limitations. After four different types of all-optical 2R regeneration methods: the SOA-based, fiber-based, EAM-based, and semiconductor-laser-based techniques are studied, we chose and focused on the semiconductor-laser-based technique since the semiconductor laser diode is cost-effective and easily available. Therefore, based on the traditional TMIL method, we propose two types of new TMIL schemes. The first type has a simplified structure without the help from external probe lasers and another one is an amplify-free method without the assistance of any outside EDFAs.

The simplified TMIL schemes for all-optical 2R regeneration are presented in Chapter 4. A cost-effective 2R device, using a compact self-seeded Fabry-Pérot laser diode (SSFP-LD) with a 10mm-long embedded fiber Bragg grating cavity, is proposed to achieve 10 Gb/s 2R regeneraton without the traditionally required external probe lasers. Furthermore, in section 4.3, this device can be incorporated in a bidirectional EDFA to form a compact 2R module with reduced number of EDFAs while maintaining the 2R performance. In addition, novel amplifier-free all-optical 2R regenerations using the proposed SSFP-LD and TMIL DFB schemes are demonstrated in Chapter 5 to execute actual 2R regeneration up to 10 Gb/s

without any commercial optical amplifier at 1.5/1.3 μm wavelength window. Such compact and amplifier-free 2R device is proved to overcome the system limitations, and what's more, it provides another promising choice for optical amplification in the EDFA-dominated network nowadays.

6.2 Future Work

Three suggestions for future development are given. The first one is compact add/drop unit using the previous proposed SSFP-LD. As we know, a commercial available laser module is usually equipped a small monitoring PD aside the LD for power evaluation. Therefore, when a signal is injected into the LD, the LD output will be modulated by the input signal, and the photon current of the monitoring PD will changes accordingly. So far, to the best of our knowledge, the concept of directly using the monitoring PD as a dropping device behind the LD has not been declared. The common architecture for modern optical transceiver includes two separated parts of adding and dropping units. If the frequency response of the monitoring PD is fast enough to catch up with the high-speed injection signal, the future design for optical add/drop unit will be more easy and elegant.

The second suggestion for future work is to expand the function of SSFP-LD to 3R regeneration. In a high-speed transmission system up to 40 Gb/s or higher, timing jitter becomes an important factor contributed to signal degradation and all-optical retiming technique is thus required. Therefore, how to extract the accurate timing information of the signal in all-optical domain is an essential task. Finally, the last objective for future development is to find other applications of the SSFP-LD.

Publication

International Journals:

1. **Hung-Chang Chien**, C. C. Lee, and S. Chi, "All-Optical 2R Regenerator Using a Compact Self-Seeded Fabry-Perot Laser Diode Incorporated in a Bidirectional EDFA," *IEEE Photon. Technol. Lett.* (SCI&EI), vol. 18, no. 12, pp. 1344–1346, June. 2006. (IF = 2.552)

2. **Hung-Chang Chien**, C. C. Lee, and S. Chi, "EDFA-Free, All-Optical 2R Regeneration Using a Compact Self-Seeded Fabry-Pérot Laser Diode," *IEEE Photon. Technol. Lett.* (SCI&EI), vol. 18, no. 9, pp. 1112–1114, May. 2006. (IF = 2.552)

3. **Hung-Chang Chien**, C. C. Lee, Y. M. Chen, K. M. Feng, and S. Chi, "All-Optical 2R Regeneration Based on a Compact Self-Seeded Fabry-Pérot Laser Diode with an Embedded Fiber Bragg Grating," *IEEE Photon. Technol. Lett.* (SCI&EI), vol. 18, no. 4, pp. 559–561, Feb. 2006. (IF = 2.552)

4. C. C. Lee, T. C. Kao, **Hung-Chang Chien**, and S. Chi, "A Novel Supervisory Scheme for OXC Based on Different Time-Delay Recognition," *IEEE Photon. Technol. Lett.* (SCI&EI), vol. 17, no. 12, pp. 2745–2747, Dec. 2005. (IF = 2.552)

5. **Hung-Chang Chien**, C. H. Yeh, C. C. Lee and S. Chi, "A Tunable and Single-Frequency S-band Erbium Fiber Laser with Saturable-Absorber-Based Autotracking Filter," *Optics Communications* (SCI&EI), vol. 250, pp. 163–167, 2005. (IF = 1.581)

6. **Hung-Chang Chien**, C. H. Yeh, K. H. Lai, C. C. Lee and S. Chi, "Stable and wavelength-tunable erbium-doped fiber double-ring laser in S-band window operation," *Optics Communications* (SCI&EI), vol. 249, pp. 261–264, 2005. (IF = 1.581)

7. C. H. Yeh, **Hung-Chang Chien**, C. C. Lee and S. Chi, "Gain-clamping erbium-doped waveguide amplifier module using optical feedback technique," *Optics Communications* (SCI&EI), vol. 246, pp. 73–77, 2005. (IF = 1.581)

8. **Hung-Chang Chien**, C. H. Yeh, C. C. Lee and S. Chi, "A stable and Tunable Fiber Double-Ring Laser Based on Erbium-Doped Waveguide Amplifier," *Optical Engineering* (SCI&EI), vol. 44, no. 4, pp. 044204-1–044204-4, Apr. 2005. (IF = 1.171)

9. C. H. Yeh, **Hung-Chang Chien**, B. C. Cheng, C. C. Lee and S. Chi, "Using optical Fabry-Perot devices for a wavelength-tunable S-band erbium-doped fiber ring laser with single-frequency operation," *Optical Engineering* (SCI&EI), vol. 44, no. 10, pp.

104203-1–104203-4, Oct. 2005. (IF = 1.171)

10. **Hung-Chang Chien**, C. H. Yeh, C. C. Lee and S. Chi, "Single-Frequency Tunable Fiber Ring Laser Based on Erbium-Doped Waveguide Amplifier and Double Filters," *Japanese Journal of Applied Physics* (SCI&EI), vol. 44, no. 1A, pp. 231–232, 2005. (IF = 1.142)

Patent:

1. S, Chi, C. C. Lee, and **Hung-Chang Chien** (2005), An All-Optical 2R Regenerator Based on a Self-Seeded Laser Diode, USA & ROC patent pending.

International/Domestic Conferences:

1. **Hung-Chang Chien**, C. C. Lee, and S. Chi, "All-Optical 2R Regenerator Using a Compact Self-Seeded Fabry-Pérot Laser Diode Incorporated with a Bidirectional EDFA for 10 Gb/s Transmission System," *Conference of Lasers and Electro-Optics/Quantum Electronics and Laser Science conference (CLEO/QELS 2006)*, no. 06-C-505-CLEO, May 2006.

2. **Hung-Chang Chien**, S. Y. Chou, C. C. Lee, and S. Chi, "A New Optical-Path Supervisory Scheme for OXC Based on Unique FSR Recognition," *Conference of Lasers and Electro-Optics/Quantum Electronics and Laser Science conference (CLEO/QELS 2006)*, no. 06-C-1724-CLEO, May 2006.

3. C. C. Lee, T. C. Kao, **Hung-Chang Chien**, K. M. Feng and S. Chi, "A Different Time Delay Technique for Supervising Switch Fabric in OXC," *Optical Fiber Communication Conference & Exposition and the National Fiber Optic Engineers Conference (OFC/NFOEC 2005)*, no 05-C-932-OFC, March 2005.

4. W. R. Peng, W. P. Lin, **Hung-Chang Chien**, and S Chi, "A novel scheme for better performance in optical code-division multiple access," *International Quantum Electronics Conference 2005 and the Pacific Rim Conference on Lasers and Electro-Optics 2005 (IQEC/CLEO-PR 2005)*, no. CThC3-P30, Tokyo, Japan, 2005.

5. **Hung-Chang Chien**, C. C. Lee, Y. M. Chen, K. M. Feng, and S. Chi, "All-Optical 2R Regeneration by Injection Locking of a Compact Self-Seeded Fabry-Pérot Laser Diode," *Optics and Photonic Taiwan (OPT 2005)*, no. B-SA-III 9-1, Dec. 2005.

6. **Hung-Chang Chien**, Y. M. Chen, C. C. Lee and S. Chi, "Single-Frequency and wavelength-tunable S-band Erbium Fiber Ring Laser based on a Saturable-Absorber-Based Autotracking Filter," *Optics and Photonic Taiwan (OPT 2004)*, no C3N-76044, Dec. 2004.

7. **Hung-Chang Chien**, C. H. Yeh, C. C. Lee and S. Chi, "A Stable and Tunable S-band Erbium-Doped Fiber Double-Ring Laser," *9th OptoElectronics and*

Communications Conference (OECC 2004), no. 16B2-2, pp. 780-781, 2004.